Characterization of the electrical properties of polyaniline in the temperature range 30 – 450 K

VENANTIO MAROVHA MZENDA

Submitted in partial fulfillment of the requirements for the degree

MASTERS OF SCIENCE

In the faculty of natural and agricultural sciences at the University of Pretoria

Supervisor: Professor S. A. Goodman
Co-supervisor: Professor F. D. Auret

August 2001

To my loved ones

ACKNOWLEDGEMENT

Firstly I would like to thank my supervisor Professor S. A Goodman for guiding me throughout this study and for being there for me.

I also would like to thank the following people for their valuable contributions:

- My co-supervisor, Prof. F.D Auret for his guidance throughout this study
- Prof. W. Folker for his help with the chemistry of conducting polymers, several laboratory instruments and polymer synthesis
- L. Prinsloo, for her help with spectroscopic analysis of polyaniline
- The metallurgy department for providing me with a mortar and pestle for making pellets
- Prof. G. Myberg, for helping me with platinum electrodes and an electrochemical cell
- Dr. N. Van de Berg, for helping me with graphite rods
- My fellow students and members off the physics department whose contribution has always been positive towards completion of this study
- My parents, sisters, brothers and cousins for letting me know what they expect of me
- Michi, for being there all the time.

Finally, God bless.

SUMMARY

Despite the poor understanding of charge transfer in conducting polymers, conducting-polymer-based devices have achieved considerable commercial success. This success is based largely on the reproducibility of the measurable properties. It is the purpose of this study to further clarify charge transfer characteristics of conducting polymers under varying conditions.

We studied a conducting polymer called polyaniline. Polyaniline was available in its doped conducting form called emeraldine salt and in its undoped form called emeraldine base. Three types of polyaniline were studied, electrosynthesized (doped by HCl), chemically synthesized (doped by HCl) and commercial polyaniline obtained from Adlrich Company and doped by camphor sulfonic acid.

Initially we investigated whether charge transfer was ionic or electronic by observing the change in resistance with time for a fixed applied current. It was concluded that conduction in this material is electronic. Electrical measurements were obtained using the four-point probe and the Montgomery methods. The samples investigated were in pellet and film forms.

We investigated charge transfer over the temperature regime 30-450 K by applying the following methods: scanning electron microscopy to investigate the surfaces of pellet and film samples, Fourier transform infrared spectroscopy and Raman spectroscopy to investigate the effect of annealing on the molecular structure of the polymer and thermal analysis to investigate the loss of substances from the polymer as a result of the annealing process. The conductivity of the material was also analyzed over the entire temperature regime.

The following were observed:

- Conductivity in polyaniline is governed my monomer units.
- The decrease in conductivity with increase annealing temperature is related to moisture loss, loss of dopant ions and polymer degradation.
- The variable range hopping model in three dimensions, satisfactorily describes charge transfer mechanism in polyaniline.
- Conductivity in polyaniline is temperature activated.
- Conductivity varies with position on the sample surface.
- The effect of pellet pressing pressure to conductivity is negligible.
- Current-voltage characteristics for polyaniline exhibit non-ohmic behavior at high current values, (> 0.2 mA for $T < 80$ K), applied between the current probes of a four-point probe measuring instrument.

TABLE OF CONTENTS

Chapter 1

Introduction

The notion that plastics could conduct electricity never came to the attention of scientists until their accidental discovery in 1977. These special plastics called conducting polymers have attracted a lot of attention in the research and scientific community because of their possible and promising applications. The combination of their polymeric nature and electronic conductivity put them in a favorable position which conventional inorganic materials are not in with regard to applications and products. Conducting polymers offer new applications in areas such as molecular electronics, electronic drug delivery, large screen displays and tunable electromagnetic interference shielding to state a few.

Despite their profound application possibilities charge transfer is still not very well understood. In this study we investigate charge transfer properties of conducting polymers in the temperature range 30 – 450 K.

Semiconductor current-voltage characteristics of the material are observed below 300 K. The effect of annealing on the current-voltage properties of the polymer is also studied at temperatures between 300 K and 450 K. Fourier transform infra-red (FTIR) spectroscopy was used in relating conductivity changes to the molecular structure of the polymer. Thermal analysis was also applied in relating conductivity changes to possible loss of substances from the polymer as a result of annealing.

Chapter 2 gives an overview of the properties of the family of conducting polymers.

In the present study, all the experimental work was done on a conducting polymer called polyaniline. Chapter 3 details the properties of polyaniline. Polyaniline was chosen

because of its easy synthesis, low cost of synthesis and stability when compared to other conducting polymers.

A number of factors contribute to the overall measured conductivity of conducting polymers. In chapter 4 charge transfer in conducting polymers is analyzed in terms of the conductivity determining factors.

In chapter 5, methods applied in the characterization of polyaniline are detailed. Chapter 6 gives some of the technological applications of conducting polymers. A full description of experimental techniques used in the present study is given in chapter 7. Chapter 8 gives the experimental results for the charge transfer study between 30 K and 450 K.

In Chapter 9 the discussion to the results obtained is given. Chapter 10 includes a conclusion to this study and suggestions for further reading.

Chapter 2

Overview of Conducting Polymers

The aim of this chapter is to describe conducting polymers (CPs) in a simplified but complete way. CPs are described here based on the approach used for the inorganic semiconductors. It is encouraging to note that this approach is reasonably successful, as evidenced by our results. The study of CPs is "relatively" new, the literature base, although rapidly expanding, is still relatively small. Most of the literature used in this chapter and the proceeding chapters are works of the pioneers and highly acclaimed researchers in this field, notably: distinguished Ohio State University Professor A. J Epstein, A. G. MacDiarmid at Pennsylvania University, J.A Heeger, B. Wessling from Ormecom Pvt. limited, M. Gosh, B. Friend, J. Bredas, S. Sethi, J. Tsukamoto, M. Conwell. R. Menon and many others.

Models from condensed matter (solid-state) physics for the treatment of semiconductors are the closest for arriving at a generalized understanding of conducting polymers, and thus have been adopted in broad measure by workers in the conducting polymer field[1]. The band structure description of CPs was first lucidly presented by J. Bredas *et al* [2] on polypyrrole. Quantum chemistry and the Su-Schireffer-Heeger (SSH) Hamiltonian and its variants have been widely used to study the electronic structure of CPs and for successfully describing the ground state of such systems[2, 3]. For more information on the theoretical study of CPs, the reader is referred to references marked with an "*" at the end of this chapter.

2.1 The background of conducting polymers

The interest in CPs began in 1977, after Heeger/MacDiarmid and the Shirakawa group discovered that polyacteylene exposed to iodine vapors develops very high and well-

characterized conductivities. However, as early as 1862 Letheby[4] reported chemical oxidative polymerization of aniline (a building unit for polyaniline (Pan)). At the beginning of the 20th century, Mecoy and Moore[4] suggested electrical conductivity in organic solids but nobody took cognisance of it for the reason that polymers were believed not able to conduct electricity[4]. Since 1957, studies of electrochemical oxidation of aromatic monomers, now widely used as one method of synthesis of CPs, have been reported under various descriptions such as "electro-organic preparations" and "electro-oxidations". As early as 1968 dall'Ollio[4] described electropolymerization of polypyrrole. From this and the above information, the discovery of CPs in 1977 was in actual fact a rediscovery of CPs[4].

After the discovery of conducting polyacteylene in 1977, the 1979 discovery of electrochemical doping of polyphenylene vinylene (PPV) opened many doors to the study of CPs[5]. Several CPs and their derivatives have been discovered since then. Another important feature of electrochemical processing has been the ability to study the doping process using the voltametry method[6].

The field of CPs is one of the most rapidly growing research fields from both a fundamental as well as a technological point of view, this is evidenced by the involvement of big companies such as Philips (Netherlands), Zipperling (Germany) (through its subsidiary Ormecon), as well as NASA (through its activity in sponsoring research) and a sizeable number of top international universities. Further evidence of how active research in CPs is, is the number of websites and patents currently registered. By 1986 the first polymeric device, a button cell, was produced by Seiko. Unfortunately the device failed to make an appreciable market impact. At present, several commercial conducting polymer (CP) based products are available on the market[7].

Despite the commercialization of CP based products, charge transfer phenomena in CPs is still not well understood. The present commercialization is based on consistence in the electronic characteristics of the material, synthesis conditions and improved properties

such as morphology and crystallinity. In our present study, we attempt to contribute towards the understanding of the charge transfer characteristics of CPs.

2.2 The Conducting Polymers

CPs are plastics made out of small building blocks called monomers just like ordinary plastics. In addition to displaying the well known properties of plastics, CPs can display special properties such as electrical conductivity, electroluminesence, photoconductivity and lazing which ordinary plastics do not. Figure 2.1 shows the monomeric units of some of the well-studied CPs.

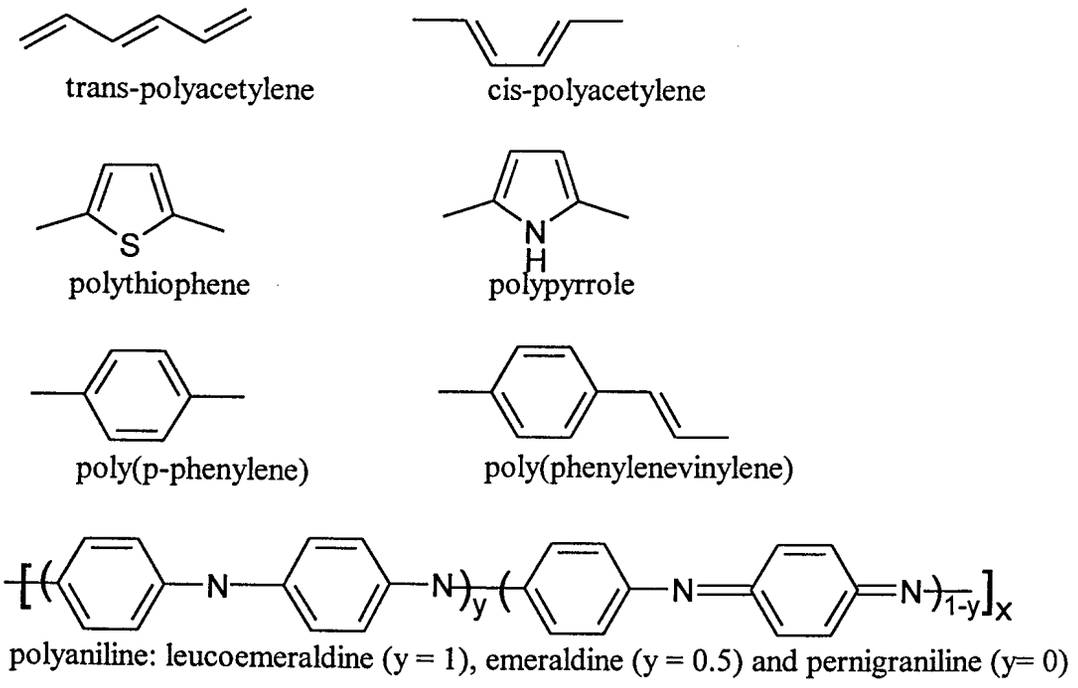

Fig (2.1): The monomers of some of the well studied CPs. Polyaniline is shown in its three possible oxidative states[8].

A common feature of CPs is the alternation of single and double bonds, at least in the backbone of the polymer structure[9]. CPs are characterized by a delocalized π-electron system along the polymer backbone. The delocalized π-electron system, figure 2.2,

confers semiconducting properties to the polymer and gives it the ability to support positive and negative charge carriers with high mobility along the polymer chain[10].

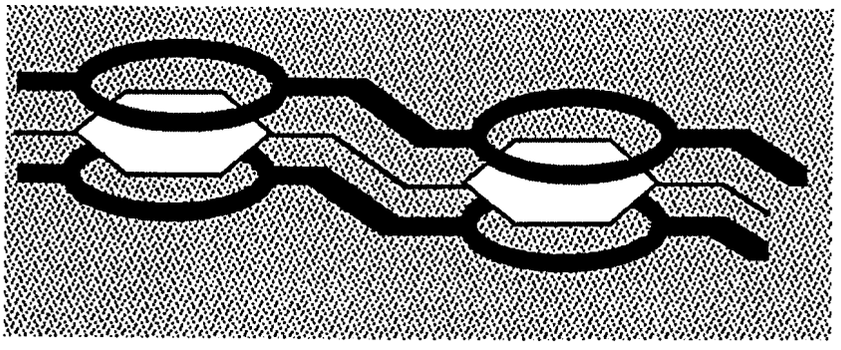

Fig (2.2): Overlap of the p-orbitals results in a delocalized π-electron cloud[10].

2.3 Attractive properties of CPs

i. They have many of the advantages of conventional inorganic semiconductors including the formation of Schottky and ohmic contacts with metals[11, 12].

ii. For application in electronics, the electronic properties are locked into the molecular structure instead of being produced by the fabrication or processing technique. This unique feature ensures a suitable control of the electronic/optical properties of a resulting device by altering/modifying the organic molecular structure before fabricating the actual device.

iii. The degree of conductivity is readily adjusted by controlling the structural order of the material and through the process of doping[13].

iv. CPs are easier to synthesize than inorganic materials, for example, compare epitaxial growth of silicon to the spinning of polymer thin films.

v. CPs display a wide variety of properties, ensuring a vast number of potential applications in a large number of technologies[14].

vi. They offer novel applications such as artificial muscles[4], electrochemical drug-delivery[6], electrochromic windows and displays[15], polymer based rechargeable batterys[16], flexible light emitting diodes[17], polymer based anticorrosion coatings[6,18], and many other applications.

vii. They stand to substitute metals and other materials in applications such as, electromagnetic interference shielding[14, 8], where they have the advantage of lightweight and a tunable electronic shielding efficiency[14].

2.4 Bonding and the semiconductor nature

To gain an understanding of the nature of CPs, we have to shed light on the structure and electrical properties of these materials. The extent of delocalization of π-electrons along the polymer backbone and the extent of interchain delocalization plays a dominant role in the electrical and optical properties of polyconjugated systems[19].

Consider the *s* and *p* orbitals of an atom. The *s* orbitals are spherical and *p* orbitals are dumbbell shaped and are oriented at 90° to each other as depicted in figure 2.3.

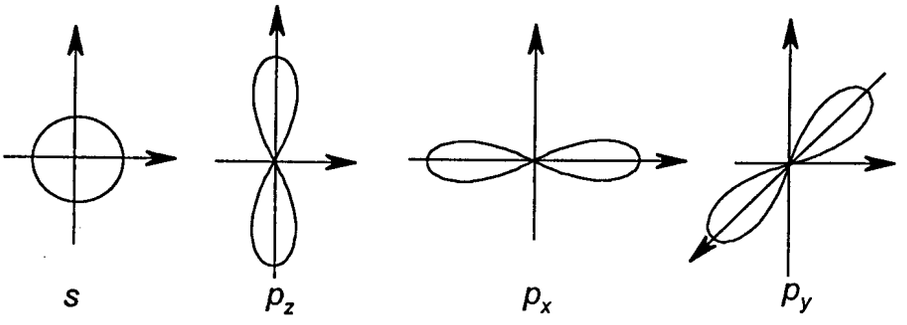

Fig (2.3): Orbital shapes for s and p_z, p_x and p_y orbitals respectively[20].

In a polymer molecule, bonding involves the *p* as well as the *s* orbitals of the atoms. The mixing of these atomic orbitals results in the chemical bonds in polymers. A covalent bond formed from end-to-end overlap of the atomic orbitals give σ bonds, while side-ways overlap of the *p*-orbitals gives π-orbitals. Figure 2.4 depicts the molecular orbitals formed from the overlap of *p* orbitals[20].

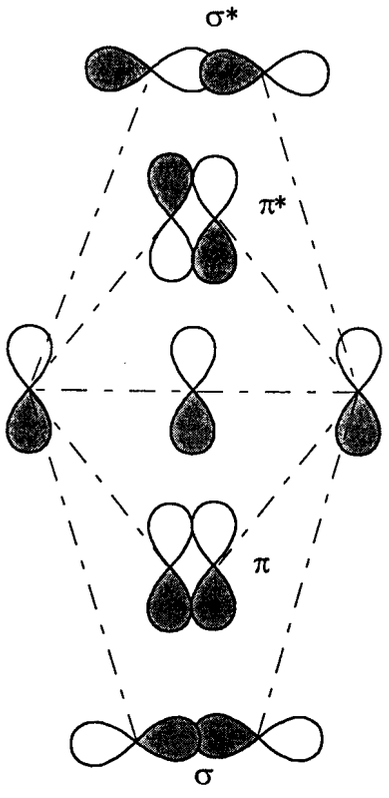

Fig (2.4): The overlap of p-orbitals to give bonding (σ and π) and antibonding (π and σ*) molecular orbitals.*

The atomic orbitals that are not available for bonding will hold lone pairs. The remainder of the orbitals will overlap with each other to form σ bonds (head to head overlap) or π - bond (sideways overlap). π bonds may cover more than two nuclei and are characterized by the increased electron density above and below the imaginary line connecting the two nuclei[20].

When describing bonding in organic substances in terms of the molecular orbital theory, we use the postulate that molecular orbitals are a linear combination of atomic orbitals LCAO[20].

If φ_A and φ_B are the interacting atomic orbitals for atoms A and B respectively, a linear combination of the two atomic orbitals will produce two molecular orbitals φ_{MOI} and φ_{MOII}:

$$\varphi_{MOI} = a\varphi_A + b\varphi_B$$

$$\varphi_{MOII} = c\varphi_A - d\varphi_B$$

In terms of electron density, *MOI* gives a high concentration of electron charge between nuclei and is called the bonding (π) molecular orbital. *MOII* gives a lesser concentration and is called the anti-bonding (π^*) molecular orbital[20], as illustrated in figures (2.4 and 2.5) for the case of diatomic molecules. As the atoms are brought together, the *s* orbitals can overlap, forming σ_s and σ_s^* molecular orbitals; the p_x orbitals also overlap, forming another set of σ molecular orbitals of different energy, σ p_x and σ p_x^*. The p_y and p_z orbitals, overlap side to side and form a different set of molecular orbitals known as the π p_y/π p_z and π p_y^*/π p_z^* respectively (figure 2.4). The energies of the molecular orbitals and their relation to the atomic orbitals from which they came are shown in figure 2.5. The bonding molecular orbitals have lower energies than the atomic orbitals p_y and p_z from which they came. Note that the atomic orbitals p_y and p_z have the same energies[20].

The energy order of molecular orbitals is as follows: σ-type orbitals (the lowest in energy), π-type orbitals (non-bonding type of orbitals such as lone pairs), π^*-type orbitals and σ^*-type orbitals being the highest in energy. Each molecular orbital has a characteristic energy. Electrons occupy these orbitals according to the Pauli exclusion principle; electrons fill the lowest energy levels first. Orbitals of the same energy will be occupied by one electron each before a second electron is added to any one of the equal-energy orbitals[20].

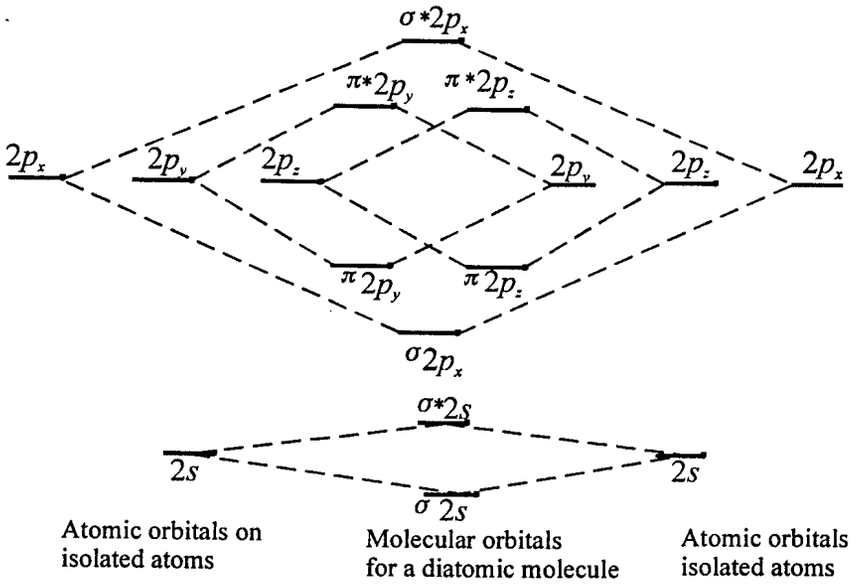

Fig (2.5): Atomic and molecular energy levels in a diatomic molecule, illustrating the concept of, σ/σ and π/π*-orbitals*[20].

The overlap of molecular electronic states produces bands. The overlap of the extended π-bands or lone pairs (non-bonding electrons) becomes the valence band called HOMO (highest occupied molecular orbital) and the overlap of the π*-bands becomes the conduction band LUMO (lowest unoccupied molecular orbital); if there is no π system empty σ* orbitals form the LUMO band. The density of states – that is, the number of energy levels per eV between the top of the π orbitals (valence band) and the bottom of the π anti-bonding (π*) orbitals (conduction band) – is zero within the bandgap (E_g). Hence when electrons are removed from the pristine (undoped) CP, they will be removed in a significant amount only from the top of the valence band. Figure 2.6 illustrates the density of states in a CP in terms of π and π* molecular orbitals.

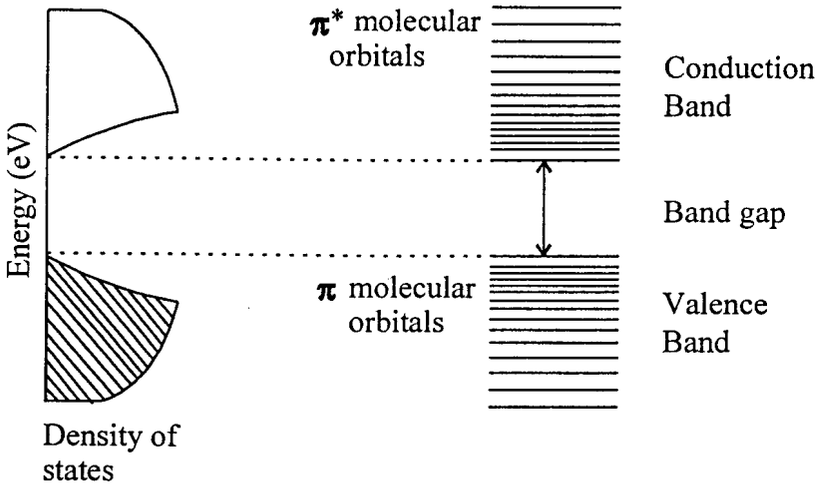

Figure (2.6): The left part of the diagram is the conventional density of states diagram for CP. The right part of the diagram depicts this in terms of π and π molecular orbitals.*

2.5 Conductivity classification

The electrical conductivity of CPs varies widely depending on a number of factors such as synthesis conditions, dopant used and the doping level. Based on these factors, CPs can be classified into the following groups: conductors (metals), semiconductors and insulators. Figure 2.7, depicts typical bandgaps of the 3 classes of materials in terms of LUMO and HOMO bands[21].

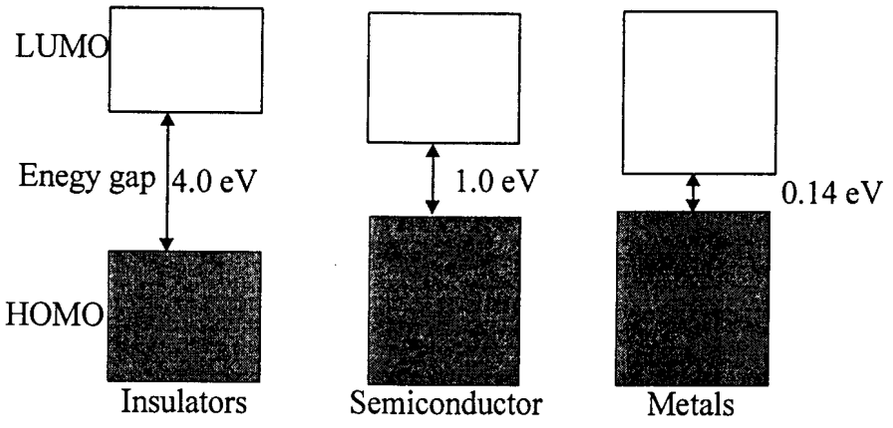

Fig (2.7): The three classes of conductivity (insulators, semiconductors and metals) are given in terms of typical energy bandgaps[21].

The range of conductivities of the different classes of materials is shown in Figure 2.8, and from this it can be readily appreciated that, in order to render a conventional polymer conductive, its electrical conductivity should be increased by several orders of magnitude[22]. Since the conductivity of CPs can be adjusted through the process of doping, attaining different conductivity levels widens the scope of applications. Thus a single CP can have insulating, semiconducting and metallic conductivities, depending on the application for which the CP based device is designed to perform, polyacetylene[5], as an example can have a conductivity range from 10^{-6} to almost 10^{6} S/cm. Such applications include gas sensors, humidity sensors, temperature controllers and adjustable electromagnetic interference shielding, to state a few. The principle of operation is based on the change in conductivity as a function of the change in conditions being measured.

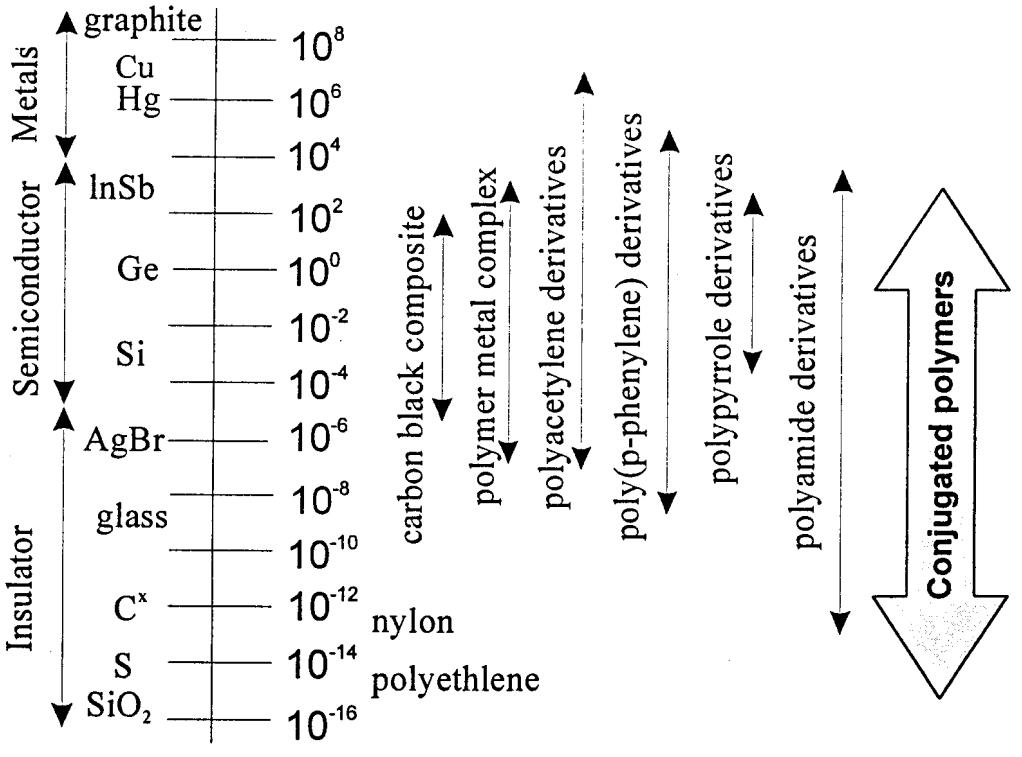

Fig (2.8): Conductivities (S/cm) of various elements, compounds and polymers[22].

2.6 Improvements in polymer conductivity

The attainable conductivity of CPs increased steadily up until about 1992, through improvement in the synthesis and doping techniques as shown in figure 2.9. In the early 1980s the observed conductivity range for polyacetylene was $10^2 - 10^3$ S/cm, whereas since 1990 samples of polyacetylene with conductivities of approximately 10^5 S/cm are routinely produced[23]. Highly conducting CPs (e.g. 10^5 S/cm for polyacetylene) are found to be unstable and therefore not suitable for device fabrication. As a result, highly conducting CPs are mainly used for charge transfer studies in the metallic region. Hence, not much research is centered at attaining extremely high conductivity

Since 1992, the conductivity of iodine doped polyacetylene has not improved beyond that of copper (slight improvements but not of much significance. This might have been achieved through varying conductivity determining variables such as stretching of the polymer and humidity).

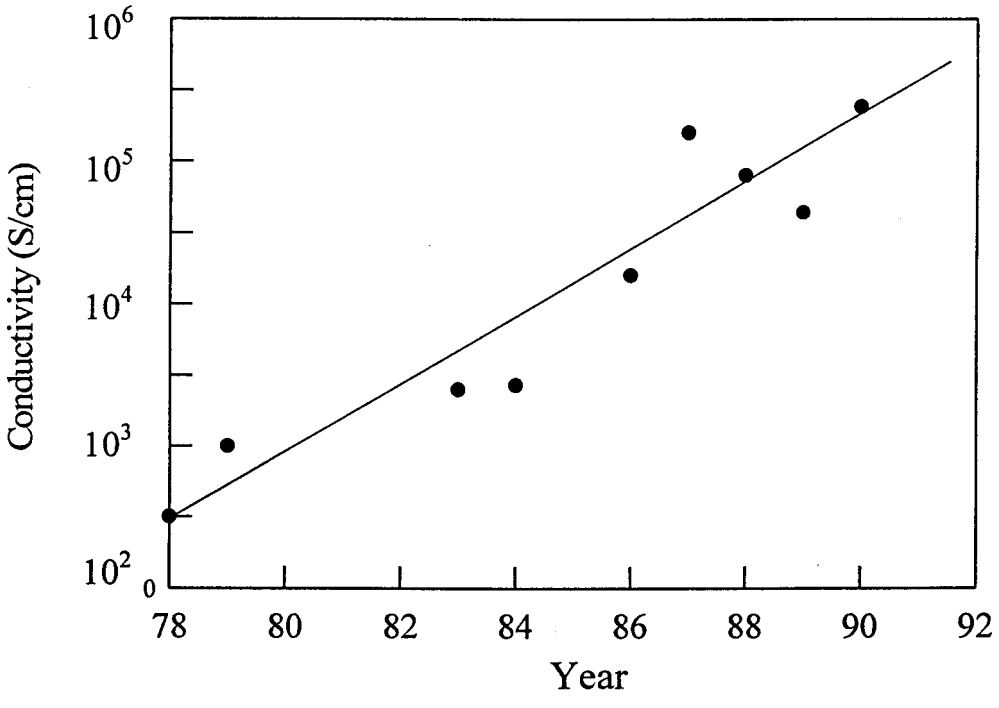

Fig (2.9): Advances in the conductivity of doped polyacetylene[5].

An important contributing factor to the conductivity of CPs is improvements in the polymer morphology. A number of factors, such as molecular weight, plasticizer used, molecular weight distribution and crystallinity, have an influence on the morphology of the polymer and thus conductivity.

2.7 Doping and dopants

Pristine (undoped) CPs can be transformed from their insulating state to either a semiconducting or metallic state through the process of doping. Because of the semiconducting band structure of CPs electron removal/addition from the valence to the conduction band is possible leading to most of the properties that are of interest in CPs. The process of doping both in inorganic and organic materials can impart conductive properties to the material. However, as shall be illustrated, doping is in effect proper oxidation and reduction, in a chemical and electronic sense and not doping/dedoping in the inorganic semiconductor sense[21].

The doping process leads to the presence of delocalized charges on CPs. These charges lead also to the relaxation of the geometry of the polymer to a more energetically favored conformation. Oxidation (anionic doping/*p-type*) generates a positively charged CP and an associated anion, while reduction (cationic/*n-type*) generates a negatively charged CP and an associated cation. These processes are illustrated below in equations 2.1 and 2.2, where *M* and *A* are any cation and anion, respectively and P represents a polymer[21]:

$$P + MClO_4 \longrightarrow P^+ClO_4^- + M^+ \quad \text{(oxidation)} \qquad (2.1)$$

$$P + NaA \longrightarrow Na^+P^- + A^- \quad \text{(reduction)} \qquad (2.2)$$

2.7.1 Dopants

Dopants are chemical oxidants or reductants incorporated into the CP by means of chemical, electrochemical, radiation and or at the time of synthesis[21]. Table 2.1 depicts some of the dopants used in chemical and electrochemical doping. The dopant is positioned on the chain so as to neutralize the charge formed from the oxidation or reduction doping reactions.

Table 2.1: Typical dopants for CPs[21]

Dopant	***Structure/formula***
Anionic (p-type)	Cl^-
Chloride	ClO_4^-
Perchlorate	BF_4^-
tetrachloroborate	$CH_3\text{-}C_6H_5\text{-}SO_3^-$
Tos, p-toluene sulfonate	$[\text{-}CH_2CH(C_6H_4SO_3)^-]_n^n$
Cationic (n-type)	
proton	H_3^+O
sodium	Na_+

The proportion of dopant ions incorporated into the polymer per monomer unit gives a measure of the doping level. Increased doping can lead to increased conduction, via the creation of more mobile charges, and the maximum doping levels achievable vary for different CPs and different dopants. Some representative doping maxima are listed in table 2.2.

Table 2.2: Typical maximum doping level

Polymer	*Maximum doping level*
Polyaniline	42% (Cl^-)
Polypyrrole	33% (ClO_4^-)
Poly(thiophene)	44% (Li^+)
Poly(p-phenylene)	30% (ClO_4^-)

2.7.2 Doping techniques

Among the most common doping techniques used are ion implantation, photochemical doping, heat treatment, solution doping and dry doping. In this study, we made use of electrochemical doping and chemical doping. We shall describe one of the two doping techniques used in the present work, namely electrochemical doping[21].

The partial removal of electrons (oxidation) from the polymer π system is referred as p-doping , and n-doping refers to the addition of electrons (reduction) of the polymer π^* system. In electrochemical doping, if a positive potential is applied to a CP immobilized on an inert anode electrode, the dopant anion moves in from the solution into the CP towards delocalized charge sites on the CP, and anionic (*p-type*) doping occurs. Oxidation produces a polycationic chain, requiring the presence of anions from the oxidizing medium for charge compensation[21] (figure 2.10). The counter ion is classified as dopant. Both *p* type and *n*-type dopants are possible for most CPs (see also equations 2.1 and 2.2).

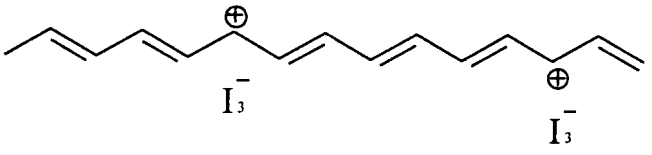

Fig (2.10): Negative ions are brought into the chain to neutralize a positive charge formed from the oxidant doping process. Iodine (I_2) will extract an electron under formation of an I_3^- ion in polyacetylene. See also figure 2.11.

The doping/dedoping reactions and the position of dopant anions (ClO_4^-) on the Pan chain are illustrated in figure 2.11.

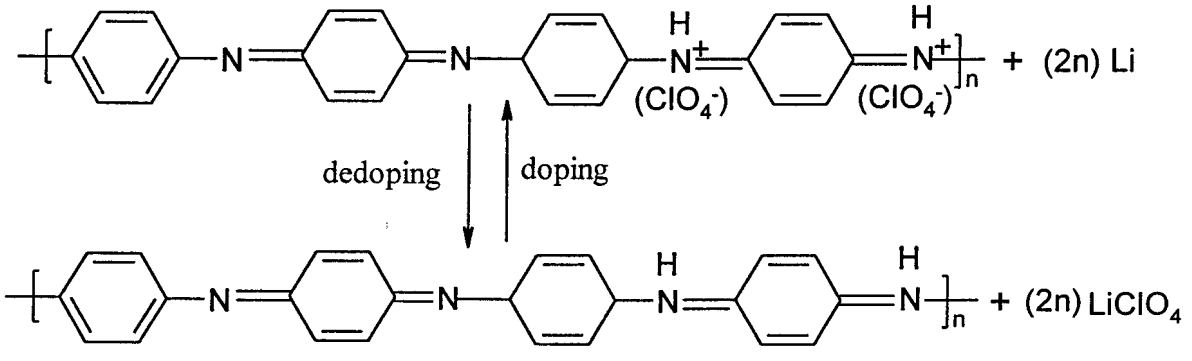

Fig (2.11): The doping and dedoping reactions of Pan[8].

2. 8 Conducting polymer ionization

Conductivity in intrinsic CPs is enhanced partly through the process of doping. Because of the polymeric nature of these organic systems, the polymer is susceptible to structural distortions. The introduction of charge during the doping process leads to a structural distortion of the polymeric structure in the region of the charge, giving an energetically favorable conformation[21]. These structural distortions are intrinsic to the development of states called polarons, bipolarons and solitons. The effects of this structural relaxation can best be visualized by first considering ionization of an organic molecule according to the Franck-Condon treatment, as depicted in Figure 2.12.

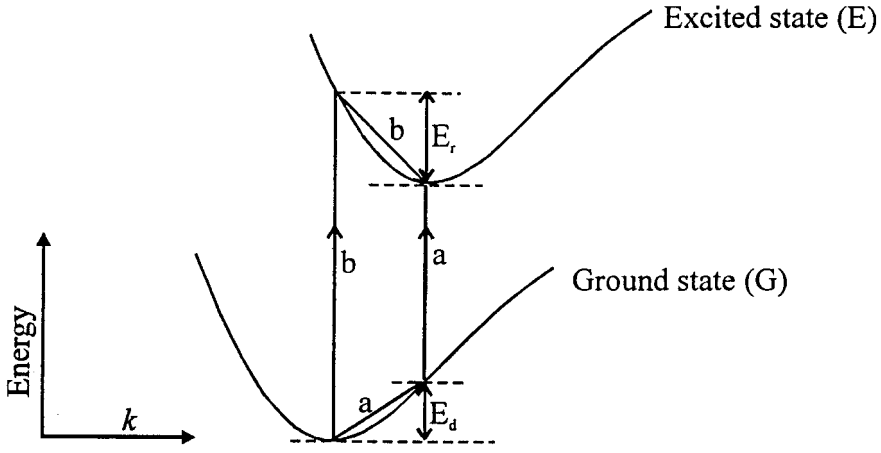

Fig (2.12): Ionization of an organic molecule according to the standard Franck-Condon treatment[21].

Ionization can be thought to occur first through the excitation of the ground state (G) to the excited state (E). According to convention, the excited state, *E*, has a different geometry compared to that of the ground state *G*. Two possible routes (ionization processes) are:

i. An initial distortion of the ground state geometry to that of the excited state, followed by the vertical excitation of the electron *(Path a)* or
ii. A standard vertical Franck-Condon excitation *(Path b)* within the geometry of the ground state followed by relaxation to the equilibrium excited state geometry[21].

If the excitation energy E_r is greater than the distortion energy, E_d, then path *b* is preferred for ionization.

2.9 The Fermi level

The Fermi level, E_F, in CPs is an equilibrium energy level corresponding to the chemical potential of the system and lies between the valence and conduction bands (π and π^* orbital bands respectively). Unlike in inorganic materials, an increase in

conduction as a result of doping corresponds to the upward and downward shift of the HOMO and LUMO bands, respectively, decreasing the bandgap in the process[21], figure 2.13.

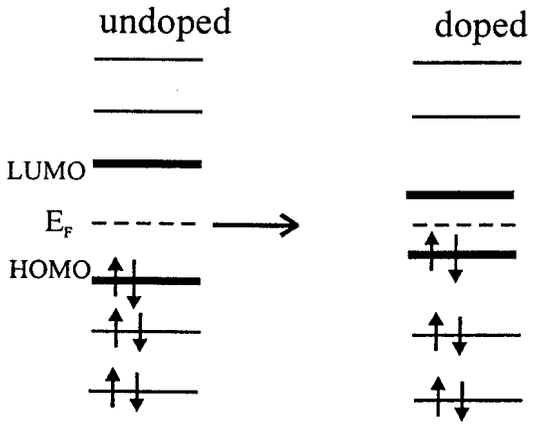

Fig (2.13): The effect of the doping process on the position of the HOMO, LUMO and the Fermi level (E_F)[21].

2. 10 Band structure treatment

The electronic conductivity of CPs is explained using the semiconductor bandgap model to describe the energy levels available to a material's charge carriers. An understanding of the band structure of CPs is important for one to be able to appreciate why CPs are described by the same treatment as inorganic semiconductors.

The ground state of a CP is that of an insulator, with a forbidden energy gap between filled and empty energy levels[14]. The energy gap arises from the pattern of single (long) and double (short) bonds with an additional contribution due to electron – electron Coulomb repulsion[14]. An overlap of the HOMO and LUMO bands results in metallic conduction[21, 2, 23]. The bandgap in doped-CP systems varies from 1eV to 4eV[2], coupled with other measured parameters. In general, doped conjugate polymers behave like inorganic semiconductors. Unlike inorganic semiconductors, the band structure of CPs has flexibility and is susceptible to structural distortions[21].

The doping and dedoping effects in CPs can be analyzed fully in terms of bandgaps, such as in inorganic semiconductors. Bredas *et al.*[1, 2] have extensively studied the spectral evolution of polypyrrole as a function of doping level. An elementary experiment based on band theory involves initially holding the polymer in its fully reduced state at a potential of 0.0 V and thus its electronic absorption from 350 nm to 2500 nm. Subsequently, the potential is stepped anodically to *p*-dope the polymer with a spectrum recorded at each potential step.

The results obtained indicate that there is one strong absorbency due to π-π* transitions of the neutral polymer. These results are satisfactorily explained with the help of the energy band diagram illustrated in figure 2.14.

From figure 2.14, there are four optical transitions possible, in decreasing order of energy: 1) From the valence band (VB) to the conduction band (π-π* transition); 2) from the valence band to the upper polaron level; 3) from the lower polaron level to the upper polaron level; 4) and from the valence band to the lower polaron level. In the case of bipolarons the transition between polaron levels is eliminated.

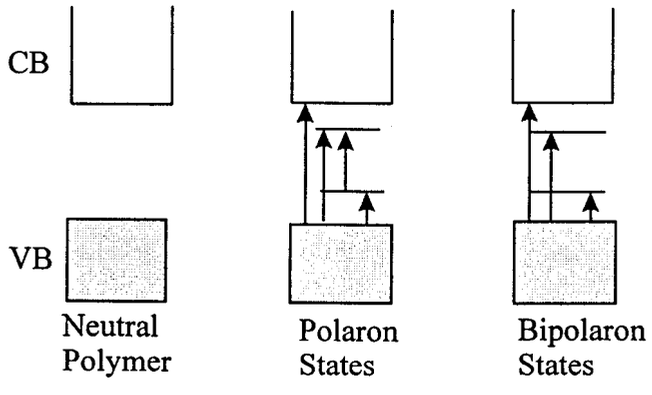

Fig (2.14): Band diagram for the optoelectrochemical spectra of a CP[21].

2.11 Structural distortions: Polarons, bipolarons and solitons

The introduction of dopant ions into the polymer, as mentioned in the previous sections, results in the creation of two localized midgap states within the bandgap. Oxidation and/or reduction processes result in the creation of charged carriers called solitons, polarons and/or bipolarons[21]. The effect of doping and doping level on the creation of such defects and their position in the bandgap are detailed below.

2.11.1 The polaron band theory

When an electron is added to a perfect chain, it causes the chain to deform, creating a characteristic pattern of bond deformation. Along with the chain deformation, there is a change in the energy level structure. An energy level is pulled out of the valence band into the gap between the valence and conduction band edges and another level is pulled out of the conduction band to form two polaron band levels or states (fig. 2.14)[9], the lower polaron level is occupied by two electrons of opposite spins as illustrated in figure 2.15a.

2.11.2 Polaron formation

As explained above localized distortion gives rise to localized electronic states in the bandgap region. Removal of a single electron from this localized state through doping results in the formation of a positive polaron, while the addition of an electron results in a negative polaron (figure 2.15 (b) and (c) respectively). The polaron as shown is a radical cation, which is associated with a structural distortion in the CP. Since we have a single charge, the lower bipolaron level is half-occupied, as shown and the species would possess spin. The half-occupied, electronic level (polaron) remains localized in the gap[21].

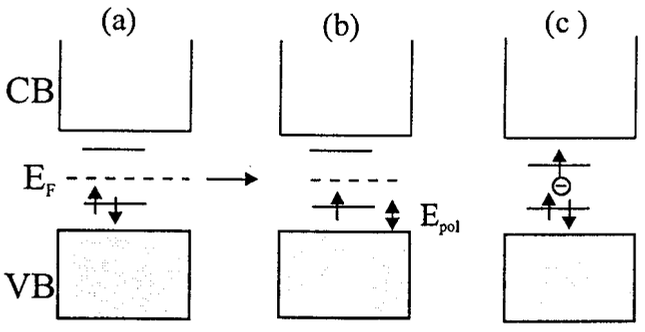

Fig (2.15): Formation of a polaron; (a) localized electronic states, (b) positive polaron formed from oxidative doping and (c) negative polaron formed from reductive doping[21].

Another approach towards the formation of a polaron will be to consider the removal of an electron from the CP structure resulting in a localized distortion in the structure, which then serves to stabilize the charge associated with the electron removal. The distortions of the local structure by a charge in an extended lattice arises from electron-phonon coupling. The polaron is said to possess binding energy equal to E_{pol} - E_{dis}, where E_{dis} is the distortion energy and E_{pol} is the difference in energy between the polaron level and the valence band (VB)[21].

2.11.3 Bipolaron formation

The removal of a second electron from the polaron results in the formation of a bipolaron, figure 2.16. This bipolaron is stable despite Coulomb repulsion of the two similar charges. The stability of the bipolaron is thought to arise from coupling of the two charges to the lattice via lattice vibrations and neutralization of the repulsion between the charges by the dopant ions. In figure 2.16, E_{bip} is the bipolaron binding energy.
Oxidative and reductive doping gives rise to positively and negatively charged bipolarons respectively, figure 2.16.

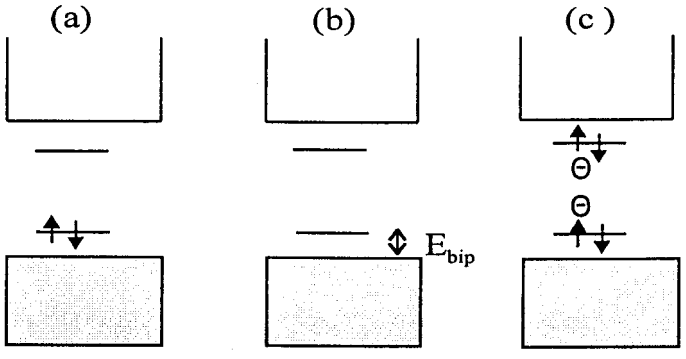

Fig (2.16): Formation of bipolaron: (a) localized electronic states, (b) positive bipolaron formed from oxidative doping of a polaron and (c) negative polaron formed from reductive doping of a negative polaron[21].

Bipolarons are either empty (p-doped) or full (n-doped) and thus they are spinless. In the formation of the polaron/bipolaron, the conduction band remains full and the valence band empty, therefore the high conductivity comes from diffusive motion of these bipolarons. Doped CPs exhibit strong anisotropy of conductivity along the polymer chains through the migration of charged defects coupled to a local deformation of the π-conjugated structure (polaron/bipolaron)[9].

2.11.4 Soliton

A soliton is an excitation that occurs only in degenerate polymers (polymers with which the exchange of single and double bonds does not result in a higher energy state). To define a soliton, lets consider trans-polyacetylene (t-PA) schematically shown in figure 2.17. With double bonds sloping to the right, as shown, take this as "A" and the one with double bonds sloping to the left as " B". A type "A" region can occur next to a type "B" region on the same t-PA chain[4]. There exists a region between them upon which a transition takes place, (see also figure 2.10).

Fig (2.17): Right and left sloping double bonds for t-PA[24].

The domain wall between different directions of the double bond, i.e. between "A" and "B", is called the soliton. A bound electron characterizes it. This bound electron, which is neither bonding nor anti-bonding, occupies a level at the center of the energy gap. Therefore a new energy level is created with a reduced energy gap. Electrons can be promoted from the valence band to the conduction band through the formation of solitons. When there is an odd number of carbon atoms in the CP chain, there remains an unpaired π-electron, and a radical, neutral soliton is said to result[21]. The schematic band structure for neutral, positive and negative solitons respectively is shown in figure 2.18.

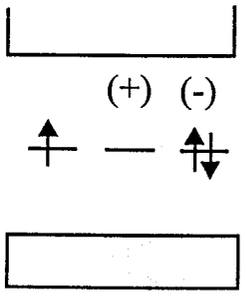

Fig (2.18): Neutrally, positively and negatively charged solitons[21].

The soliton level can accommodate zero, one and/or two electrons and thus it may also be positively or negatively charged, giving the unusual property of separating spin and charge, with neutral solitons possessing spin; but no charge. Both positively and negatively charged solitons possess charge but no spin. For doped CPs, charge is located in the mid-gap states, since these provide the HOMO for the charge removal and the LUMO for charge injection[21]. However, because various kinds of defects in polymers, such as crosslinks between chains and bends, and kinks, are common, conduction should

be to a larger extent a combination of the three modes described above in most of the cases.

2.11.5 Polarons, bipolarons and solitons in a polymer chain

Polarons, bipolarons and solitons are confined to, and delocalized over, about four to six monomer units. A counter-ion (dopant ion) is located in the vicinity of the entity for charge neutrality[21], as indicated previously for the case of Pan (figure 2.10). The appearance of these defects in the polymer chain is shown in figure 2.19.

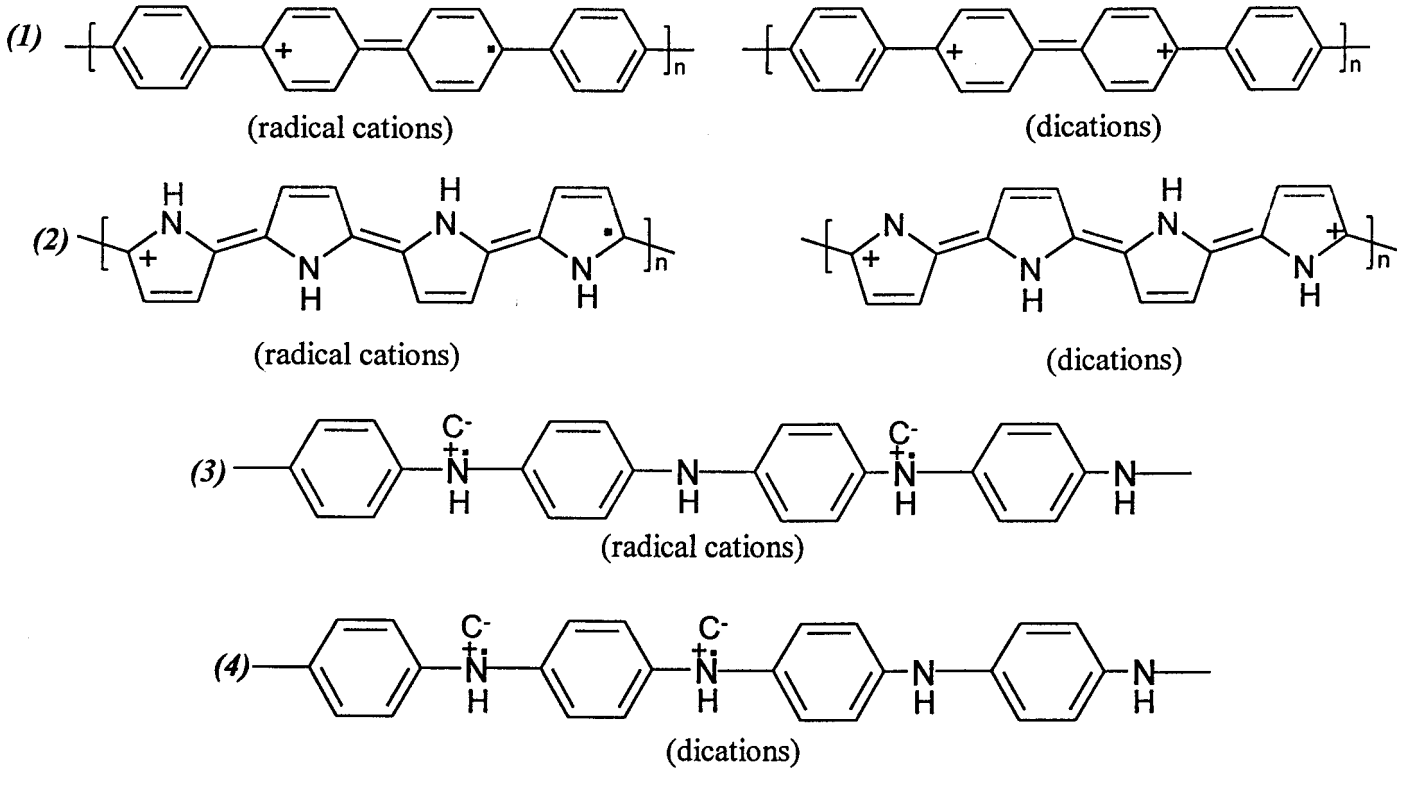

Fig (2.19): Polarons (radical cations) and bipolarons (dications) for (1) PPV[21], (2) polypyrrole[21] and Pan[8] (3) and (4) respectively.

2.12 Band structure evolution

Figure 2.20 depicts the evolution of band structures, (polypyrrole taken as an example), based on semi-empirical theoretical and experimental studies on CPs, first presented by Bredas *et al*[1,2]. Removal of an electron from the polymer chain produces a polaron, with two-polaron levels at about 0.5eV from the conduction and valence band edges, according to the approximate calculations of J. Bredas *et al*[21].

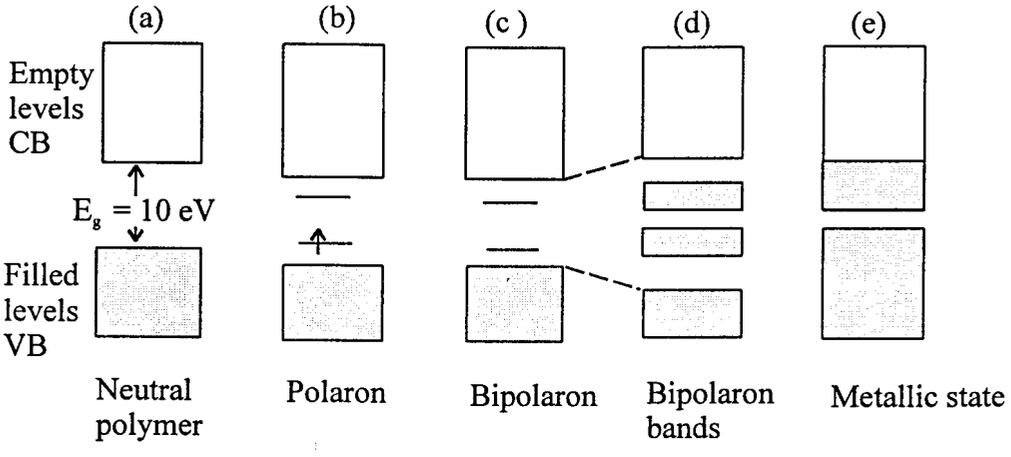

Fig (2.20): Hypothetical evolution of band structure to a metallic state for CPs[21].

The polaron has a band structure like that depicted in figure 2.20, with the single positive charge delocalized over about 4 to 6 monomer units. Removal of a second electron produces a bipolaron[21]. On increased doping (a maximum of about 35 % for polypyrrole), the individual bipolaron states of figure 2.20 (c) coalesce into bipolaron bands (figure 2.20 (d)). Bipolaron bands arise from electronic states taken from the valence and conduction band edges, and the gap between these bands consequently increases.

Assuming a hypothetical doping level of 100 % (one dopant ion per monomer unit), the two bipolaron bands would gradually broaden enough to coalesce into the valence and conduction bands (figure 2.20(e)), producing metal-like conduction[21]. At these high dopant concentrations, the bipolarons, which are spinless, can become mobile under the application of an electrical field, thus giving rise to high conductivity.

The width of the polaronic levels are affected by the influence of chains of different length, disorder, interchain coupling, electron-electron interactions, and interactions between chains and dopants[1].

In summary, this chapter aims at giving a comprehensive introduction to the study of conducting polymers. A description of the molecular structure concomitant with conductivity in this special type of polymers is detailed. Following is the description of charge carriers and the process of conduction enhancement. CPs have the same band gap structure as other inorganic semiconductors and their conductivity can also be improved through the process of doping.

References

1. J. L. Bredas, J. C. Scott, Phys. Rev. **B 30**, 1023 (1984).
2. J. L. Bredas, D. Beljonne, Z. Shuai, Conjugated Oligomers and Dendrimers, From PA to DNA, (Ed. J. L. Bredas), De Boek Universite: Paris (1998).
3. U. Sum, H. Buttner, Phys. Rev. **B 40**, 6166 (1998).
4. C. Trivedi, Handbook of Organic Conductive Molecules and Polymers **2** (Ed. H. S Nalwa), John Wiley and sons: New York, 506 (1997).
5. J. Tsukamoto, Adv. in Phys. **41**, 509 (1992).
6. T. F. Otero, Handbook of Organic Conductive Molecules and Polymers **4** (Ed. H. S Nalwa), John Wiley and sons: New York (1997).
7. K. Gurunathan, Materials Chemistry and Physics **61**, 173 (1999).
8. A. J. Epstein, A. G. MacDiamird, Science and Application of conducting polymers, (Ed. W. R. Salaneck), Bristol: England (1991).
9. E. Conwell, Handbook of Organic Conductive Molecules and Polymers **4** (Ed. H. S Nalwa), John Wiley and sons: New York (1997).
10. Source: Internet: WWW.lumex.com/tech_notes/polymer.htm
11. M. Rusu, G. Rusu, Appl. Surf. Sc. **126**, 245 (1998).
12. A. G. MacDiarmid, Synth. Met. **84**, 27 (1997).
13. P. Yam, Trends in Material Sc. (Scientific American), 75, July (1995).
14. A. J. Epstein, MRS Bulletin, **22**, 16 (1997).
15. E. Kim, K. Lee, S. B. Rhee, J. Electrochem. Soc. **144**, 227 (1997).
16. C. Arbizzan, B. Scrosati, Handbook of Organic Conductive Molecules and Polymers **4**, (Ed. H. S Nalwa), John Wiley and sons: New York (1997).
17. Y. Yang, MRS Bulletin **22**, 31 (1997).
18. B. Wessling: source: www.zipperling.de/Research/abstract/corros
19. R. Menon, Handbook of Organic Conductive Molecules and Polymers **4,** (Ed. H. S Nalwa), John Wiley and sons: New York (1997).
20. Chemistry a study of matter, (Ed. A. B. Garret), Xerox corporation: Toronto (1972).
21. Conducting polymers, Fundamentals and Application, (Ed. P. Chandrasekhar), Kluwer academic publishers: Boston (1999).

22. S. R. Sethi, M. T. Goosey, Elec. Prop. of polymers, 1, Ed. C. C. Ku (1993).

23. D. O. Cowain, F. M. Wlygul, C & EN, 28, July, (1986).

1*. M.E. Jozefowcz, R. Laversanne, H. H. Javadi, J. A Epstein, A. G. MacDiarmid, Phys. Rev. **B 39**, 12958 (1989).

2*. U. Sum, H. Buttner, Phys. Rev. **B 40**, 6166 (1988).

3*. R. P. McCall, J. M. Ginder, A. G. MacDiarmid, Phys. Rev. **B 41**, 5202 (1990).

3*. J. M. Ginder, J. A Epstein, Phys. Rev. **B 41**, 10674 (1990).

4*. J. L. Bredas, J. C. Scott, Phys. Rev. **B 30**, 1023 (1984).

Chapter 3

The structure and properties of different forms of Pan

In the group of materials known as CPs, polyaniline (Pan) an oxidative polymeric product of an aniline under acidic conditions is one of the more studied materials due to its:

(1) Easy synthesis[1]
(2) Environmental stability[1]
(3) Simple non-redox doping by protonic acids[1]
(4) Diversified applications[1,2]
(5) Can assume diverse incarnations, including thin films and patterned surfaces[2]

Pan is a phenylene-based polymer with a chemically flexible –NH– group in a polymer chain flanked on either side by a phenylene ring[1]. The –NH– group is important for the physico-chemical properties of Pan such as the protonation and deprotonation (non-redox doping). This non-redox doping by protonic acids is an important aspect where a number of electrons in a polymer chain remain unchanged during the doping process. The protonated form is electrically conducting, and the magnitude of increase in its conductivity is a function of the level of protonation as well as the functionalities present in the dopant[1].

Pan and its related CPs such as poly (p-phenylene oxide) PPO and poly (p-phenylene sulfide) PPS have been shown to contain large equilibrium phenyl ring torsional displacements (upwards of ± 30 °C or more) out of the plane defined by the ring bridging atoms (amine/imine nitrogens in the case of Pan and sulfur for PPS)[2]. The chemical and structural flexibility surrounding the amine/imine nitrogen linkages in Pan creates enormous diversity: the geometry, electronic structure, and dynamics of the defect states are quite different from those of the carbon-backbone-conjugated polymers. There is an

overall reduction in the effective intrachain conjugation length and a marked decrease in the tendency to form crystalline phases. This also implies that there are implications to the electronic transport properties of the polymer[2]. Despite the experimental evidence for the long-lived massively charged defects in Pan, as well as the demonstration of the importance of ring flipping as a relaxation mechanism, the role of ring conformational changes in the self-trapping of charged defect states has received little attention[2]. Ring flipping shall be illustrated together with the conventional representation of the molecular structure of polymers in the following sections.

In order to form a reasonable understanding of CPs, knowledge of the structure and terminology used is necessary.

3.1 The different forms of Pan

Pan can be transformed through four different oxidation states, each oxidation state having different electronic and optical properties. The different forms of Pan are determined[4] by the fraction of imine (–NH=) nitrogen atoms per 4-ring repeat unit, which is labeled *1-y*. Where *1-y* is equal to 0.5, 0 and 1 for half-oxidized (emeraldine), fully reduced (leucoemeraldine) and fully oxidized (pernigraniline) forms, respectively. The chemical formula which most broadly describes this polymer is presented in figure 3.1.

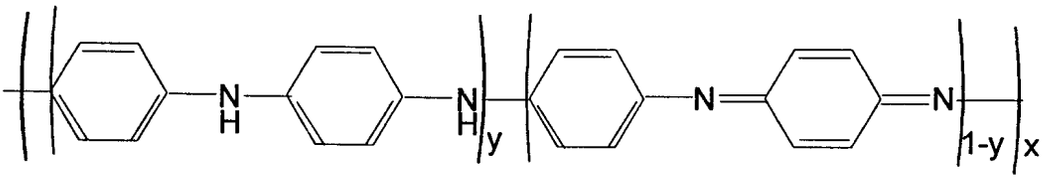

Fig (3.1): The base form of Pan: leucoemeraldine (y = 1), emeraldine (y = 0.5), and pernigraniline (y = 0)[5].

The emeraldine base (EB) insulating form of Pan is the most important form, because it can be doped to high conductivity and it is easily processible in this state (that is through dissolving it in appropriate solvents). The comparison of Pan to other CPs is based on the

EB form of Pan. The EB form differs substantially from other CPs in several important aspects:

1. The C_6 benzoid rings of Pan can rotate or flip, significantly altering the nature of electron – phonon interactions[6].
2. Emeraldine can be converted from an insulating to a metallic state if protons are added to the *–N=* sites while the number of electrons on the chain is held constant[6].
3. Pan comprises an alternating ring-heteroatom backbone structure. Both carbon rings and nitrogen atoms are within the conjugation path, forming a generalized "*A – B*" polymer[4,6].
4. It does not display charge conjugation symmetry in contrast with the most studied polymers polyacetylene and polythiophene[6].
5. The polymerization mechanism affects the properties in as much as it influences the microstructure, the molecular weight and the molecular weight distribution[4].

A summary of the properties of the different forms of Pan is shown in table 3.1.

Table 3.1: Forms of Pan and their electrical properties

Forms	***Oxidation state***	***Electrical properties***
Emeraldine base (EB)	Half-oxidized	Can be doped to high conductivity
Emeraldine salt (ES)	Half-reduced	Conducting
Leucoemeraldine base	Fully reduced	Insulating
Pernigraniline base	Fully oxidized	Insulating

Pan has excellent electrochemical reversibility and stability in aqueous media. The color of a Pan film in aqueous solutions can change very quickly with applied potential. In a solution containing $ZnCl_2$ and NH_4Cl, at pH>4 in a phosphate buffer, the color of Pan film changes from reddish purple to blue–*fully reduced*, green–*half oxidized*, and transparent yellow- *fully oxidized states* when the potential is swept from 0.8 to – 0.10 V[7]. A detailed description of each of these forms is presented in the coming sections.

3.1.1 Emeraldine base (EB)

This is a half-oxidized insulating Pan with a large extrinsic gap (E_g ~3.6eV) and *1-y = 0.5*[4](fig. 3.2). EB can be converted from an insulating to a metallic state if protons are added to the –NH= sites while the number of electrons in the chain are held constant[6]. Because of this property, EB is the most important form of Pan.

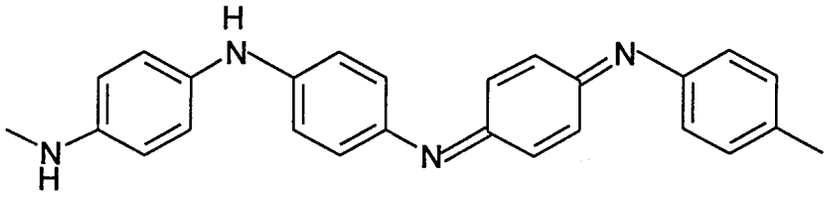

Fig (3.2): Emeraldine base structure.

The degree of crystallinity is typically low and, even in the best samples, never exceeds 50 %. In the approximate structure of Jozefowicz *et al.*[8], the deviation from planarity by the phenyl rings is sequentially alternated between $\pm 30^0$ as one moves along the backbone as illustrated in figure 3.3.

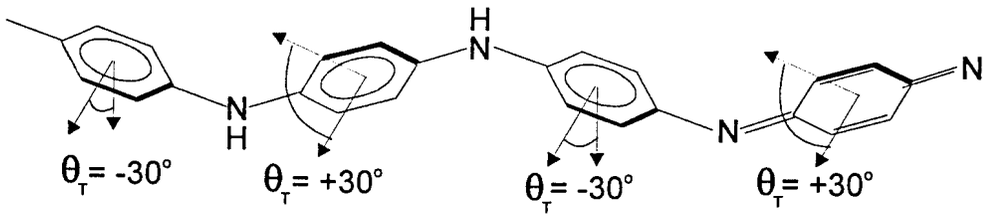

Fig (3.3): Schematic diagram of a four-monomer repeat in Pan EB showing the deviation from planarity of the four rings, three benzoid and one quinoid for crystalline EB[8].

3.1.2 Leucoemeraldine base (LEB)

In the LEB form illustrated in figure 3.4, Pan exists in the fully reduced state, *1-y = 0.* LEB is an insulator whose large extrinsic energy gap (E_g ~ 3.6 eV)[9] originates predominantly from the difference in energy between the bonding and anti-bonding molecular orbitals of benzene involved in the overlap of molecular orbitals of neighbouring phenyl rings and nitrogen atoms.

The presence of amine (-NH-) groups allows chemical flexibility so that other electronic states of the polymer can be obtained by removal of protons (or hydrogen atoms), as well as electrons, from the polymer[4].

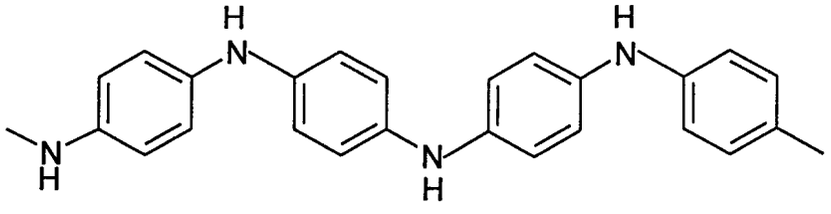

Fig (3.4): Leucoemeraldine base structure[4].

The ground state configuration of LEB consists of adjacent phenyl rings twisted out of the nitrogen-nitrogen plane by equal but opposite angles, $\theta \sim \pm 30^0$ figure 3.5 [9,10]. Changes in the number of electrons along the polymer backbone results in new ring angles which

are different from the ground-state configuration. p-Doping of LEB results in the formation of a hole polaron, (P^+) described as a ring-centered distortion in which the center phenyl ring twists out of its ground-state configuration toward the plane formed by the nitrogens. This distortion causes neighboring rings to distort toward planarity and away from the ground-state angle; figure 3.5[10].

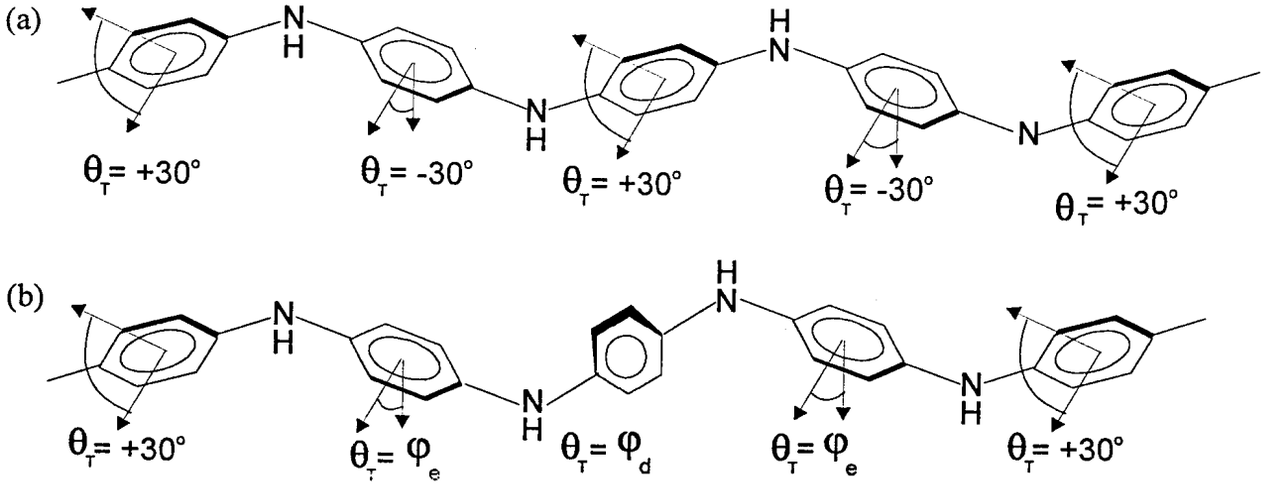

Fig (3.5): (a) A segment of a LEB chain showing the phenyl rings rotated by ±30° out of the plane formed by the nitrogens. (b) Representation of a ring-rotational hole polaron in LEB where the center phenyl ring and the phenyl rings rotate toward the nitrogen plane to new angles φ_d and φ_e [10]

A negative polaron (P^-) causes almost no ring-rotational effects, although bond-length effects produce very small asymmetrical splittings from the conduction and valence bands less than a few tenths of an eV[10].

3.1.3 Pernigraniline base (PNB)

This fully oxidized (*1-y = 1*) and insulating form of Pan, shown in figure 3.6, has an energy gap (E_g ~ 2.3 eV) that is intrinsic due to electron-phonon interactions[4]. The electronic structure of PNB is characterized in terms of a Peierls ground state[10] that supports soliton and polaron defects. The half-filled π-band is split by an energy gap caused by an effective bond-length alternation, resulting in the constituent phenyl rings of

the Pan backbone taking on an alternating quinoid-benzenoid character analogous to the double-bond-single-bond alternation in dimerized *trans*-polyacetylene[10]. The resulting degenerate ground state of PNB supports bond-alternation defects, particularly solitons and polarons, which accommodate doping-induced and photo-induced charge in the polymer[10].

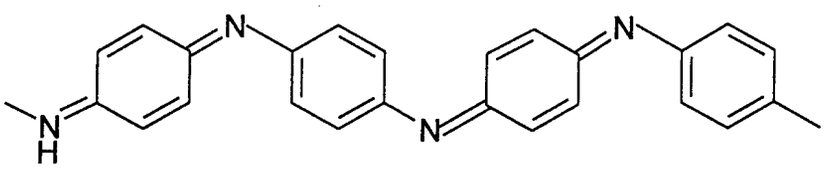

Fig (3.6): Pernigraniline base structure[4].

3.1.4 Emeraldine salt (ES)

ES is the conducting form of Pan formed by the protonation of EB by exposure to protonic acids (a process which is a variation of either the number of protons, electrons or both *(on the unprotonated –N= sites)* or on n- and /or p- doping of LEB[4,5]). Figure 3.7 shows the two processes leading to one form, ES. Doping causes the orders of the undoped insulating forms to change, resulting in a reorganized electronic structure described as a metallic polaron energy band[11].

The conductivity of pristine Pan increases by several orders of magnitude upon doping and depends on a number of factors including, dopant used and processing in different solvants[11]. Upon protonation of the formerly unprotonated –N= sites of EB, the conductivity increases by a factor of 10^{10}, reaching about 1S/cm, despite the unchanged electron concentration[6].

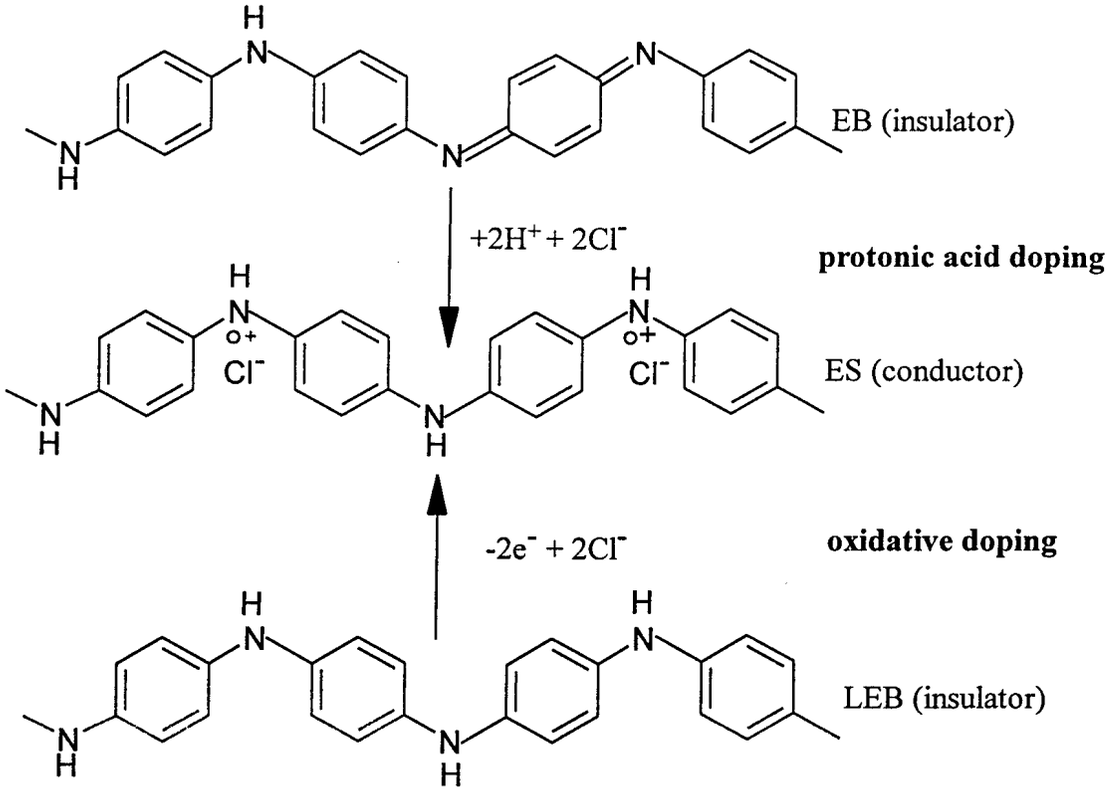

Fig (3.7): Illustration of the oxidative (p-doping) of LEB and protonic acid doping of EB, leading to the same final product, ES[11].

3.2 Polyaniline derivatives

The derivatives of Pan are obtained from doping the EB form of Pan with organic or inorganic acids, with the subsequent substitution of one of the benzene hydrogens by an anion from the acid. Pan derivatizing improves the material's processibility and compatibility[10]. Examples are: the sulphuric acid substituted derivative, where a hydrogen on the C_6 ring is replaced with a $SO_3^-H^+$ unit (figure 3.8), poly (orthotoluidine) POT-EB where a single hydrogen at the C_6 ring is replaced with a single CH_3 unit (figure 3.9)[10], and the hydrochloric acid salt of POT-ES, (figure 3.9(b)). The covalent bonding of protonic acids to the Pan backbone gives important properties that are not available in the emeraldine hydrochloride (HCl doped Pan). $SO_3^-H^+$ substituted Pan (figure 3.8a and b) is

soluble in water and aqueous base media. Pan POT-EB has been useful in the study of the effects of ring derivatization and interchain electronic properties of the polymer[6,12].

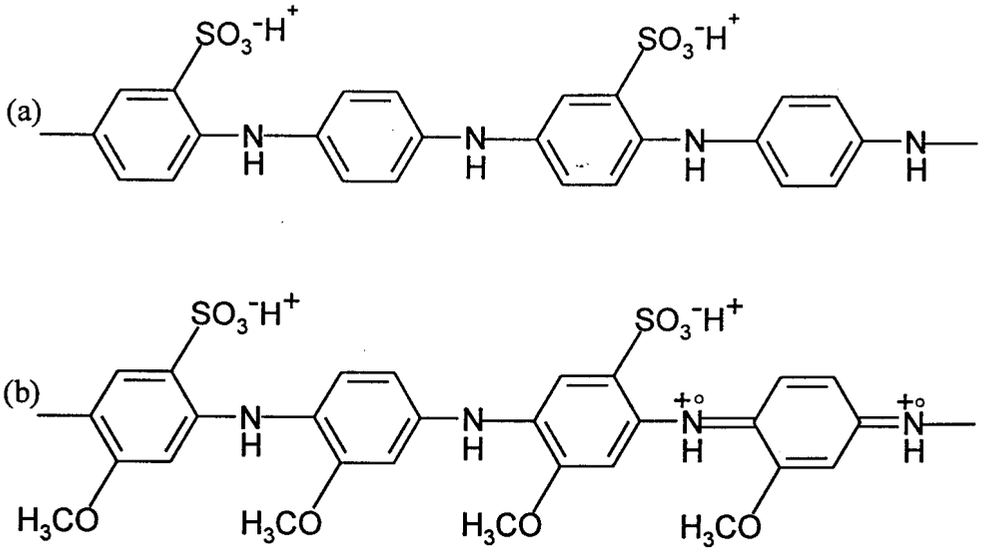

Fig (3.8): Schematic illustration of derivatives of Pan (a) 50% sulfonated and (b) 100% sulfonated Pan (self-doped forms) [12].

The interest in Pan stems from the fact that many different ring- and nitrogen- substituted derivatives can be readily synthesized and that each derivative can exist in several different oxidation states which can, in principle, be "doped" by a variety of different dopants either by non-redox processes or by partial chemical or electrochemical oxidation.

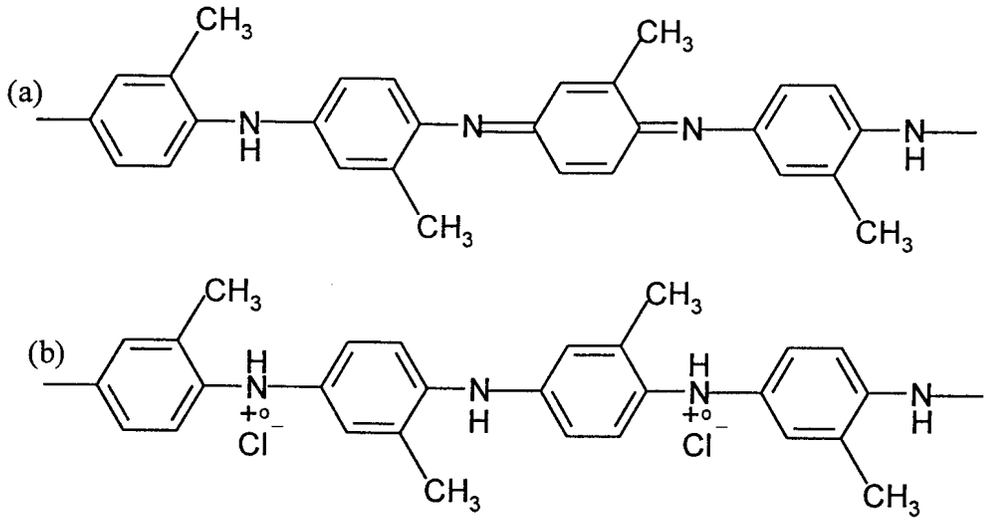

Fig (3.9): The structure of (a) POT-EB and (b) HCl salt of POT- ES derivatives of Pan [12].

3.3 Switching properties

The potential applications of Pan are related to the ability of this polymer to change its oxidation state, irrespective of the effect which induces this change: standard chemical or electrochemical oxidation and reduction, variation of the pH of the medium and effect of various types of energy (solar and radiation)[2]. Variation of the oxidation state results in changes of the whole spectrum of chemical, physiochemical and physical properties of the polymer: oxidation potential, light absorption, dielectric constant, refractive index, acid dissociation constant (pK_a), conductivity, crystallinity, dimensionality and a number of properties not stated here[2].

The chemical, conductive and electrochromic properties of Pan, can be controlled by application of a potential and /or an acid or base. Pan switches vice versa from the fully undoped form, LEB, that is less conductive to fully oxidized PNB that is insulating upon reaction with acids or bases that protonate and deprotonate the base sites of the polymer[13].

3.4 The polaron lattice of polyemeraldine

The geometric structural representation summarizing the formation of a polaron lattice in Pan is represented in figure 3.11. A model based on a two-step transition from isolated, doubly charged, spinless bipolarons to a polaronic metal [figures 3.11 (b) - (d)] was suggested by Stasftrom *et al*[12]. The first step relates to the instability of a bipolaron on a polyemeraldine chain [figure 3.11 (b)], with respect to the formation of two polarons [figure (3.11(c)], and the second step is their separation to yield a polaron lattice[11].

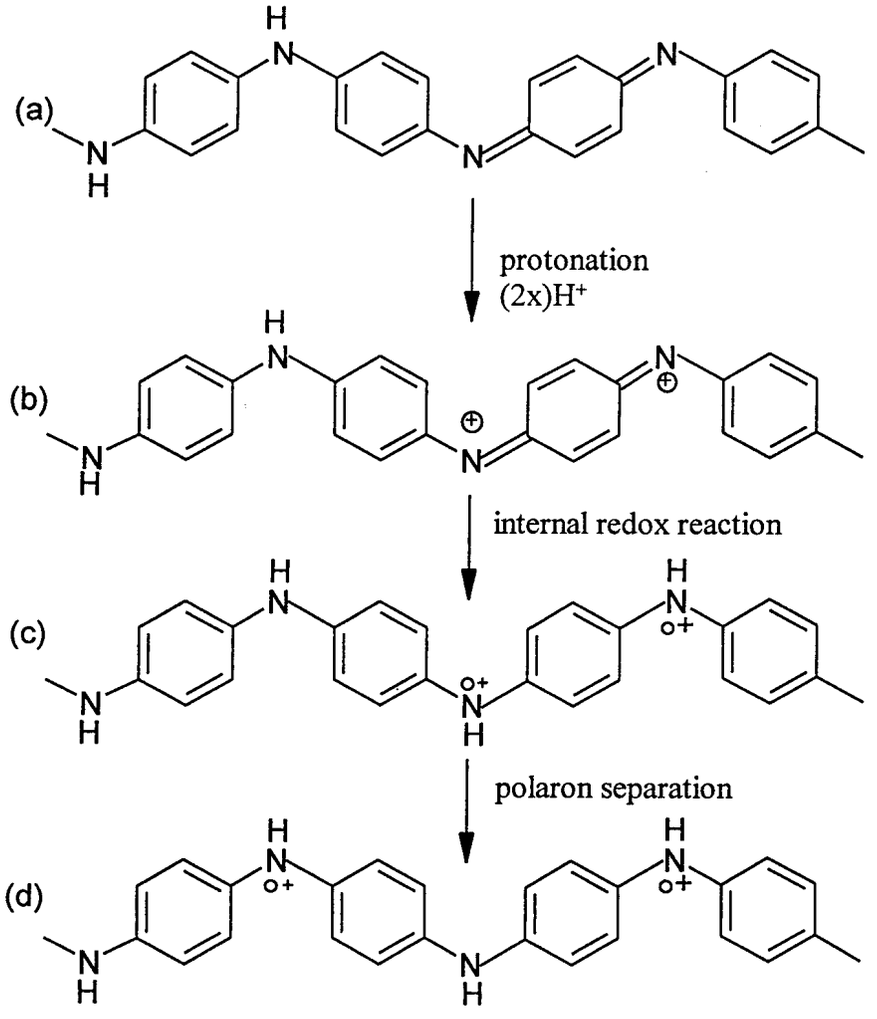

Fig (3.11): The geometric structure of Pan (a) before protonation and (b)-(d) after 50% protonation: (b) formation of bipolarons and (c) polarons; (d) the polarons separate, resulting in a polaron lattice[11].

3.5 The mass of charge carriers in polyaniline

The mass of polarons is very large $M_{polaron} > 60m_e$, where m_e is the mass of an electron[13]. Experimental evidence has shown that $M_{polaron}$ increases with an increase in the moment of inertia of the rings through addition of substituents. A further increase in the defect mass may result from interchain effects (due to increased interchain distances), causing changes in the ground state and excited state ring angles, as well as an increase in the average ring angle resulting from an increased intrachain steric effect of the methyl groups in poly (*o*-toluidine)[14]. Table 3.2 lists the defect (polaron) masses for LEB, EB, PNB, and half-oxidized poly (o-toluidine)[5].

Polarons, bipolarons and/or solitons are delocalized within a polymer chain and can travel along a chain as an entity, the atoms in their path changing their positions so that the deformation travels with the electron or hole. The fact that the atoms must move as these particles drift along a chain, results in an increase in the effective mass of the particles (table 3.2) [15].

Table 3.2: Masses of long-lived defect states for various forms of Pan[4].

Material	*Defect mass*
Leucoemeraldine base (LEB)	~ 60 m_e
Emeraldine base (EB)	~ 60 m_e
Pernigraniline base (PNB)	~ 300 m_e
Half-oxidized poly (o-toluidine) POT	~ 200 m_e

References

1. D. C. Trivedi, HandBook of Organic Conductive Molecules and Polymers **2** (Ed. H. S Nalwa), John Wiley and sons: New York (1997).
2. N. Gospodinov, L. Terlemezyan, Prog. Poly. Sci. **23**, 1443 (1998).
3. P. Yam, Trends in Material science, Scientific American, 75, July (1995).
4. J. Epstein, R. P. McCall, J. M. Ginder and A. G. MacDiarmid; Spectroscopy of advanced Materials, (Ed. R. J. H. Clark), Chichester: Wiley (1991).
5. A. J. Epstein, MRS Bulletin **22**, 16 (1997).
6. M. E. Jozefowicz, A. J. Epstein, A. G. MacDiarmid, Phys. Rev. **B 39**, 12958 (1989).
7. M. Shaolin, L. Jincui, www.chemistrymag.org/1999/011001pe.htm
8. http://romano.phsics.wisc.edu/winoku/
9. J. Fan, D. Zhu, Solid state communications **110**, 5762 (1999).
10. R. P. McCall, J. M. Ginder, J. M. Lang, A. G. MacDiamird; Phys. Rev. **B 41**, 5202, (1990).
11. S.Satafstrom, J.L.Bredas, Phys. Rev. Lett. **59**, 1464 (1987).
12. A. J. Epstein, A. G. MacDiamird, 141-150, Science and Application of conducting polymers, (Ed. W. R. Salaneck), Bristol: England (1991).
13. Conductive Electronic Polymers, (Ed. G. Gordon. Wallace, G. M. Spinks, P. R. Teasdale), Lancaster (1997).
14. E. Ehrenfreund, S. Vardeny, Phys. Rev. **B 36**, 1535 (1987).
15. J.P Pouget, M. E. Jozefowcz, Macromolecules **24**, 779 (1991).

Chapter 4

Charge transfer in Conducting Polymers

Some of the factors which can substantially influence the conductivity of CPs will be discussed in this chapter. By noting the contribution of each of these different factors, we will be able to determine the characteristics of charge transport in CPs. There are two basic mechanisms of single-particle transport in the solid state[1]:

i. *Band transport mechanism*: this is based on coherent diffusion: electrons move ballistically and are scattered by phonons and by disorder. This type of conduction is realized in metals with weak disorder or, in a more general case, for electronic states above the mobility edge[1]. For a given degree of disorder, all states may either be localized or extended as a function of energy. The boundary separating these two regimes is called the mobility edge. The metal-insulator transition takes place when the electrons' Fermi energy crosses the mobility edge.

ii. *Nonmetallic (phonon-assisted hopping) mechanism*: electrons jump between localized states by absorbing and emitting phonons. This hopping motion takes place for electrons with energies below the mobility edge[1].

iii. *Reduction/oxidation (Redox) mechanism*: this is a charge exchange phenomenon most thought to contribute to the overall conductivity in either of case i or ii above. This redox mechanism is explained in more detail below[2].

Charge hopping among fixed polaron and bipolaron sites shall be considered as the primary charge-transport mechanism in the lightly doped EB systems. At high protonation levels, the polarons are arrayed to form a polaron lattice with metal-like transport within the partially filled polaron energy band[3].

4.1 Charge exchange phenomena

Maximum conductivity is achieved when Pan is in the ES state, in this state the polaron states overlap to form mid-gap bands[2]. The electrons are thermally promoted at ambient temperatures to the unfilled bands, which permit conduction. Because of the presence of structural defects, the occurrence of a charge exchange phenomenon, as depicted in figure 4.1, is thought to be necessary to produce the degree of conductivity obtained[2].

In CP hosts, electronic charge transport requires motion of charge both along the backbone and between chains to create a three-dimensional conducting matrix. In these materials, subtle variations in both the intra- and inter-chain organization can generate profound changes in the measured transport properties[2]. Conductivity involves inter-chain or intra-chain proton exchange as well as electron transport. This explains the observed dependence of conductivity on the ambient humidity, as the presence of water in the polymer lattice would facilitate this proton-exchange phenomenon[2]. This inter-chain charge hopping is represented in figure 4.1.

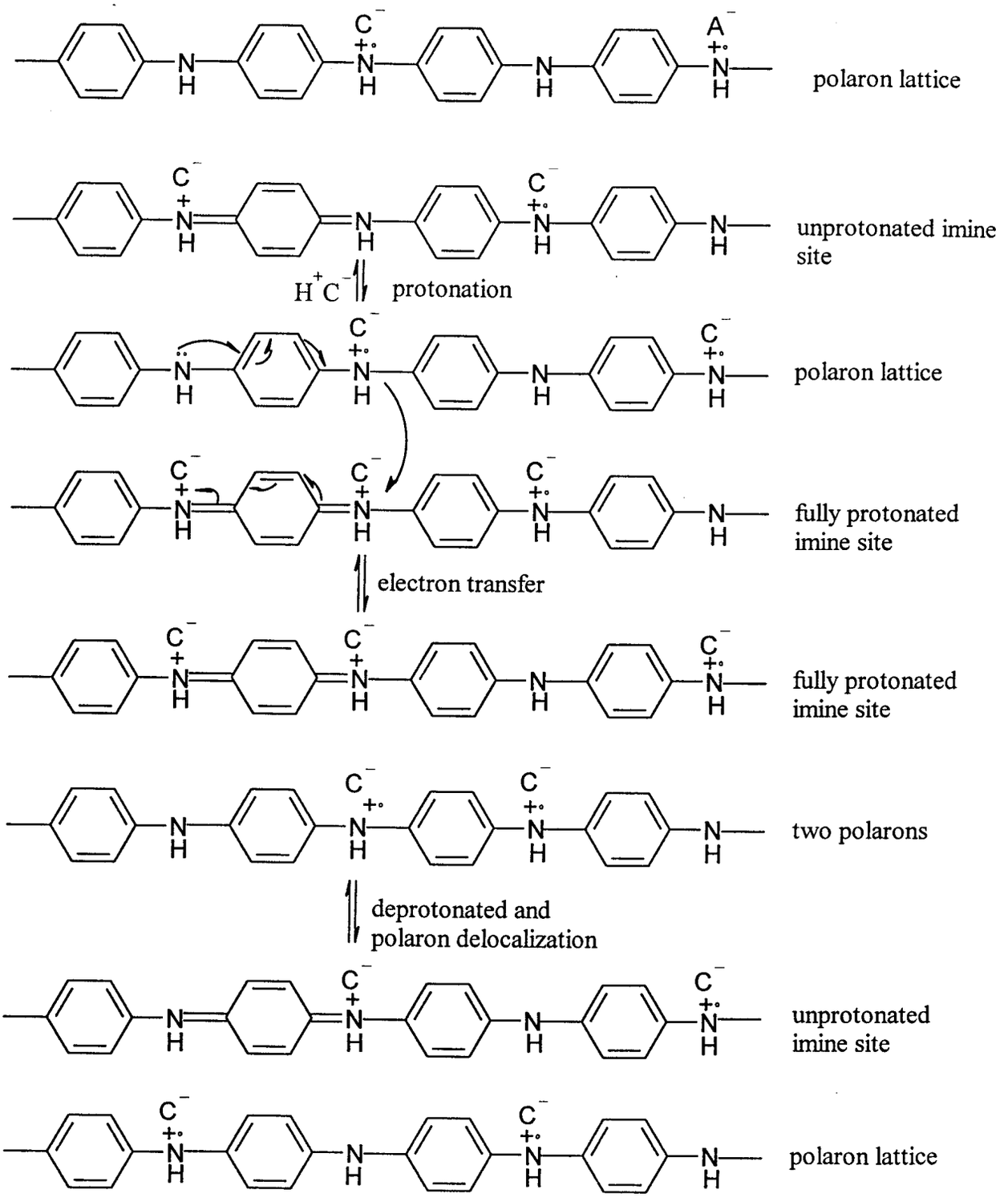

Figure (4.1): The inter-chain charge hopping mechanism for Pan[2].

4.2 Factors affecting electrical conductivity

In CPs, electrical conductivity is dependent upon temperature, humidity, functional groups on the polymer and counter-ion species including the solvent it is cast from. In addition, the conductivity depends on preparation conditions, as they relate to the formation of structural defects and polymer morphology[4].

4.2.1 Moisture content

The presence of moisture in Pan doped with HCl can increase the conductivity and significantly affects the other electronic properties. Figure 4.2 and 4.3 [2, 5-9] show the effect of humidity on conductivity and the role of moisture in the polymer's conductivity, respectively. While some water molecules are tightly bound, others are found to be relatively free and mobile[9] The resulting increase in conductivity has been argued to be due to reduced potential barriers between the metallic islands[9]An almost similar argument on the role of water in electrical conduction is that the presence of moisture in the polymer lattice facilitates the process of inter-chain or intra-chain proton exchange[2]. The proton exchange takes place between the polymer solid phase and the water mobile phase[10].

The temperature dependence of resistivity increases upon annealing of the Pan sample, indicating that the conduction mechanism has been affected. The conductivity of annealed samples can recover upon exposure to moisture[8].

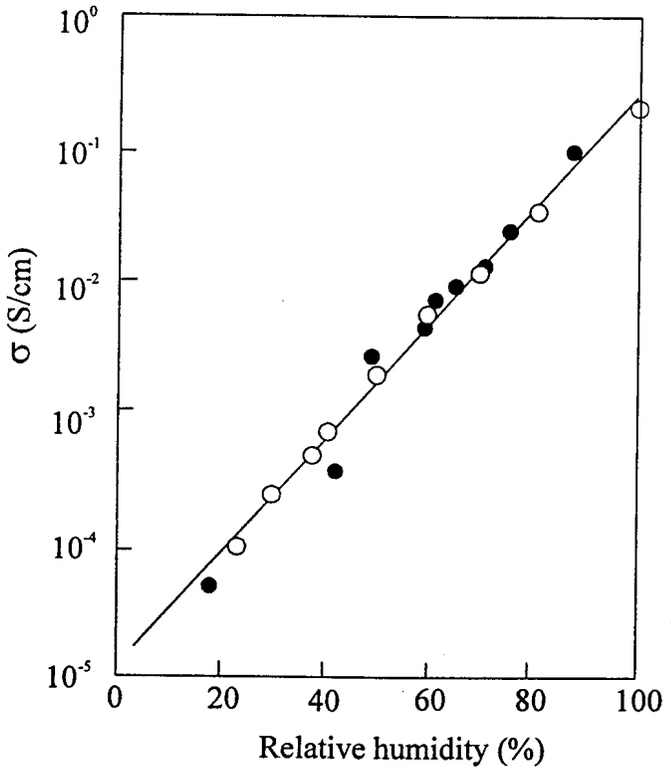

Fig (4.2): Relationship between the conductivity and relative humidity in the (o) desiccating and (•) moistening processes for a Pan-polyvinyl alcohol composite film[10].

The mechanism by which the Pan film senses water molecules is shown in Figure 4.3, where "A" represents the dopant anion. At high humidity the doping of Pan is high and the polymer conducts. When water molecules are removed from the polymer, the dopant anions are de-doped in the acid form (HA) from the CP, resulting in a decrease in conductivity. This process is reversible and the conductivity changes with change in moisture[10].

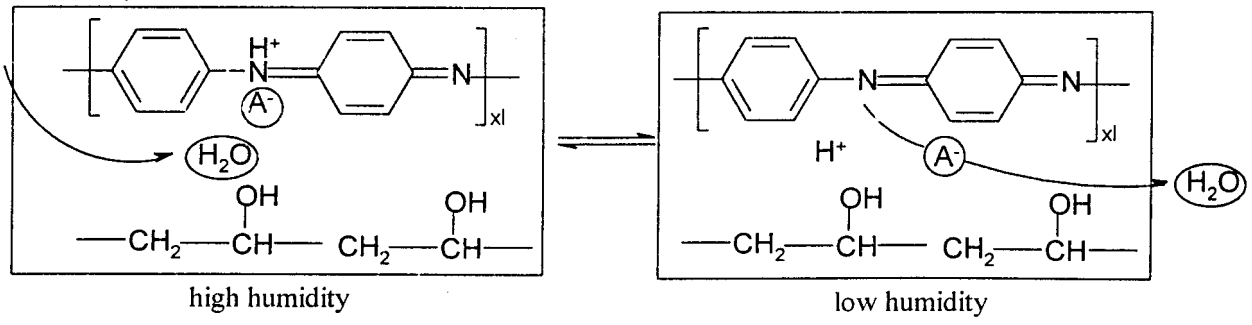

Fig (4.3): The role of moisture in the doping and de-doping of the polymer[10].

4.2.2 Morphology and the heterogeneous media

The importance of morphology on conduction can be visualized from figures 4.4 and 4.5. The existence of defects or discontinuities in the extended conjugation (for example, cross link or ortho branch in the idealized head-to-tail chain of Pan and the attraction of the charge carriers to dopant counterions which pin them), localize the charge carriers[11].

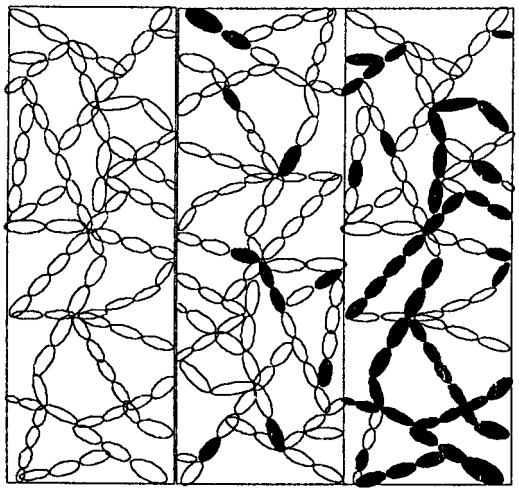

Fig (4.4): The relation of CP morphology to conduction. Doped segments (dark) in an interpenetrating structure, showing how increased doping finally provides a complete conduction pathway, left to right: undoped, partially doped (semiconducting) and partly doped (metallic) states[11].

It is perhaps more accurate to characterize the conduction process in CPs as the hopping of electrons between these charged carriers, a basis for the "hopping" models of conduction. CPs are considered as **disordered semiconductors** and, defects or breaks in the conjugation scatter electron transport[11]. The inter-chain configuration of Pan in the base form (EB) significantly impacts the overall properties of the polymer[11].

The micrographs of CPs pellets and films demonstrate that the polymer solids consist of a heterogeneous structure of fibres and grains. An idealisation of this structure is shown in figure 4.5[11].Points 1 to 4 represent microprobes used to take electrical measurements. Probes 1 and 2 sit on the same chain and would permit direct conductivity – *intermolecular conduction.* Probes 2 and 3 would permit a hopping or tunneling process – *intermolecular hopping.* Probes 3 and 4 permit transport between fibres - *interfibrillar* conduction[11]. In real experiments we measure transport between points 1 and 4 therefore we have a complicated superposition of various conduction processes. This superposition can be expressed as a series of resistances:

$$R_{1,4} = R_{1,2} + R_{2,3} + R_{3,4} \qquad [4.1]$$

The largest resistance determines the material behavior. For lightly doped samples $R_{2,3}$ dominates and inter-polaron hopping takes place. In highly doped samples $R_{3,4}$ dominates. Hence hopping mechanisms are of paramount importance for charge transport in amorphous polymers[11].

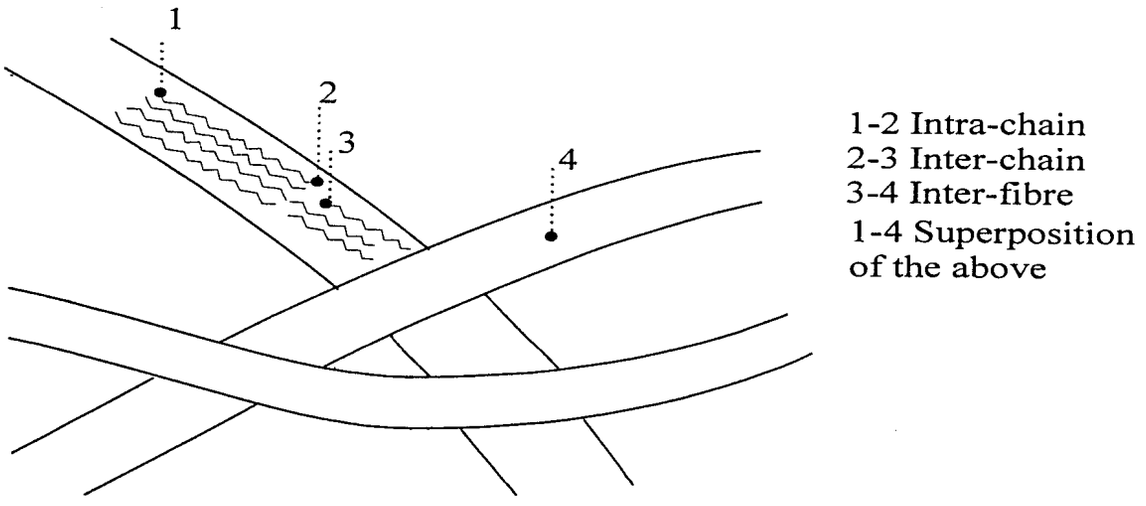

Fig (4.5): Schematic view of the fibrillar structure of a CPs[11].

Kaiser and Graham[11]ave shown that the overall conductivity can be built up using standard expressions for different regions and they proposed a simple heterogeneous model as shown in figure 4.6.

Two key components of this model are:

i. Temperature dependant conductivity is strongly influenced by thin barrier regions but is amplified by geometrical factors depending on the relative length of the highly conducting region (σ_1) to the total length[12].

ii. The presence of a disordered metal region (σ_4) and phonon assisted transport in barrier regions (σ_3) [12].

The overall conductivity is expressed as in equation 4.2 where *a*, *c*, *d*, and *q* are the parameters including geometric factors. The first term ($a\exp(-[(h/2\pi)\omega_o]/k_BT)$ corresponds to conductivity in the in metallic regions from Kevelson and Heeger, $(h/2\pi)\omega_o$ is the energy of the phonons that backscatter electrons and *h* is the Planck's constant.

$$\sigma^{-1} = a\exp(-[(h/2\pi)\omega_o]/k_BT) + \{c\exp[-(To/T)^{1/2}] + d + qT^{1/2}\}^{-1} \qquad [4.2]$$

The first term in the bracket corresponds to the hopping/tunnelling mechanism from Sheng and Klafter[11].The remainder of the terms in the brackets ($\{cexp[-To/T)^{1/2}] + d + qT^{1/2}\}^{-1}$)comes from the electron-electron interaction in the disordered metal region, which occur parallel with the hopping/tunnelling region. In CP samples, contributions due to metallic regions are very small and the conductivity is mainly governed by the tunnelling/hopping process with a decreasing conductivity, presumably due to the lack of the metallic path in the barrier regions[12].

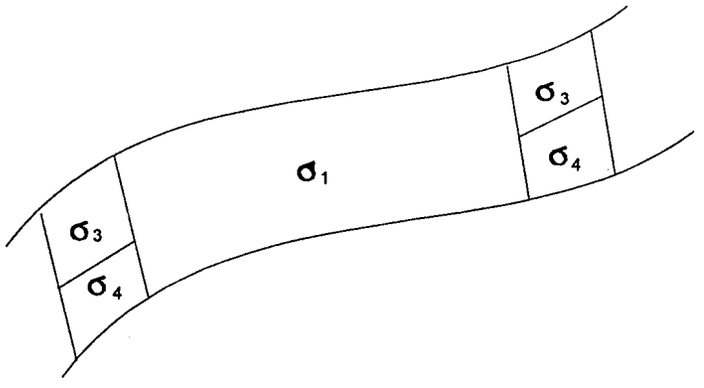

Fig (4.6): Conduction model in a fibril by Kaiser and Graham. Barriers consist of disordered regions in which hopping or tunneling occurs (σ_3) in parallel with a region showing metallic conductivity (σ_4). The larger regions in series with the barriers are metallic with high conductivity (σ_1)[11,12].

4.2.3 Impact of aggregation

Aggregates are formed in EB as a result of inter-chain interaction via hydrogen bonding between amine and imine sites. Reduction of the leucoemeraldine form eliminates the H-bonding and the aggregation[7]. The extent of aggregation on the polymer will impact on the solubility and solution characteristics of the polymer. The degree of aggregation on the polymer will depend on the conditions used to synthesize the polymer. Deaggregation facilitates a conformational change through chain expansion. Since doping results in a polar chain, the electrostatic repulsion of the ions on the doped chain also favors a chain expansion[7].

4.2.4 Minor structural defects

Figure 4.7 (a) and (b) are micrographs of pellet and film surfaces for Pan doped with HCl respectively. Defects indicated from the surface profile, such as cracks in the material, have a direct effect of reducing conductivity. At the same time the volume of the conducting material imposes limitations on conductivity.

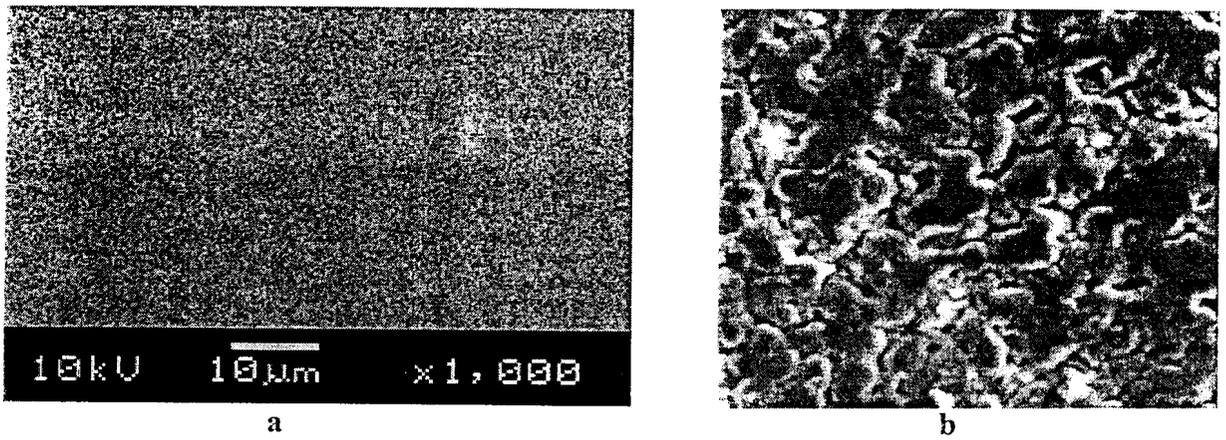

a b

Fig (4.7): Surface SEM images for a doped Pan ES, film (a) and pellet (b), the pellet image was magnified at X 3,000.

4.2.5 Carrier mobility

The carrier mobility is the magnitude of the drift velocity per unit electric field. Carrier mobilities give an indication of the degree of perfection of the structural organization, purity and whether charge transport is due to hopping or band motion. Room temperature mobilities for CPs range from less than 10^{-7} to ~ 0.5 $cm^2/V/s$, whereas they are typically 1350 and 3600 for n-type silicon and germanium, respectively. Mobilities depend on temperature as a modest power law.

For thermally activated charge transport, the mobility describing 3-dimensional hopping is obtained using the Einstein diffusion relation[13].

$$\mu = \left(\frac{ea^2\omega}{6k_BT}\right)\exp\{-E_A / k_BT\} \qquad [4.3]$$

where a is the hop distance (this distance is not the average chain separation but the average distance that carriers are able to travel along the chain between the thermally-activated inter-chain transfer processes), E_A and ω are the barrier to hopping (energy gap) and the average frequency of the optical phonons which modulate the chain dimerization, respectively. The mobility (μ), from the above equation can be increased through improving the structural order in the polymer and/or to move from the regime in which bipolaron hopping model applies to the metallic regime in which screening by other charges present removes the barrier to transport[13].

4.2.6 Doping level

The conductivity of a CP increases with increasing doping across certain critical doping level ranges. The conductivity increase within a narrow applied potential range follows an exponential relation of the form[11]:

$$\sigma(E) = \sigma_o \exp([E - E_o]/s) \qquad [4.4]$$

Where σ_o is the conductivity at reference potential E_o, and s is the slope of $\log(I_s)$, (I_s is the steady state current at potential E) vs. E plot[11].

The variation of room temperature conductivity $\sigma_{(300K)}$ of ES as a function of dopant concentration (Cl/N)% is shown in figure 4.8. The conductivity of the sample gradually increases with an increase of dopant concentration. At high doping levels, the resistance between the fibres, $R_{3,4}$, dominates (figure 4.5) and the model of fluctuation-induced tunneling should be applicable[11].This model assumes elastic tunneling at low temperatures and at high temperature, an activated process is added[8].

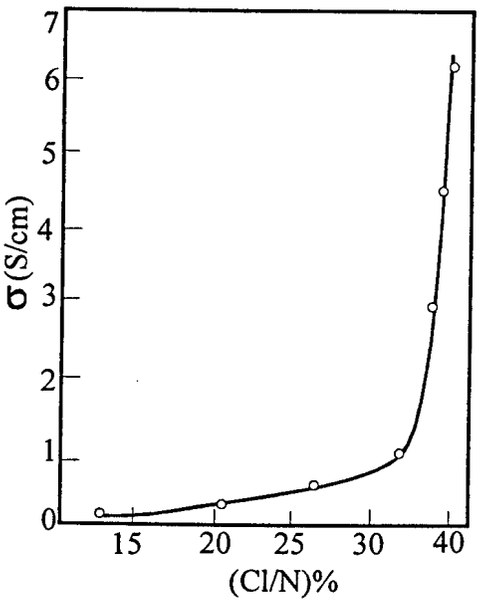

Fig (4.8): Variation of conductivity of ES with dopant concentration at 300 K [6].

For DC conductivity this should be variable range hopping, hopping between localized electronic states, which are distributed at random in space and energy[11].

4.2.6.1 50% doping

As shown in the previous chapter, (figure 3.3,) EB consists of amine (-NH-) and imine (=N-) sites in equal proportions[2, 4]. The imine sites are protonated to give the bipolaron (dication salt). However, they dissociate to form the delocalized polaron lattice[5], (figure 3.10). At doping levels higher than 50%, some amine sites are protonated. At doping levels lower than 50%, some imine sites remain unprotonated. In both instances, delocalization of the charge carriers over the polymer backbone is disrupted, thereby, reducing the polymer conductivity[2].

If a significant proportion of these unconducting phases occur, polyaniline behaves in a manner equivalent to a conducting system in which metallic islands are dispersed throughout a non-conducting media. In such a system, charge transport is through "charge energy-limited tunneling", involving long-range hopping[2].

4.2.7 Temperature

The electrical properties of CPs are strongly dependent on the extent of disorder present in the material. The extent of disorder is characterized in terms of the temperature dependence of conductivity[6]. By considering the temperature range from near absolute zero, metals, semiconductors, disordered semiconductors and insulators have the following conductivity dependencies:

- A metal's DC conductivity increases slightly with decreasing temperature, and reaches a finite limiting value near absolute zero[1-5].
- A semiconductor's conductivity decreases with decreasing temperature and remains finite at temperatures below 50 K[1-5].
- Conductivity of a crystalline semiconductor vanishes exponentially approaching absolute zero, while disordered semiconductors vanishes slowly[1-5].
- An insulator's conductivity decreases with decreasing temperature and vanishes at temperature near absolute zero[1-5].

Figure 4.9 shows the conductivity/temperature relationship of Pan. The conductivity increases as the temperature increases from 30 K, implying a hopping charge transfer mechanism where as conductivity decreases with temperature for band transport. In order to explain such behavior, the DC data are presented in the light of several models: Arrhenious plot, CELT model, Kivelson model and Mott's VRH model[13]. A detailed explanation of the models is presented in the next chapter. Because of the weak temperature dependence of conductivity, charge transport is analyzed here as 3–dimensional among localized states as described by Mott for non-interacting carriers[6] At high temperature, phonon scattering dominates impurity scattering. This destroys the elastic scattering interference responsible for electron localization and explains the observed high conductivity. With decreasing temperature the localization effects become strong, and this interplay between the disorder and the phonon scattering leads to the observable decrease in conductivity with temperature[1].

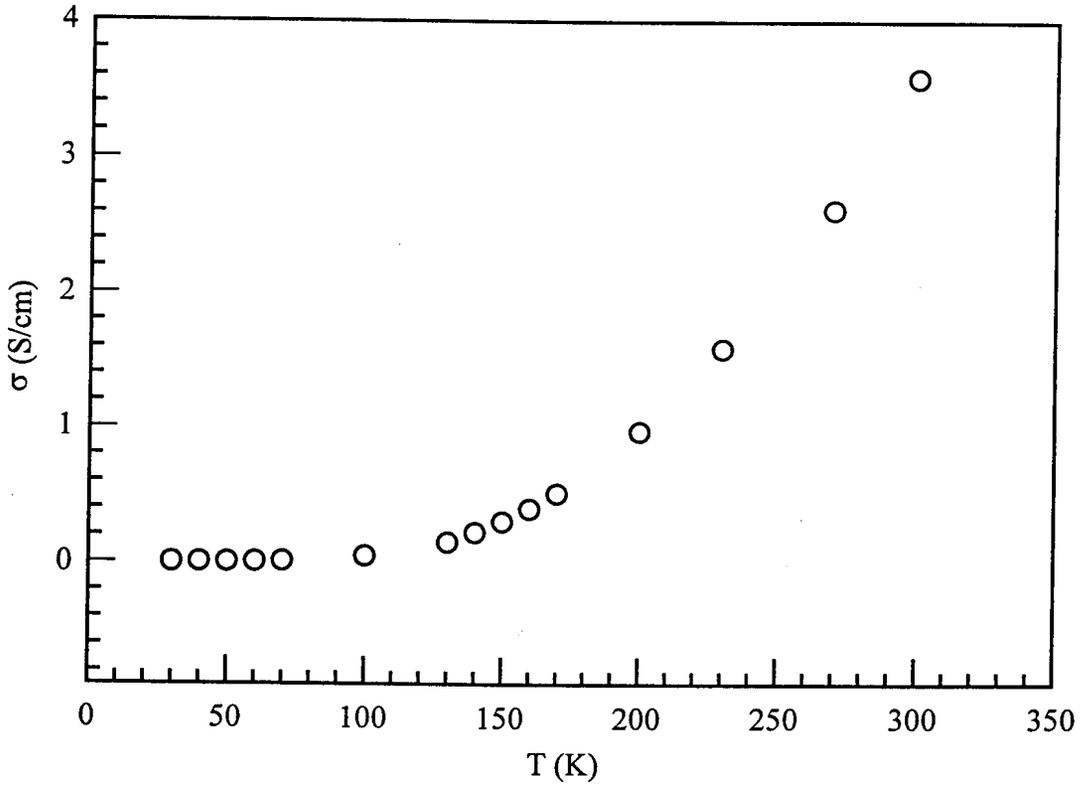

Fig (4.9): Variation of conductivity of Pan with temperature[6]

4.2.8 Conjugation length

A further property, which can influence conductivity, is the conjugation length, which can be defined as the extent of delocalization along the chain before a defect is encountered[11]. Studies on CPs have indicated that the conductivity decreases with decreasing conjugation length[11]. An increase in inter-molecular interaction results in an increased conductivity. It is noted in this respect that a short conjugation length is one of the key limiting factors for the conductivity of CP's. Hypothetical calculations have shown that conductivities up to 10^7 S/cm, far exceeding that of copper, could be obtained if one were truly able to synthesize a CP with extended conjugation along its entire chain[11].

4.2.9 Orientation and coherence length

One characteristic of highly conducting Pan is a high degree of orientation[11]. Electrosynthesised polymers are produced with higher orientation, contributing to their higher conductivity compared to chemically synthesized material. Higher orientation results in more order, which seems to introduce the 3-D carrier transport[12]. Crystallite size is represented by the coherence length (L_c) and is expressed as:

$$L_c = 0.9\lambda/B\cos\theta \qquad [4.5]$$

where λ is the wavelength of the radiation, B is the reflection width of the half-height and θ is the Bragg angle[12].

4.2.10 Plasticizer

The addition of a plasticizer (for example: N-methylpyrrolidinone (NMP)) to the EB solution, results in highly crystalline EB films with no mechanical deformations. Crystallinity is due to the effect of deaggregation and the local mobility that the plasticizer provides which allows chains to crystallize. The solvent can solvate the individual chains and, thus a conformational change can occur in which chains become more expanded[7].

4.2.11 Processing solvents and solutions

The solution characteristics determine the morphology of EB films derived from such solutions. EB films will have different levels of deaggregation and chain expansion, depending on the solvent from which they have been processed and therefore, will exhibit different properties[7].

The amorphous phase exists in various conformations, such as "coil", "expanded–coil" and "rod–like" conformation. These conformations are obtained depending on the

processing solution, for example, Pan processed from m-cresol and NMP/LiCl, has a more expanded coil type of conformation and exhibits higher conductivity than the same salts processed from solvents such as NMP[7]. Samples of the same chemical composition prepared from different solvents may have different local orders, thus very different conductivities[15].

4.2.12 Dopant molecules

A dopant not only generates a charge carrier by chemical modification, but also provides intermolecular links and sets up a microfield pattern affecting charge transport. Any disturbance of the periodicity of the potential along the chain induces a localized energy state. Localization also arises in the neighborhood of the ionized dopant molecule due to the Coulomb field[16].

4.2.13 Solution concentration and crystallinity

The crystallinity of EB films depends on the degree of aggregation in the polymer. Films cast from highly concentrated solutions, where the structure is more aggregate, are more amorphous compared to films cast from less concentrated solutions[7].

4.2.14 Synthesis procedure

A comparison is made between electrochemical and chemical synthesis of Pan.

In **electrochemical synthesis**, different experimental conditions and/or dopant ions do not necessarily give identical results[17]. By varying the conditions, for example, Pan (BF_4^- doped) film grown on a platinum electrode at a constant potential of *0.7 V* (vs. saturated calomel electrode (SCE)) for *16 hours* was observed to have a compact microspheroid morphology, whereas a film (ClO_4^-) doped and grown on indium tin oxide (ITO) at a constant current of $50\mu A$ for *90 minutes* had a highly fibrillar morphology on a micropsheroid underlayer of the polymer[15]. The final oxidation state of Pan produced

during electrochemical synthesis can vary greatly depending on preparation conditions (the different oxidation states of Pan).

In **chemical synthesis,** it is possible to obtain a polymer of varying: molecular weight distribution, polydispersity index (chain length), morphology and oxidation states. These variables impact on the polymer conductivity and device shelf life[17].

4.2.15 Stretching

The conductivity of a CP increases steeply with increasing draw ratio l/l_o, where l is the length after drawing and l_o is the original length before drawing (figure 4.10). The initial stretching results in higher orientation and denser packing in fibrillar structure but additional stretching causes sliding of different fibrils against each other and finally small cracks develop[12]. X-ray diffraction studies of EB subjected to increasing draw ratio l/l_o show an increase in cystallinity (see figure 4.11). The draw ratio, cystallinity and conductivity data show that the conductivity of fibers increases monotonically with increases in apparent crystallinity[18].

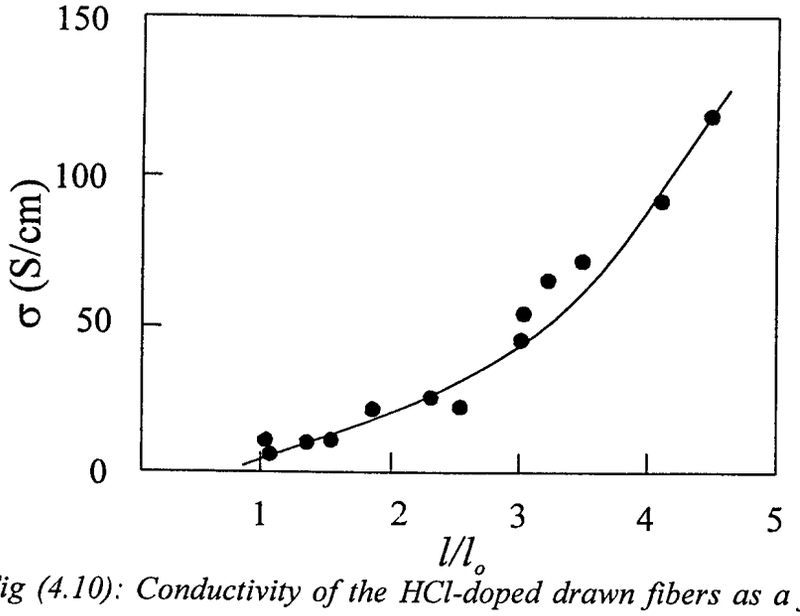

Fig (4.10): Conductivity of the HCl-doped drawn fibers as a function of increasing draw ratio l/l_o[18].

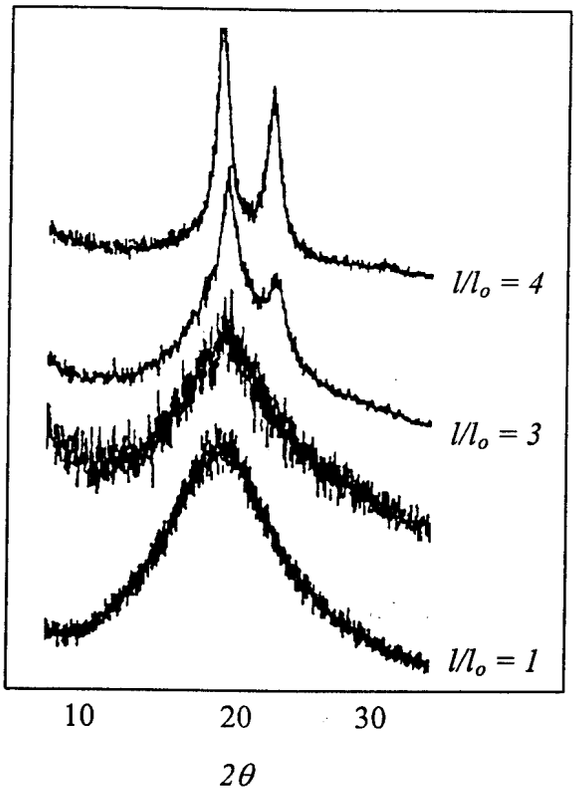

Fig (4.11): X-ray diffraction spectra of ribbons of EB of increasing draw ratio l/l_o[18].

4.2.16 Molecular weight

In figure 4.12 it can be seen that the conductivity of a doped (1M HCl) ES rises monotonically with molecular weight (Mw) up to a value of 150 000 (~1.600 ring-nitrogen repeat units), after which it changes relatively little. However, samples with different molecular weights, and therefore different conductivities, exhibit approximately the same crystallinity as determined by X-ray diffraction studies[18].

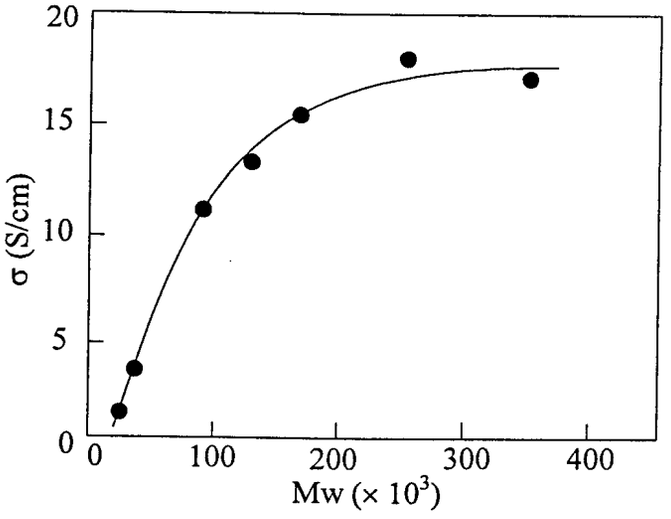

Fig (4.12): Dependence of conductivity of ES on molecular weight[18].

4.3 The metallic behavior of polyaniline

In general, the conductivity of Pan can be said to depend on the inter-link of metallic regions with insulating regions. An abundance of metallic regions results in the following metallic characteristics displayed by heavily doped CPs:

- Relatively high conductivity: 200 S/cm for doped Pan pellets, Pan-CSA (camphor sulphonic acid) has a room temperature conductivity of 200-400 S/cm, comparable to Mott's minimum metallic conductivity[19, 20].
- Pauli temperature independent magnetic susceptibility[20].
- Linear term in the specific heat capacity[20].
- Absorption throughout the infrared region with no energy gap[20].

However, these metallic features in the bulk transport, are severely limited by strong disorder. The polymers cannot display the following traditional signatures of metallic transport:

i. Resistivity (ρ) with a positive temperature coefficient, $d\rho/dT > 0$;
ii. Thermoelectric power (S) proportional to temperature[20].

Disorder results in the localization of states. If the magnitude of the disorder potential is large compared with the bandwidth, all states become localized and the system will be an insulator. In such a state, there is no energy gap. Consequently, the insulating property results since the Fermi level (E_F) lies in an energy interval in which all states are localized – the system is a Fermi glass. In such a system, the conductivity is temperature activated. At high temperatures, the activation energy is a measure of the energy difference between E_F (which lies in the region of localized states) and the mobility edge. At lower temperatures, variable range hopping (VRH) transport results from the existence of unoccupied localized electronic states near E_F [20].

References

1. J. Joo, V. Prigodin, A. G. MacDiarmid, A. J. Epstein, Phys. Rev. **B 50**, 12226 (1994).
2. Conductive Electroactive Polymers, (Ed. G. Wallace, G. M. Spinks, P. R. Teasdale), Lancaster (1997).
3. J. Ginder, A. J. Epstein, Phys. Rev. **B 41**, 10674 (1990).
4. K. Lee, A. J. Heeger, Phys. Rev. **B 20**, 14884 (1993).
5. M. E. Jozefowicz, A. J. Epstein, A. G. MacDiarmid, Phys. Rev. **B 39,** 12958 (1989).
6. M. Gosh, A. Barman, S. K. De, Chatterjee, J. Appl. Phys. **84**, 806 (1998).
7. M. Angelopoulos, R. Dietro, W. Zheng, A. G. MacDiarmid, A. J. Epstein, Synth. Met. **84**, 35 (1997).
8. N. J. Pinto, P. K. Kahol, B. J. McCormick, Phys. Rev. **B 53**, 10690 (1996).
9. A. Atushi, H. Ishikawa, K. Amano, M. Satoh, J. Appl. Phys. **74**, 296 (1993).
10. K. Ogura, T. Saino, H. Shiigi, J. Mater. Chem. **7**, 2363 (1997).
11. Conducting Polymers, Fundamentals and Applications, (Ed. P. Chandrasekhar), Kluwer academic publishers: Boston (1999).
12. J. Tsukamoto, Adv. in Phys. **41**, 509 (1992).
13. R. H. Friend, J. H. Burroughes, K.E Ziemelis, Science and Application of conducting polymers, (Ed. W. R. Salaneck), Bristol: England (1991).
14. M. Gosh, A. Barman, A. K. Meikap, S. Chatterjee, Phys. Lett. **A 260**, 138 (1999).
15. A. J. Epstein, MRS Bulletin **22**, 16 (1997).
16. A. G. MacDiarmid, W. Zheng, MRS Bulletin **22**, 24 (1997).
17. D. C. Trivedi, Handbook. of Organic Conductive Molecules and Polymers **2** (Ed. H. S Nalwa), John Wiley and sons: New York (1997).
18. A. G. MacDiarmid, A. J. Epstein, Science and Application of conducting polymers, (Ed. W. R. Salaneck), Bristol: England (1991).
19. R. Pelster, B. Wessling, Phys. Rev. **B 49**, 12 718 (1994).
20. R. Menon, A. J. Heeger, Y. Cao, Phys. Rev. **B 48**, 17 685 (1993).

Chapter 5

Characterization of Polyaniline

One of the aims of this study has been to clarify the transport mechanisms in CPs. To this end, different characterization methods have been employed for the characterization of CPs. The mechanisms behind charge transfer in CPs is still under debate and we have employed different methods during this work in order to try and narrow down possible mechanisms. Electrical characterization provides an excellent and very sensitive way to determine the electrical characteristics of CPs. In the present study the following techniques were used in assessing and explaining electrical properties of such materials:

- Scanning electron microscopy (SEM) for morphology analysis,
- Fourier transform infrared spectroscopy (FTIR) for molecular level analysis,
- Differential scanning calorimetry (DSC) and thermal gravimetry analysis (TGA) for analysis of decomposition behavior and crystallinity.
- Temperature dependant current – voltage (I-V) measurements.

From the various experimental results such as conductivity, magnetic susceptibility and spin dynamic measurements, it seems that doped Pan segregates into either granular 3-d metallic islands surrounded by armophous regions or an isolated conducting chain in an insulating polymer matrix[1]. However, conductivity in Pan shall be analyzed in terms of the models summarised in table 5.1, these models shall be described in more detail in section 5.8.

Table 5.1: Summary of conduction models

Model	*Area of application*
Mott's Variable Range Hopping (VRH)[1] ($\ln\sigma$ vs. T^{-025})	- Disordered semiconductors, including CPs - Temperatures above 30K, being also dependant on the dimensionality of charge transfer process
Arrhenius plot[2] ($\ln\sigma$ vs. T^{-1})	- Temperatures above 250 K for most Pan samples
Kivelson [2] ($\ln\sigma$ vs. $\ln T$)	- Highly doped Pan samples
Activation energy[2] ($\ln\sigma$ vs. $T^{-0.5}$)	- Temperatures above 280 K - Over a wide doping level range - Assumes conduction is attributed to electron hopping
Sheng[2] ($\ln\sigma$ vs. $T^{-0.5}$)	- Assumes a system of metallic particles embedded in a dielectric matrix - Highly doped Pan (about 50%), ratio of dopant ions per monomer units

5.1 Current-voltage measurements at ambient temperatures

Current-voltage measurements were first made to ensure that no significant contribution to conductivity occurred due to ionic conduction; this was achieved by passing a constant current through a sample and monitoring the potential difference as a function of time. If an ion contribution to conductivity occurred, it would have been manifested as a decrease in the sample conductivity as the number of ions were depleted. Since this did not occur it was assumed that conduction was occurring in all samples by an electronic mechanism. Current–voltage characteristics were found to be ohmic in all samples in the current range 5nA to 5mA.

5.1.1 Ohmic contacts

The electrical properties of Pan were measured using the four-point probe and the Montgomery techniques. These two methods are based on point-electrodes and thus assume a spherical symmetry of the electric field, meaning that they are not really applicable to strongly inhomogeneous materials. For both methods the measurement of conductivity relies on passing a stabilized current through the sample and measuring the voltage drop at the voltage electrodes. The simplest device structure is a bar of the polymer with two electrodes connected via ohmic contacts. The conductivity (σ) of a bar of p-type material is given by[3]

$$\sigma = e\mu_p p \qquad [5.1]$$

where e is the electronic charge, μ_p the (hole) mobility and p the hole density. Because both the *free-carrier density* p and the *mobility* μ_p are functions of temperature, the conductivity is strongly temperature dependent[3]. The hole density is given as

$$p = 2^{\frac{1}{2}}(N_A N_V)^{\frac{1}{2}} \exp(-E_A / k_B T) \approx T^{\frac{3}{4}} \exp(-E_A / k_B T) \qquad [5.2]$$

Here N_A is the acceptor concentration, N_V the density of states at the top of the valence band, E_A the activation energy of the acceptor, k_B the Boltzmann constant and T the temperature. The hole mobility depends on the limiting mechanisms described in chapter 4. The following models are equally possible:

Acoustic phonons: $\mu_p \sim m^{*\,-5/2} T^{-3/2}$ [5.3]

Ionized impurities: $\mu_p \sim m^{*\,-1/2} T^{3/2}$ [5.4]

Optical phonons: $\mu_p \sim m^{*\,-3/2} T^{1/2}$ [5.5]

In principle, we determine the activation energy for bulk conduction through the measurement of the conductivity as a function of temperature. In this model, the resistivity of the sample does not depend on the voltage.

5.1.2 Conductivity in the bulk samples

As stated in the previous chapters, several charge carriers contribute to the overall conductivity of the polymer, many structural imperfections are present in all polymers and thus, when discussing mechanism of bulk conductivity, these defects need to be considered. Conductivity is not only a result of charge transfer along the chain, but is also due to electron hopping between chains and between different conjugated segments of the same chain. In addition to these effects which act at a molecular level, bulk conductivity values are also dominated by electron transfer between grain boundaries and variations in morphology[3]. Thus the bulk conductivity (σ) can be represented by[2]:

$$\sigma = \sum \frac{n_i Z_i e v_i}{E} \qquad [5.6]$$

Where,

n_i = number of charges carried by each type

Z_i = carrier type

e = electronic charge

v_i = drift velocity of an electron

E = electric field strength.

Equation 5.6 takes into account different charge carrier types, which contribute to the overall observed conductivity in the bulk polymer[2].

5.2 Four-point probe measurements

Considering a collinear four-probe array as in figure 5.1, current (I) is applied by two outer points and the voltage (V) is measured between two inner probes. For a semi-infinite sheet with thickness ($d >> s$), where s is the separation between probes[4,5]:

$$\sigma = I / 2\pi s V \qquad [5.7]$$

This method was applied in measuring the current-voltage characteristics of Pan pellets.

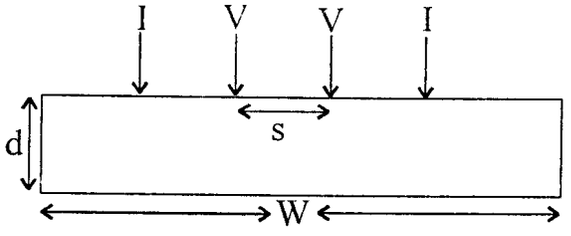

Fig (5.1): Outer electrodes on Pan pellet are current (I) electrodes while inner electrodes are voltage electrodes (V).

5.3 Montgomery method

This method was used in the measurement of the conductivity of thin films. Point electrodes are attached at the four corners of a square thin film, (fig. 5.2) and resistivity ρ, is given as[5]:

$$\rho = HER \qquad [5.8]$$

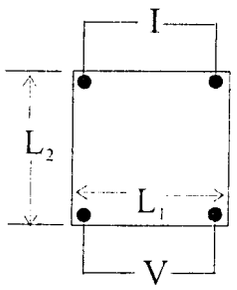

Fig (5.2): Current and voltage electrodes are attached to the four corners of the square sample (film/pellet)

Where H is a function of L_2/L_1 as shown in Table 5.1. R is the ratio of measured voltage to current (V/I). E is an effective thickness, which is equal to the actual thickness L_3 when $L_3 <<< (L_1L_2)^{1/2}$, but never gets much greater than $(L_1L_2)^{1/2}$. In the present study, L_1 was made equal to L_2 and therefore $H \sim 4.531$ according to table 5.2 [6]. The average for L_3 for our films was about $50\ \mu m$, while L_1 and L_2 were about $0.4\ cm$ respectively.

Table 5.2. Selected values of the function H [6]

L_1/L_2	0.25	0.5	0.6667	**1.0**	1.5	2.0	4.0
H	0.3207	0.8911	1.562	**4.531**	21.86	105.1	56 300.0

5.4 Conductivity measurements at T > 300 K

Pellets of emeraldine salt (ES) were subjected to temperatures between 300 and 450 K at atmospheric pressure. The current-voltage characteristics were determined using the four-point probe method described above. The results from these relatively high temperature measurements were related to thermogravimetry results and the effect of moisture loss on conductivity was determined.

5.5 Conductivity measurements at T < 300 K

These investigations were performed to verify which of the conduction models studied, best describes electrical conduction in Pan. Current-voltage measurements of Pan samples were taken and conductivity was calculated using the Montgomery and four-point probe methods. The intrinsic metallic state and also its dimensionality can be detected from the low temperature conductivity values. In the present work, we made an extensive study on the transport properties at low temperatures[1].

5.6 Measurement of the extent of disorder in a polymer

The extent of disorder in the polymer is characterized in terms of the resistivity ratio (ρ_r). The higher this value the more disorder is present in the material. ρ_r is described by the relationship:

$$\rho_r = \rho_{T(K)} / \rho_{300K} \qquad [5.9]$$

Where $\rho_{T(K)}$ represents the resistivity at a temperature between 30 and 300 K[7].

5.7 The metal -insulator transition

Menon *et al*[1] describes the metal-insulator (M-I) transition behavior in Pan depending on the ratio values (ρ_r). Three types of behavior are identified:

i. metallic region ($\rho_r < 2$)
ii. critical region ($2 < \rho_r < 6$)
iii. insulating region ($\rho_r > 6$),

for $\rho_r = \rho_{30\,(K)} / \rho_{300\,(K)}$ [5.10]

5.8 Conduction models

A model of best fit is deduced from the measurement of the deviation of the experimental results from linearity when we plot curves of the variation of conductivity as a function of temperature for the models stated in the following section. While these and many other models have been proposed for conduction in CP, conduction remains a complex phenomenon, and to date no single model is comprehensively accurate. In varying degrees, the various models are able to account for the conduction behavior within a specific temperature range or doping range or dopant type, but then fail for other CPs. In one case, a 3-dimensional conduction model may be indicated, whereas in another case, it is not[8].

5.8.1 The Mott – Variable Range hopping (VRH) model

The lack of ordering in CPs produces localized electronic states (polarons, bipolarons and solitons). The model of VRH assumes that localization is not very strong and differs at different locations within a material and thus postulates that conduction occurs by variable range hopping of electrons between these localized states. This electron hopping is assisted by phonons and sometimes depends on the initial and final energies (overlap of wave functions) of the states between which hopping occurs[1].

Mott's model is applicable to *1*–, *2*– and *3*– dimensional conduction. However, since the one-dimensional model arises due to strong interchain coupling between bundles, the one-dimension conduction fails if all bundles are coupled.

Due to the weaker resistivity–temperature dependence, the model such as metallic islands arising due to large inhomogenity and strong disorder is not valid for our samples. Our experimental results were analyzed according to 3-D conduction among localized states[1]. The magnitude of the hopping conductivity is expected to be much less than that of Mott's minimum metallic conductivity (200 – 400 S/cm), while the conductivity of metallic states above the mobility edge remains higher than this boundary value[8]. In the

argument developed by Mott, conductivity as a function of temperature for three-dimensional hopping is given by:

$$\sigma(T)=\sigma_O \exp(T_O/T)^{1/(n+1)} \qquad [5.11]$$

Where, n = dimensionality of the material's conductivity, σ_o is the room temperature conductivity [9].

From the values of the fitting parameters σ_o and T_o, we can calculate the values of the density of states, $N_{(EF)}$, and average hopping distance R, from the following equations:

$$T_o = 24/[\pi L_{loc}^3 k_B N_{(EF)}] \qquad [5.12]$$

$$\sigma_o = (3/4)e^2 \gamma_o R N_{(EF)} \qquad [5.13]$$

$$R = [3L_{loc}/\{2\pi N_{(EF)} k_B T\}^{1/4}] \qquad [5.14]$$

Where k_B is the Boltzman constant and L_{loc} the localization length (localization length is the range in which a charge carrier in the CP can move without encountering a barrier) which is determined from the magnetic field dependence of conductivity data. L_{loc} (Å) was assumed to be 72 Å, after the work of M. Gosh *et al*[1]. Temperature dependence should change with pressure, because the density of states at the Fermi level changes[9].

A condition for application of the hopping theory is that: $R >> L_{loc}^2$

5.8.2 The conductivity Arrhenius plot

Conductivity follows the Arrhenius behavior at temperatures above 250 K for most Pan samples.

$$\sigma = \sigma_e \exp(|E_F - E_C|/k_B T) \qquad [5.15]$$

E_F - E_c (activation energy) is the energy difference between the Fermi energy (E_F) and the mobility edge (E_c) and σ_e is the conductivity at the mobility edge[2].

5.8.3 Activated energy model

This model directly follows from Mott's model described above for conduction in 2-D. At lower temperatures, where the Arrhenius law fails, conduction is satisfactorily represented by the expression 5.16 for thermally activated conductivity[2].

$$\sigma = \sigma_o \exp(-\sqrt{T_o / T}) \qquad [5.16]$$

Where T_o and σ_o are described by equation 5.12 and 5.13 respectively.

Conduction is attributed to electron hopping, the origin and size of electronic localization centers and barriers have not yet been identified[11]. The hopping activation energy decreases as conductivity increases, as would be expected for higher state densities, since the conductivity increases as the hopping sites get closer together.

5.8.4 Kivelson model

This model represents the conductivity of lightly doped Pan samples. The conductivity follows the power law[2]:

$$\sigma(T) \propto T^n \qquad [5.17]$$

where, $n > 10$.

In Kivelson's model, there should be the same temperature dependence at all pressures [9].

5.8.5 Sheng's model

This model applies mostly to highly doped polymers. It assumes conduction between the "metallic islands" within the polymer and yields the following temperature relation:

$$\sigma = \sigma_o \exp(-T_1/(T + T_o)) \qquad [5.18]$$

Where T_o is described by equation 5.12. T_1 is an additional fitting parameter, and the fitting parameters are dependant upon the properties of the potential barriers (insulating islands or interfibrillar spaces) between the highly conducting islands[8]. The charge transport is thought to result from tunneling induced by thermal fluctuations. The above equation predicts conductivity monotonically decreasing with temperature but still yielding a finite value at near absolute zero (due to quantum mechanical tunneling) and a saturation value of conductivity at higher temperatures. Several variations of Sheng 's model exist[8].

Each of all the above models are but one part of the whole truth, being valid under different ranges and conditions of doping, temperature and other variables.

5.9 Polymer sample morphology

The morphology of the polymer has an effect on the electrical conductivity of the material. As shown in the previous chapter, amorphous regions disturb conduction through band to band hopping allowing only fiber to fiber hopping conduction which is more unlikely and thus we end up with low conduction material and very low charge mobility. Transport in the crystalline regions is metallic like and the magnitude of conductivity is higher. Charge mobility is also high. A *50%* crystalline polymer is more conductive as compared to a *20%* crystalline polymer. The following techniques were used to analyze polymer morphologies.

5.9.1 Scanning electron microscopy (SEM)

Polymer structure and morphology are greatly affected by synthesis conditions such as electrode materials for electrosythesis, solvent and electrolyte salts, oxygen and water content of the system and the current density used for electropolymerization. SEM is used for the analysis of polymer samples in the film and pellet form. Films appear generally smooth, while pellets show uneven surfaces and the possible existence of macroscopic defects such as cracks (see chapter 8 figure 8.4).

5.10 Fourier-Transform-Infrared (FTIR) and Raman spectroscopy

The vibrational frequencies of a molecule can be determined by infrared spectroscopy and Raman spectroscopy. Both techniques depend on the interaction of electromagnetic radiation with matter, but the physical causes are different. In many molecules it is therefore possible to observe vibrations of different symmetry by different spectroscopic techniques.

i. Raman spectroscopy was used initially for the analysis of the changes in the molecular structure of Pan as result of the annealing.
ii. Infrared spectroscopy was used to evaluate the effect of annealing on the molecular structure of emeraldine base and emeraldine salt, as well as to compare the Pan we synthesized in our laboratory with commercially available Aldrich Pan in their doped and undoped forms.

FTIR spectroscopy is commonly used to study organic compounds as it provides information about:

i. the presence or absence of certain functional groups in a molecule
ii. the extent of hydrogen bonding (intra- and inter molecular hydrogen bonding)
iii. conformational orientation of molecules

The theoretical basis of FTIR spectroscopy can be explained in the following way:

5.10.1 Molecular vibrations

A polyatomic molecule possesses several vibrations and these may be infrared active or inactive according to the symmetry of the vibrational mode. The energy of these vibrations corresponds to that of the infrared region. Therefore, absorption of infrared radiation of the appropriate wavelength results in a vibrationally excited state. Infrared radiation is absorbed if the frequency of the radiation matches that of an allowed vibrational transition. The bond(s) undergoing the vibrational transition must have a dipole moment and the absorption of radiation must result in a change of that dipole moment, that is, vibrations in a molecule must give rise to an unsymmetrical charge distribution. The greater the change in the dipole moment, the more intense the absorption. The vibrations of homonuclear diatomic molecules (e.g. O_2, N_2, etc.) do not result in infrared absorption and therefore we apply Raman spectroscopy in which light is scattered rather than absorbed.

5.10.2 Types of oscillations

Molecules can undergo different types of oscillations and thus may absorb energy at more than one wavelength. During vibration, the molecule's bonds stretch, contract and bend so that the structure oscillates around the most stable configuration.

(a) Stretching vibrations (b_{u1} and b_{u3}).

Stretching vibrations can be symmetric (b_{u1}), i.e. expansion and contraction of the molecular bonds occur in phase or asymmetric (b_{u3}), formed by combining the expansion of one bond with the contraction of the other, i.e. out of phase.

This symmetric and antisymmetric combination occurs in all cases where two bonds are equivalent due to molecular symmetry.

(b) Bending vibrations (b_{u2})

Bending vibrations can be relatively complicated motions such as scissoring, rocking, wagging or twisting. An infrared spectrometer measures the frequencies of the infrared radiation, which have been absorbed by a given sample. Most FTIR spectra are complex because of the overtones and coupling peaks.

5.10.3 Infrared spectra of polyaniline as from the work of Epstein *et al*[12]

Results from chapter 8, show that the peak positions vary to a low degree, depending on whether the Pan was obtained from electrosynthesis, doped in HCL or Aldrich Pan (camphor sulfonic acid doped). The spectral shifts/changes are taken as adequate indicators of molecular changes in the polymer.

i. EB spectrum shows strong absorption at *827, 1150, 1320, 1501,* and *1591* cm^{-1}.

ii. Upon protonation of EB to ES the existing features show an increase in the oscillator strength and the bands at *1501* and *1591* cm^{-1} show a red shift to *1486* and *1568* cm^{-1} respectibvely. No new band appears upon doping.

iii. p-doping of LEB with *HCl* to ES results in a significant change of the spectra, a new band is seen at *1150*cm^{-1} and the bands at *1500* and *1591* cm^{-1} change intensity and /or shift. Several of these features are observed for EB as it changes to ES.

iv. The *1591* cm^{-1} band for EB is consistent with the presence of quinoids in this material.

v. The infrared spectra of EB is described in terms of *para*-disubstituted benzene and additional modes are associated with symmetry breaking of the benzeoids due to the presence of quinoid groups.

vi. The band at *816* cm^{-1} for LEB is assigned to a b_{u2} *C-H* out-of-plane deformation of the benzoid groups. The band at *1284* cm^{-1} for LEB is due to b_{u3} benzenoid-amine stretching vibration. The intense band at *1497* cm^{-1} is for b_{u3} *C-C* ring-

stretching mode; the relatively weak one at *1613cm^{-1}* is likely to arise from the disorder–induced b_{u1} *C-C* ring stretching mode.

vii. For EB, two new bands are present at *1150* and *1591 cm^{-1}* corresponding to two strong Raman bands of LEB at *1188* and *1623 cm^{-1}* respectively The *1166 cm^{-1}* mode is assigned as either a b_{u1} *C-H* in-plane ring deformation or a b_{u1} ring-amine stretching vibration. The *1591 cm^{-1}* mode has two contributions: *C-C* ring stretching vibration of the quinoid groups and b_{u1} *C-C* ring stretching mode of the benzenoid groups (as in LEB, but much stronger). Again the symmetry-breaking role of the quinoid groups present in EB causes the Raman mode to become infrared active[12].

The relative intensity of the two bands at *1150* and *1591 cm^{-1}* can be used as a measure of the oxidation state (i.e. the number of quinoid groups) in Pan between LEB (*1-y = 0*) and PNB (*1-y = 1*). The monotonic increase in the intensity of the *1590 cm^{-1}* absorbency is taken as indicating the continued growth in the number of quinoid-like rings in the polymer chain[13]. Doping of ES results in an overlap of the infrared bands with the electronic continuum of the polaron band. The resulting absorption can be described in terms of a Fano effect causing shifts and large enhancement of the infrared bands[12].

Reference:

1. M. Gosh, A. Barman, S. K. De, S. Chatterjee, J. App. Phys **84**, 806 (1998).
2. M. Gosh, A. Barman, S. K. De, S. Chatterjee, Phys. Let. A **260**, 138 (1999).
3. http://www.sci.port.ac.uk/aeg/jrsmith/chapter1.htm
4. W. Pukacki, Mat. Sc. Forum **122**, 255 (1993).
5. S. M. Sze, Physics of semiconductor devices, (Ed. S. M. Sze), New York (1981).
6. H. C. Montgomery, J. App. Phys. **42**, 2971 (1971).
7. M. Gosh, A. Barman, S. K. De, S. Chatterjee, J. App. Phys. **84**, 806 (1998).
8. Conducting Polymers, Fundamentals and Applications, (Ed. P. Chandrasekhar), Kluwer academic publishers: Boston (1999).
9. J. Joo, V. N. Prigodin, A. J. Epstein, Phys. Rev. **B 50**, 12226 (1994).
10. S. Curran, Handbook of Conductive Molecules and Polymers **2** (Ed. H. S Nalwa), John Wiley and sons: New York 25 (1997).
11. R. Pelster, V. B. Wessling, Phys. Rev. **B 49**, 12718 (1994).
12. http://lifshitz.physics.wisc.edu/www/rguest/re_winokur_over.htm
13. A. J. Epstein, R. P. McCall, J. M. Ginder and A. G. MacDiarmid; Spectroscopy of advanced Materials, (Ed. R. J. H. Clark), Chichester, Wiley (1991).

Chapter 6

Application of Conducting Polymers

The study of CPs is a challenging exercise from both a fundamental point of view and the commercial potential these materials have. Many of the applications are based on the fundamental principles of physics and we concentrate on these issues in sections 6.1 – 6.6. In the applications arena, CPs are bringing radical innovations such as in electromagnetic interference shielding[1], CPs as pixel drivers in displays and electronic alfactometer (nose)[2]; completely new applications such as in electrochemical drug delivery[3] and novel applications such as artificial muscles[4] and bioaffinity sensors[2]. CPs have the potential of creating their own market segment as has been proved in the case of plastic batteries and organic light emitting devices in large screen displays[5]. Taking these factors into consideration, it is a plausible technological strategy for any industry that feels its technology would be threatened in the near future and/or wishes to be first on the market with an innovation to embark on researching CPs. As mentioned earlier, there is ample evidence indicating immense worldwide interest in CPs and astonishing applications successes thus far.

The combination of metal-like or semiconducting conductivity and processibility of classical polymers has created opportunities for a large range of applications for CPs[6]. The unique properties of inherently CPs stem from:

(i) the possibility of fine-tuning the conductivity by adjusting the amount of dopant incorporated within the polymer
(ii) doping/dedoping reversibility
(iii) the optical absorption characteristics in the ultraviolet, visible and near infrared spectra, as well as its electromagnetic absorption characteristics[6,7]. Some of the advantages of CP based devices compared to inorganic materials for the same functions include low weight, cost, flexibility and ability to form large surface areas as compared to conventional semiconductor materials[7].

Several polymers have been tested and proven to work in a variety of applications. Figure 6.1 illustrates some of the applications of Pan[6]. Despite the relatively poor success in providing a satisfactory explanation of the charge transfer mechanism in CPs, a number of products have achieved commercial success. In most instances the success has been attributed to consistent and reproducible responses of CP material to different stimuli. Individuals, companies and universities currently own several patents on the synthesis and device fabrication of these materials. Some of the commercialized products based on Pan are:

- Antistatic layers in computer disks by Hitachi Maxwell [2].
- Camouflage by Milliken and Co[2].
- Dispersible Pan powder version - jointly developed by Allied Signal, Americhem and Zipping Kessler[2].
- Electrostat loudspeaker - 0.1 μA Pan on 6 μm polyester film.
- Incoblend electrostatic dissipation. This technology is being utilized as an antistatic component for computers[1].
- 3V - coin-shaped batteries by Bridgestone-Seiko[2].

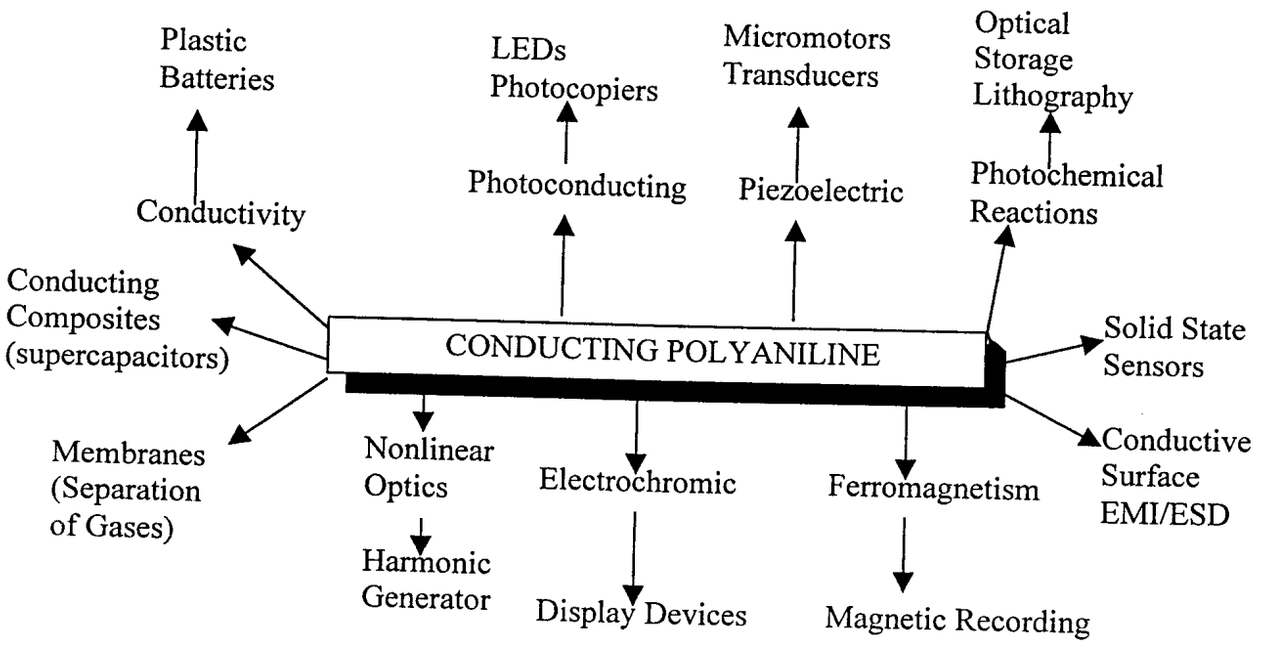

Fig (6.1): Applications of Pan[6].

6.1 Photoelectric conversion

CPs can be used in place of inorganic materials to convert solar irradiation into electric signals. Advantages of using CPs over inorganic materials include: ease of fabrication, lower cost of fabrication and environmentally friendly disposability. Grandstrom *et al*[8] obtained open-circuit voltages greater than 2 V, whereas *p*-type silicon based solar devices produce less than 1 V. This result implies that, compared to silicon, fewer polymer-based devices need to be cascaded to obtain the same net output voltage[8].

A bandgap exists between the (HOMO) and (LUMO) molecular orbitals. The bandgaps of most photovoltaic polymers lie in the range 1.5 – 3 eV, and as such are comparable to the energies of photons whose frequencies lie within (or just outside) the visible spectrum. This makes the polymers ideally suited for fabricating optoelectric devices. An incident photon has sufficient energy to excite an electron from the HOMO into the LUMO band of the polymer. This event creates an electron coupled to a hole – the exciton, and their motion through the material remains coupled. Figure 6.2 illustrates an **exciton** in a polymer[8].

The bound electron and hole are split at the electrode/polymer interface, as illustrated in figure 6.3. The electrons are collected at the lower work function electrode and holes at the higher work function electrode. The voltage output depends on the work function difference between these two electrodes.

In general there are two principles for photoelectric conversion[5]

(a) Utilize junctions of semiconductors such as *pn* junction or Schottky contact.
(b) Photochemical processes which produce electrical output from a photochemical reaction.

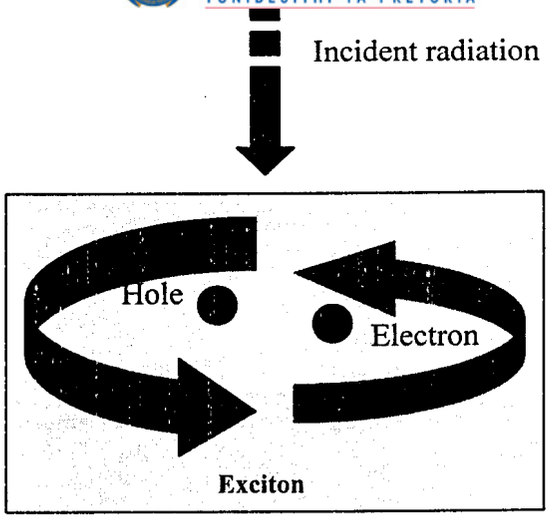

Figure (6.2): Excitons are produced in a CP. An incident photon produces bound electron-hole pairs called excitons, which transport charge in photovoltaic polymers[8].

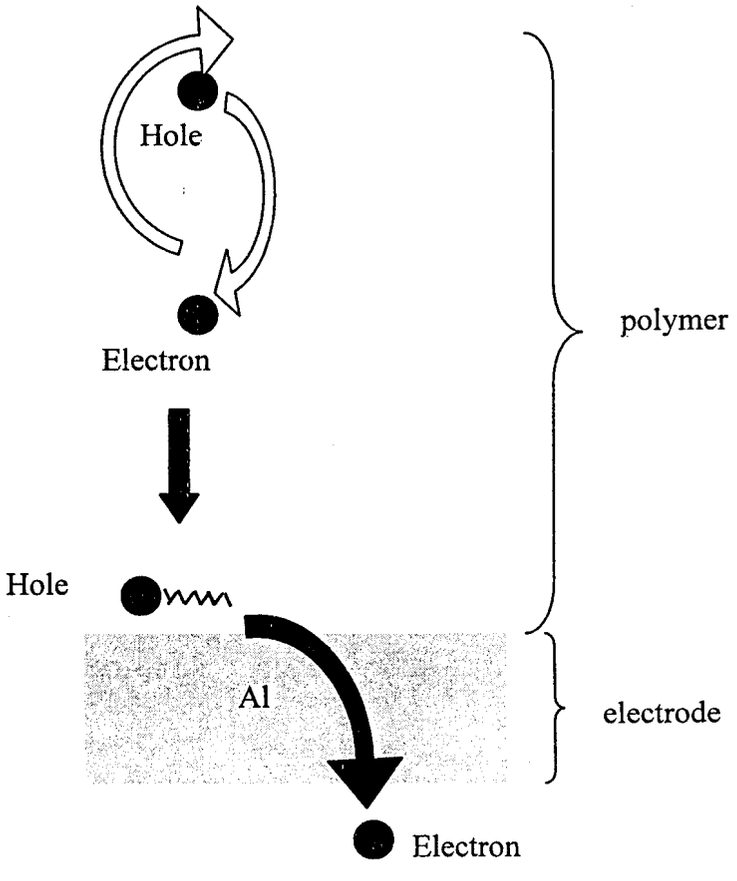

Fig (6.3): Excitons dissociate at the interface between materials having different ionization energies and electron affinities[8].

6.1.1 Design principle

The lifetime of excitons is short and only excitons that are formed within ~10 nm of the junction will ever reach it. Hence, when considering the mobility range of charge carriers in CPs (10^{-7} to 0.5 $cm^2V^{-1}s^{-1}$) their lifetime is in the region of picoseconds[8]. By creating interfaces among CP molecules of differing electron affinities, it is possible to enhance the probability of electron transfer between molecules. Interpenetrating networks of electron-accepting and electron-donating polymers can be used in the place of polymer/metal heterojunctions. Research into polymeric photovoltaics is at an early stage and we shall briefly describe such a device formed using a metal/polymer/metal structure, as depicted in figure 6.4[9].

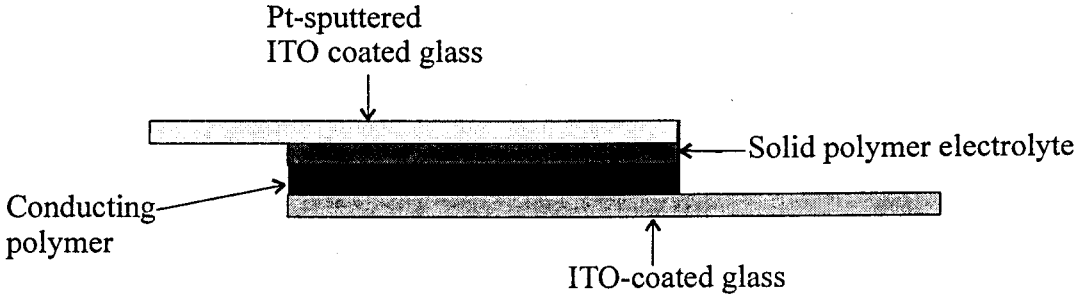

Fig (6.4): Construction of a photovoltaic device[9].

Although the photoelectric conversion of these devices is not high (2 % for polythiophene in sunlight), they can be used as sensors and for photoelectric devices. Recent advances in the efficiency of solar cells, based on organic dyes, encourages the development of devices with high performance at low cost[1]. The problem with durability could be overcome in the future by both fundamental and application-directed research. The variety of polymeric and organic materials should promise to open a new era of photoelectric conversion devices[8].

6.2 Organic light emitting devices (OLED)

OLED emit light as a result of the radiative recombination of electrons and holes electrically injected into the luminous polymer, which is sandwiched between two electrodes on a transparent glass. Typical OLED are constructed by sandwiching a

layer of luminescent CP between an anode (usually Indium Tin Oxide (ITO), because of its high work function) and a cathode (metals such as calcium, aluminum or magnesium/silver alloy with work functions 2.9, 4.3 and 3.7 eV respectively) on top of a glass substrate[10]. Figure 6.5, depicts a simple design of an OLED with poly (p-phenylene vinylene) (PPV) as the electrochromic CP.

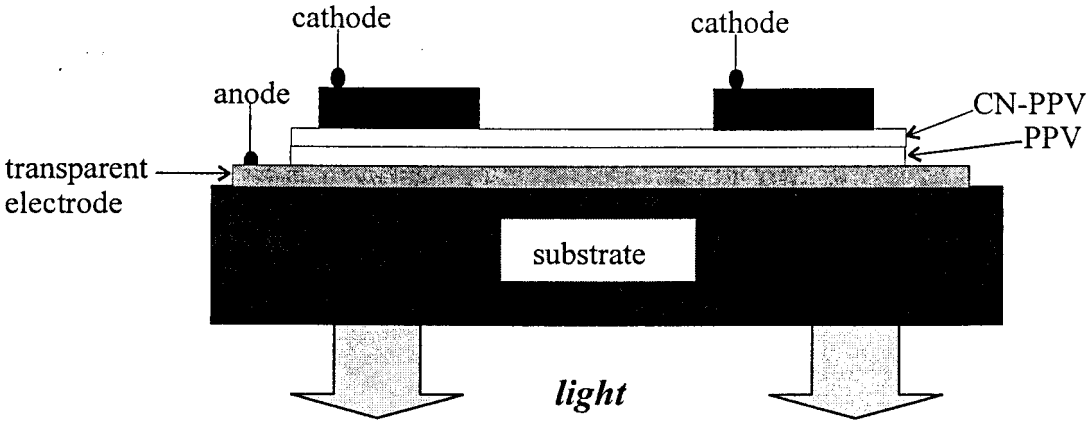

Fig (6.5): A light emitting device from CN-PPV[5]. CN-PPV stands for Poly(2,52',5'-tetrahexyloxy-8,7'-dicano-diphenylvinylene).

6.2.1 Operation

When an electric current is applied across the cathode and anode contacts, the potential developed between the electrodes ensures that electrons (negative charge carriers) flow into the polymer. Discharge of electrons by the anode results in holes being left in the polymer. Electron/hole recombination results in photon emission. The current-voltage curves of the device are diode characteristic[10]. At reverse bias conditions (ITO as the cathode and calcium as anode), charge injection is difficult and only leakage currents are measured. At forward bias, holes and electrons are injected into the polymer films from the ITO cathode and calcium anode, respectively. The energy level diagrams for such a device are shown in figure 6.6[5].

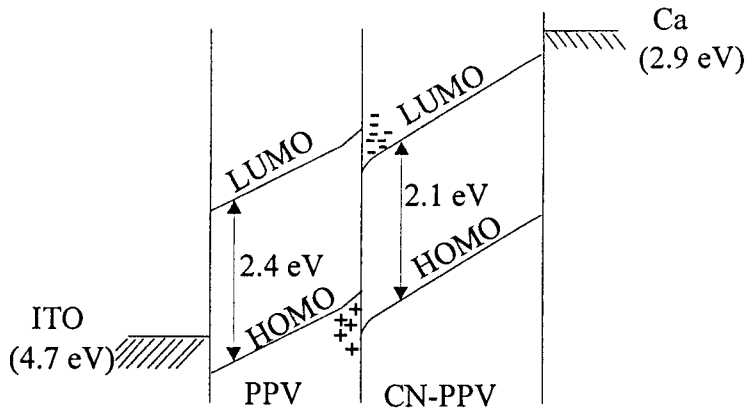

Fig (6.6): Energy level diagram for an OLED under forward bias[5].

The polymer/metal interface determines charge injection and therefore plays a crucial role in the operation of the devices. Due to a low dopant concentration the luminescent CPs are often treated as intrinsic semiconductors with a rigid band structure. The primary mode of electron injection in OLED is proposed to be field emission tunneling at high electric fields[5,10].

Applications of OLED include bright light for large area displays, alphanumeric displays and light emitting diodes[5, 10].

The advantages include: low cost, ease of fabrication, power efficiency, large surface area, bright, multi color display, mechanical flexibility and light weight[5].

6.3 Electrochromic windows

Electrochromic windows utilize the property that electroluminescent CPs such as Pan change color during electrochemical oxidation/reduction processes. For example, Pan changes color from pale yellow to green to violet and during reduction the color will change from violet to green and then to yellow[9]. By utilizing this property, the amount of light passing through a window of this material can be controlled.

Electrochromic windows are fabricated on thin semitransparent layers of conducting glass usually ITO. A schematic representation of an electrochromic window using a transparent solid polymer electrolyte is shown in figure 6.7.

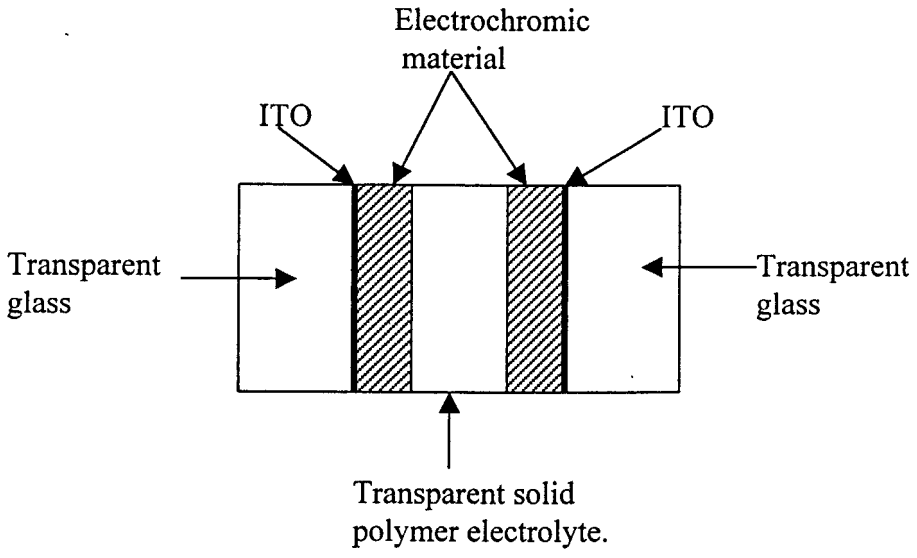

Fig (6.7): A schematic of an electrochromic window; Pan is used as the electrochromic material and polyethylene oxide containing $LiClO_4$ is used as the transparent solid polymer electrolyte[9].

Possible applications include: smart windows that are made opaque by simply applying a current, and the use by defense force industries[9].

6.4 Artificial muscles

Artificial muscles are devices made out of intrinsic CPs, which transform electrical energy into mechanical energy through electrochemical reactions occurring at the molecular level in the solid CP[4].

These electrochemomechanical actuators function by using electrochemically induced:

- changes in dimensions of the CP
- changes in relative dimensions of the polymer and a counter electrode or,
- changes in total volume of a CP electrode, electrolyte, and counter electrode[11].

When intrinsic CPs are used as electrodes in ionic media, they are oxidized and reduced in a reversible way. Linked to this electrochemical process, a reversible change in volume takes place[4]. Therefore, by applying a voltage to such a cell, its

volume can be changed in a defined manner[4]. Emerging applications include: devices for microrobotics, microvalves, microdevices and medical instrumentation (see figure 6.8: microtweezers).

6.4.1 Operation

An electric pulse, generated by electrochemical equipment, arrives via metal wires at the CP films, driving an electrochemical reaction. The device operates by the electrochemical transfer of dopant between the CP layers, separated by an adhesive ion-conducting layer[12]. The electrochemical reaction promotes a change in the volume of the film, giving a concomitant macroscopic movement of the bilayer and mechanical energy. The electrochemical reaction is linked to the conformational changes of the polymer chains together with a flow of ions and water through the polymer - solution interface[4].

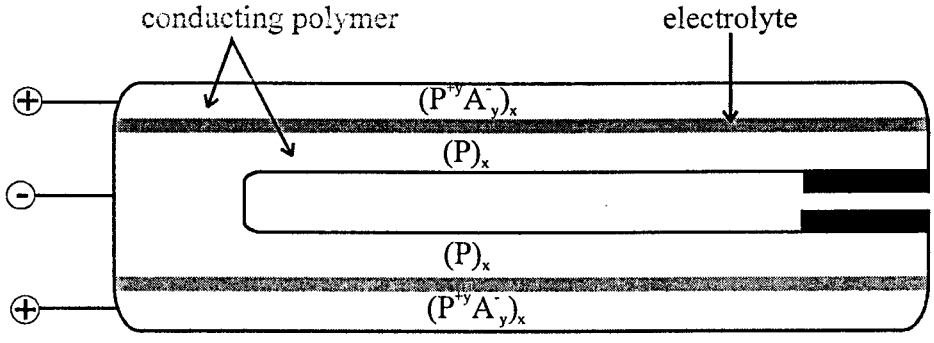

Fig (6.8): Paired bimorph actuators used as micromechanical tweezers. $(P)_x$ represents any CP, e.g. Pan and $(P^{+y}A^{-}_{y})_x$ represents a CP doped by an anion A^-. Electrochemical transfer of dopant from the outer layer to the inner layer as a result of reversing the electrode potentials of each bimorph causes the opening of the tweezers[4,12].

Advantages of these actuators include: low voltage needed for operation (1V) compared to 100V for electrostatic tweezers and high mechanical advantage as compared with piezoelectric polymers. The disadvantages include limitation on cycle time (2.56 seconds were required to reach a 90^0 turn) for the device[12].

6.5 Humidity sensors

Recently, the demand for humidity control has increased in fields such as air conditioning systems, electronics manufacturing and drying processing for ceramics and foods[11]. However, commercial humidity sensors are far from satisfactory since a linear response is valid for only a limited humidity range and hysteresis is often involved in the measurement of the response and humidity curves[11].

A humidity sensitive film has been synthesized consisting of soluble Pan 0.28% volume and 99.72% polyvinylene alcohol (PVA). The conductivity of Pan – PVA composite was proportional to the relative humidity, and the linearity was valid from 3×10^{-5} to 1.5×10^{-1} S/cm. The conductivity of the composite film varied depending on the doping level of Pan, which was dependent on the concentration of water molecules around the conducting polymer[11]. The conductivity versus humidity curves for Pan-PVA composites are shown in figure 6.9.

The excellent linear dependency of conductivity on humidity, reflecting the reversible incorporation and ejection of water molecules occurring in the composite film, is favorable for the construction of a humidity sensor[11].

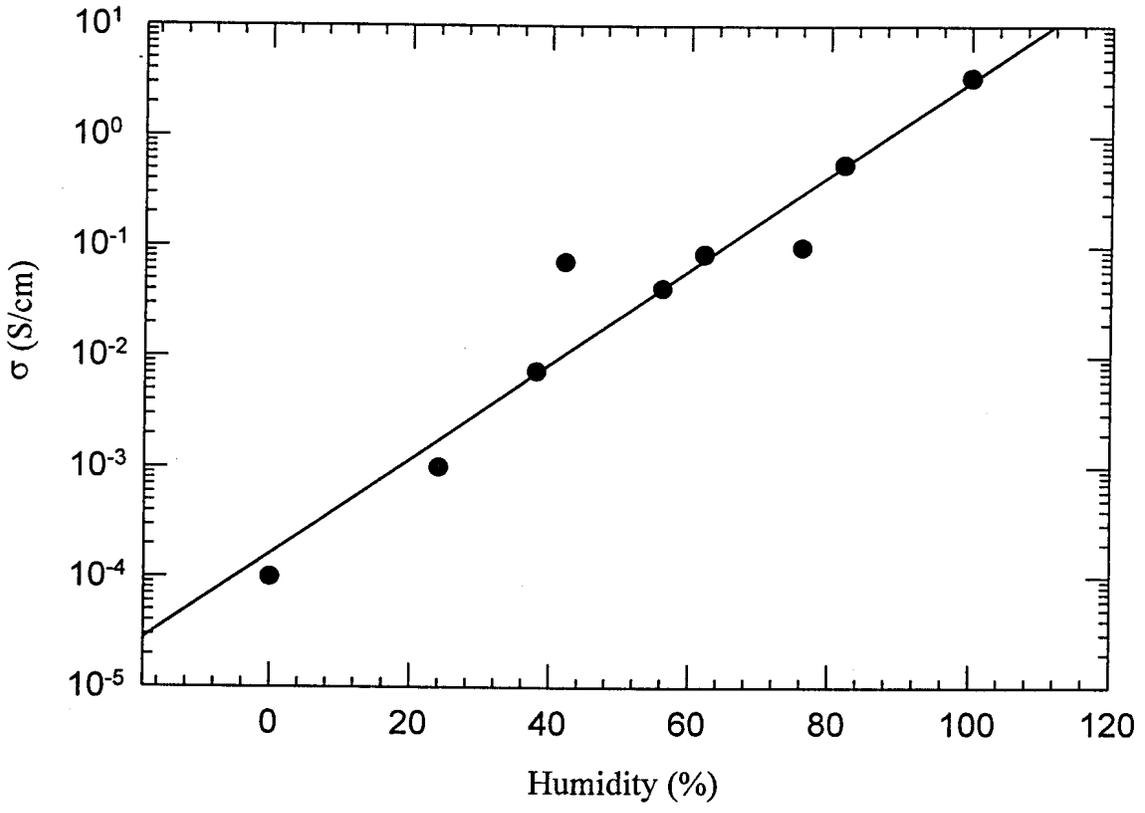

Fig (6.9) A schematic illustration of the relationship between humidity and temperature of a Pan–PVA composite film[11].

6.6 Corrosion prevention

The use of CPs as anti-corrosion coatings addresses the following issues, which the traditional methods (coating the metal with a material, chemical "conversion coatings" and cathodic protection) do not:

- Environmental issues, such as the unacceptability of chromates (used in conversion coating).
- Ease of application and practicality, e.g. contrary to cathodic protection.
- Cracks and pinholes, as well as slow corrodant diffusion to the metal surface. This problem is rampant in the conventional coating.

A CP, such as Pan, can be used to coat metal surfaces in order to prevent corrosion. Various methods are used for coating, including painting with the polymer, spraying and dipping the metal in liquid polymer. The use of a CP coating on a metal creates a built-in electric field, resulting from the interfacial, positive dipole space charge

layers[5]. This creates a force (F = -eE, figure 6.10), that opposes electron transfer from the metal to oxidizing species in the external environment (such as oxygen). A bending of the CP bands occurs at the metal/CP interface (figure 6.11)[5]. An important and distinctive feature of this method is that the electric field created is intrinsic and extends up to 250 μm in dimension (the field extends across small pinholes and cracks) providing protection[5]

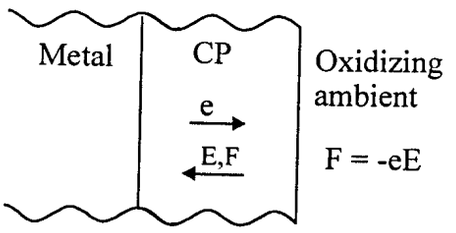

Fig (6.10): The metal/CP interface, showing the intrinsic electronic barrier to corrosion generated by the coating of CP[5].

Promising applications are in the industrial cooling-water treatment plants where phosphates and heavy metal salts traditionally used raise environmental pollution concerns[3, 5].

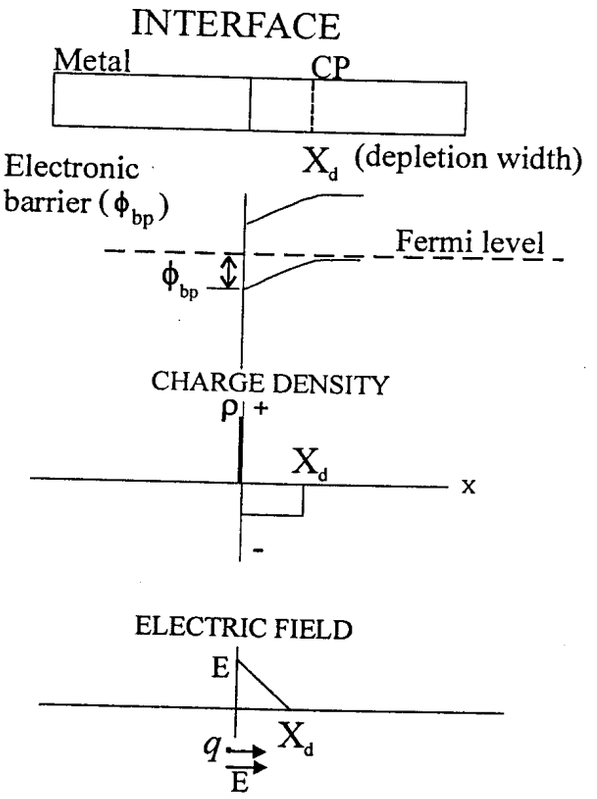

Fig (6.11): The metal/CP interface, showing band bending and development of interfacial space charge and electronic barrier to corrosion[5].

Reference:

1. J. Joo, A. J. Epstein, App. Phys. Lett. **65**, 2278 (1994).
2. O. A. Sadik, Electroanalysis **11** Number 2, 839 (1998).
3. A. J. Epstein, MRS Bulletin **22**, 16 (1997).
4. T. F. Otero, Handbook of Organic Conductive Molecules and Polymers **4** (Ed. H. S Nalwa), John Wiley and sons: New York (1997).
5. Conducting Polymer Fundamentals and Applications, (Ed. P. Chandrasekhar), Kluwer academic publishers: Boston (1999).
6. D. C. Trivedi, Handbook of Organic Conductive Molecules and Polymers **2** (Ed. H. S Nalwa), John Wiley and sons: New York (1997).
7. K. Gurunathan, R. Marimuthu, D. P. Amalneker, Mat. Chem and Phys. **61**, 173 (1999).
8. http://pubs.acs.org/hotartcl/ci/oo/apr/065wallace.html
9. E. Kim, S. B. Rhee, Electrochem. Soc. **144**, number 1, 227 (1997).
10. Masao Kaneko; Handbook of Organic Molecules and Polymers **4** (Ed. H. S Nalwa), John Wiley and sons: New York (1997).
11. F. Krok, Mat. Sc. Forum **122**,150, Ed. J. Przyluski & S. Roth, (1993).
12. R.H. Baughman, L.W. Shacklette, Science and Application of Conducting Polymers, 52, (Ed.: W R Salaneck), Bristol: England (1991).

Chapter 7

Experimental Techniques

In order to determine charge transfer phenomena in CPs, direct current (DC) current-voltage measurements were done on Pan films and pellets at temperatures above 300 K and at low temperatures down to 30 K. Fourier transform infrared spectroscopy (FTIR) and thermal analysis methods were applied to determine the effect of annealing on the polymer. The following types of Pan were used in the present work:

- Electrosynthesised Pan (HCl doped).
- Chemically synthesized Pan (HCl doped).
- Commercial Pan (Aldrich).

Chemically synthesized and commercial Pan were available in both the doped and undoped form. The undoped form was dissolved in N-methyl-2-pyrrolidinone (NMP) and spun to form thin films. Doped forms were pressed to form pellets and used in FTIR, thermal analysis and annealing experiments. The experimental work described in this chapter covers all the steps in electrochemical and chemical synthesis. This chapter comprises two sections,

(i) *Experimental procedures, covering polymer synthesis and*
(ii) *Experimental techniques, covering the experimental set-ups and measurements*

The flow chart, figure 7.1, summarizes the processes from polymer synthesis, sample preparation to material characterization in this work. The synthesized Pan is in its doped state, which is insoluble in most common solvents besides strong acids. To process Pan into thin films, we dedoped the chemically synthesized Pan before dissolving it in an organic solvent (NMP).

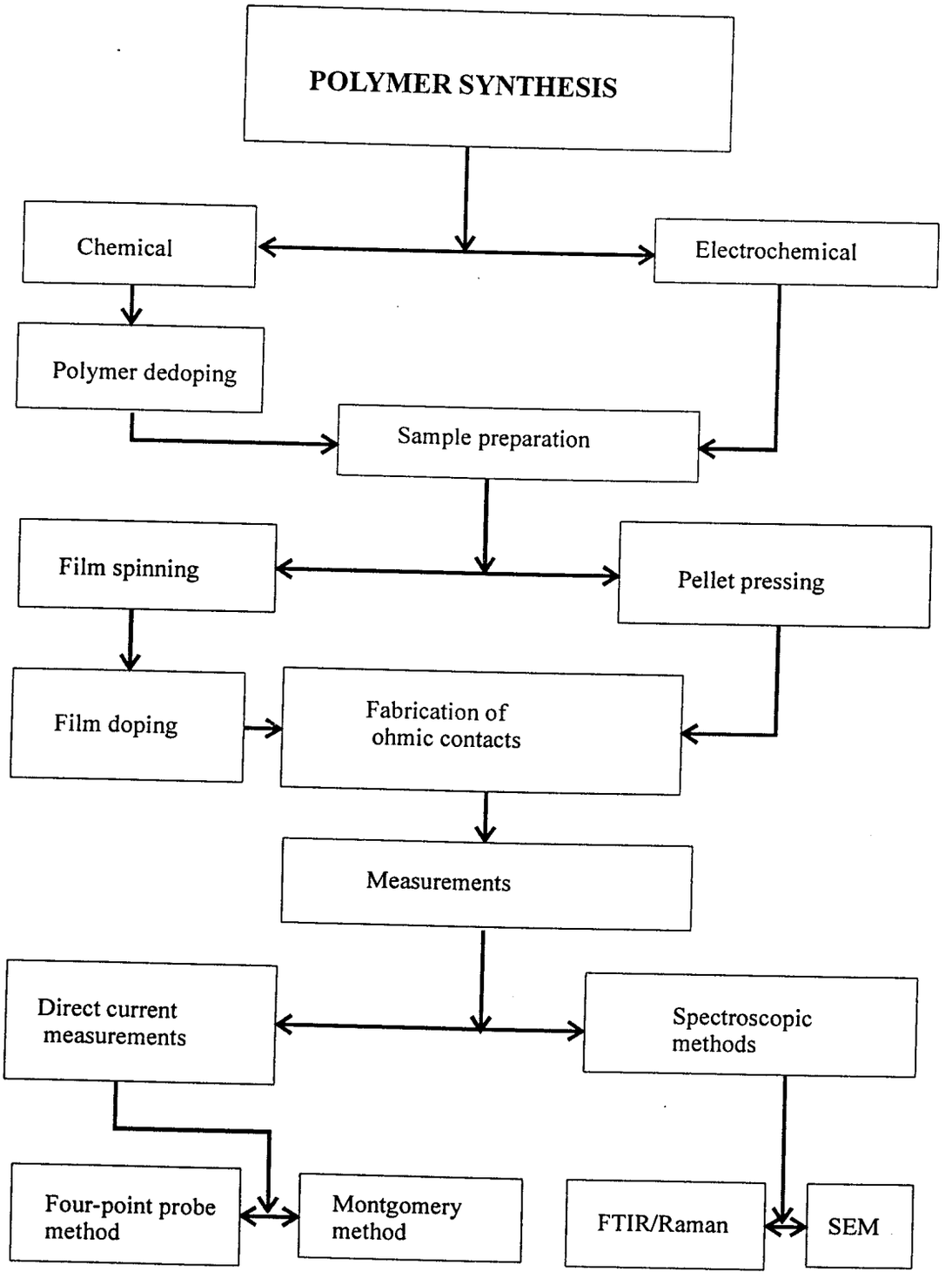

Fig (7.1): A schematic layout of the procedures used in the present work

7.1 Chemical synthesis of polyaniline

Chemical synthesis was the preferred method to obtain high quantities of the polymer. Through applying the method described below, we were able to obtain a Pan emeraldine yield of approximately 14 g. An oxidant, ammonium persulphate $(NH_4)_2S_2O_8$, was used to effect chemical polymerization of aniline under acidic conditions, pH 1-3[1]. The function of the oxidant was to withdraw a proton from an aniline molecule, without forming a strong coordination bond with either substrate/intermediate or with the final product. The selected pH conditions favored the formation of Pan, which was not suitable for the formation of strong metal chelates [1].

7.1.1 Requirements

i. 50.005 g $(NH_4)_2S_2O_8$
ii. 20.002 g aniline
iii. 750 ml 1.0M HCl
iv. excess 3 wt % NH_4OH
v. 20 liters distilled H_2O

7.1.2 Procedure

50 g of $(NH_4)_2S_2O_8$ was dissolved in 500 ml of ice-cold 1M HCl. This was added to a stirred solution of 20 g aniline in 250 ml ice-cold 1M HCl[2]. An ammonium persulphate solution was added over a time of abut 30 minutes. Stirring of the solution was continued for 2 hours after which the mixture was suction filtered using a Buchner funnel and washed with distilled water until the filtrate was colorless[2]. During washing the water level was always above the polymer coke to prevent drying which might cause uneven washing. Pan (ES) was obtained as a dark green precipitate.

7.1.3 Preparation of emeraldine base

The freshly prepared precipitate – ES was deprotonated by stirring in excess 3 wt% ammonium hydroxide solution. The deprotonated precipitate was washed in distilled water until the filtrate (EB) was colorless. To remove excess oligomeric impurities we washed the precipitate in 500 ml of acetone [2].

7.2 Glass substrate preparation

Polymer films were formed on glass substrates, which had to be cleaned initially to improve the contact between the glass and the polymer. Wax used for fixing the glass on a silicon wafer before dicing was removed by firstly heating the wafer and the glass until the wax softened. The glass was put in boiling acetone for 15 minutes and then rinsed in distilled water before immersing it in boiling propanol for 10 minutes. Finally the glass was rinsed in distilled water and blow dried with nitrogen gas.

7.3 Polymer spinning

A film of Pan was produced through spinning a drop of the polymer solution onto a glass substrate[3]. The Pan solution was prepared through dissolving Pan EB in NMP [3] until the solution saturates. It was then centrifuged for two hours at 4000 rpm to separate lumps of the undissolved polymer. This solution was then spun onto a square glass substrate at 1000 rpm [3] for a minute.

Two methods were used for film drying, drying in an oven under a fan at a temperature of 40°C and drying in a natural environment at room temperature for 48 hours. An average film thickness of 50 μm was obtained. Pan films were used for conductivity measurements over the temperature range ($30 \leq T\,(K) \leq 300$).

7.3.1 The EC101D photoresist spinner (*instrumentation*)

The major components of the photoresist spinner are as listed below:

i. Motor controller: consists of a tachometer for controlling the speed of the spinner, a cycle timer for controlling the spin cycle and a motor speed controller that works together with the tachometer.

ii. A vacuum pump: for fixing the substrate in position.

7.4 Film doping

A thin film of EB was exposed to vapors of HCl for 1 minute. The film was doped by the vapor to green ES from purple EB. Uniform doping was ensured, through exposing both sides of the film to the HCl vapors.

7.5 The depth profiler

An Alpha-Step 200-depth profiler measured the thickness of soft Pan films spun onto glass slides. Thickness was analyzed as the difference in the height between the virtual zero level and the surface of the film. Figure 7.2 illustrates the movement of a stylus in measuring thickness.

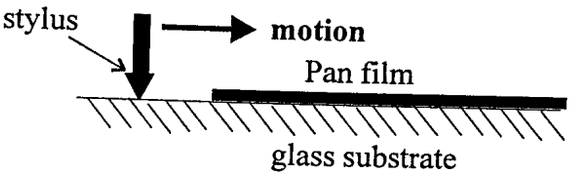

Figure (7.2): Stylus motion during thickness measurement

The Alpha-Step 200 samples up to 2000 data points on each scan, providing up to one sample every 400Å. It can identify discontinuities in the film in tens of Angstroms and can measure surface profiles below 200Å and up to 160 microns.

7.6 Electrochemical synthesis of polyaniline (Pan)

The anodic oxidative polymerization of aniline is the preferred method to obtain a clean and thin coherent film of Pan [1,4]. Electrochemical synthesis was achieved by sweeping the potential between two potential limits – 0.2 to 0.8 V versus silver in silver chloride (Ag /AgCl) counter electrode at a scanning rate of 50 mV/s [1, 5, 6, 7]. The electrolyte was a solution of 0.2M aniline in 1.0M HCl with a pH of about 1. Dark green Pan (ES) was deposited onto the anode [7].

After removing electrodeposited Pan (ES) from the platinum electrode by stripping it off with a blade, the electrodes were cleaned of excess polymer by immersing them in nitric acid until the polymer disappeared. Then a process involving rinsing the electrodes in distilled water, boiling in acetone for about 5 minutes followed by immersing them in boiling propanol was applied. Finally, the electrodes were rinsed in distilled water.

7.6.1 Instrumentation

The electrochemical cell is constructed from a vessel containing a solution of a monomer (aniline) together with an acid (HCl) [4]. Electrochemical polymerization was carried out using an EG & G Model 362 scanning potentiostat. A three-electrode cell was employed with platinum foils (2 cm x 2 cm) used as both counter and working electrodes. Silver in silver chloride was the reference electrode. Pan ES deposits on the working electrode were stripped off and filtered in distilled water. Alternative cell configurations used in this work included graphite as working electrode versus platinum counter electrode, indium tin oxide as both working and counter electrodes, platinum coated glass was also used as both working and counter electrodes.

7.6.2 Problems encountered during synthesis

i. Electrochemical deposition using indium tin oxide (ITO) coated glass as working electrode and graphite rod as counter electrode produced a very small yield. It was later discovered that ITO was dissolving in the solution. We therefore decided to use platinum-coated glass instead of ITO.

ii. Using platinum coated glass also resulted in problems because platinum was easily removed by the crocodile clamp grips used to suspend the glass in the solution. Considering the cost of platinum and the deposition process, it was found economically necessary to find an alternative source of working electrode. We obtained platinum foils measuring 1.5 cm x 1.5 cm and a thickness 0.07cm.

iii. Using graphite as working electrode, Pan deposits were too loosely bound onto the electrode plate such that by withdrawing the electrode from solution, all the deposit was lost into the solution.

iv. Accumulation of air bubbles on the working electrode, which were insulating, stopped the deposition process. A suitable current of 10 mA was chosen for the potentiostat.

7.7 Deposition of metal contacts

A resistive evaporation system was used to deposit metals onto the glass substrates for the making of platinum and gold electrodes. An attempt was also made to form ohmic metal contacts on the polymer films using this method. The first and most important step was the cleaning of the glass substrates. Glass substrates were boiled in aqua regia (a mixture of hydrochloric acid and nitric acid in the ratio 3:1) for 10 minutes. The glass was then rinsed in distilled water and then boiled in trichloroethlyene (TCE) for 3 minutes. From TCE, the glass was put into boiling iso-propanol for 3 minutes, rinsed in distilled water and dried with nitrogen gas.

Deposition of thin ohmic gold films onto a glass substrate and a doped Pan surface was accomplished by use of an evaporation system. The main components of the deposition

system include a bell jar, a substrate holder, a thickness monitor, a shutter, a source, a lower shield/reflector, a transformer and a vacuum pump[8].

The gold was placed into the source and a vacuum of about 10^{-5} Torr (7 mbars) was attained before evaporation could start. The Joule heat created by the current passing through the source resulted in evaporation of the gold. The temperature was controlled through slowly increasing the current. A deposition rate of 4 Å/second was maintained through adjusting the current output. The maximum temperature on the Pan sample was maintained below 40°C.

For making platinum electrodes, platinum was deposited onto a titanium coated glass surface to a thickness of about 2000 Å. The titanium/glass substrate was first annealed at 250 °C in an argon environment to improve the adhesion between the glass and metal contact.

7.8 Electrical measurement techniques

Two methods (the four-point probe and Montgomery) were applied in the measurement of the electrical properties of Pan. In applying the Montgomery method, graphite paste was used to attach copper wires at the four corners of the sample (figure 5.2 chapter 5).

7.8.1 Fabrication of Ohmic contacts

Pan ES (Aldrich, electrosynthesised and one synthesized in our laboratory) were pressed to form pellets of thickness between 0.02 and 0.5 mm at pressures between 8 and 20 tons. The resistive evaporation technique (as explained in the previous section) was used to make ohmic contacts by the deposition of gold onto the surface of the materials through a mask to create contacts with a diameter 0.75 mm. For the Montgomery method, graphite paste was used for making the ohmic contacts, between the connecting wires and the sample surface.

7.8.2 The four-point probe method

The four-point probe method was used in the measurements of the I-V properties of Pan in pellet form, see figure 5.1, chapter 5.

A small current was passed through the outer two probes and the voltage was measured between the inner two probes [9, 10]. The current source was a model HP 3245A and the voltage source was model HP 3457A with an internal impedance of 10 GΩ. The conductivity is defined by Ohm's law, as the ratio of the current (I) flowing through the sample and the electric field (E) [9, 10]. For all pellets with dimensions W << d and d >> s, the conductivity, σ, was calculated as:

$$\sigma = I/u2\pi s \qquad [7.1]$$

Where, I is the measured current, u is the applied potential difference and s is the pellet thickness.

7.8.3 Montgomery method

In the Montgomery method, electrodes were attached at the four corners of a square polymer sample, (figure 5.2, chapter 5) [10, 11]. Current was applied on electrodes *1* and *2*, while electrodes *3* and *4* measured voltage. From the current-voltage measurements, resistivity was calculated[11]. For thin samples resistivity is expressed as:

$$\rho = Hl_3R \qquad [7.2]$$

where H is a function of l_2/l_1. The value of H used in the result analysis was 4.531, since l_1 was made equal to l_2[11]. R is the ratio (V/I) of the voltage between the two contacts and the current. After mounting the sample on the sample holder, the temperature was lowered to 30 K. Thereafter, the temperature was increased in intervals of 10 K from 30

to 380 K. For each temperature interval a set of current and voltage measurements were taken. Low temperatures were achieved using a cryostat.

7.9 Temperature controller for heating pellets

A power supply and controller supplied a voltage to an element over which a pellet of Pan rested. A feedback loop of the thermocouple was used to control the temperature and, using the temperature controller, it was able to adjust the rate at which temperature increased and the time taken between ramps. The voltage measurements were made using the four-point probe method.

7.9.1 Experimental setup

In order to anneal a pellet while monitoring the current-voltage behavior of the sample, a state of the art instrument was designed through interfacing, the four-point probe, a voltage source, a controller unit and a heating plate from "Linkman Scientific Instruments ltd." model TMS 93.

7.9.2 Operating modes

Experimental conditions were varied through use of the following operating modes of the system:

- The element was allowed to heat the pellet from room temperature to a maximum set temperature at rates typical of 20°C / min. A hold time of 10 minutes was deemed sufficient for the temperature of the pellet to homogenize. Current-voltage measurements were done within the 10^{th} minute.
- The heating element was able to heat the sample at different ramp rates. Different rates from 5 °C/min to 20 °C/min were used. The voltage was measured using the four-point probe technique.

- A current of 8×10^{-4} A was maintained on the pellet. Whilst the temperature rose at a rate of 5°C / minute, I-V measurements were taken.

7.10 Thermal analysis techniques

Thermal analysis is the measurement of changes in the physical properties of a substance as a function of temperature, whilst the substance is subjected to a controlled temperature variation[12]. Different samples and different conditions may alter the mass loss/temperature relationship and, for this reason, we used the simultaneous thermal analysis technique. This involved measuring the temperature and mass changes on the same portion of the polymer sample during a single temperature program[13]. Differential scanning calorimetry (DSC) and thermogravimetry analysis (TG) were performed simultaneously in this work.

7.10.1 Thermogravimetry (TG)

Thermal gravimetry was used in the detection of changes in the mass of the sample by reaction or evaporation. The mass of the sample is monitored against time or temperature while the temperature of the sample, in a specified atmosphere, is changed[12].
The apparatus comprises four main parts[12]:

- An electro-balance and its controller
- A furnace and temperature sensors
- A computer
- A data acquisition device[12].

Deviation of the balance beam from the null-position is measured using an electro-optical device with a shutter attached to the balance beam. The shutter partly blocks the light beam between the source and a photocell. Movement of the beam alters the light intensity on the photocell and the amplified output from the photocell is a measure of mass change[12].

7.11 Infrared spectroscopy

Fourier-transform infrared spectroscopy (FTIR) allows wavenumbers in the range 400-4000 cm^{-1}. Fourier transformation, is used to convert the measurement (interferogram) into a spectrum of the polymer. The region 400 to 4000 cm^{-1} is considered to be the mid-infrared region where vibrational and rotational bands are observed[14]. The effect of temperature and the period of heating on Pan salt and the base form were analyzed using FTIR spectroscopy.

7.11.1 FTIR Instrumentation

The optical system features a modular construction of the vacuum cabinet with infrared radiation focused on a beam splitter with an effective diameter of 10 mm. Interferograms were recorded at a vacuum of 100 mBar.

7.11.2 Sample preparation for FTIR

1000 mg of potassium bromide (KBr) kept at 100 °C in an oven was mixed with 50 mg of Pan. The mixture was finely ground in a pastel and mortar. A pellet was formed by pressing the KBr/Pan powder at a pressure of 8 tons[15].

References

1. D.C. Trivedi; Handbook of Conductive Molecules and Polymers **2**, 510, (Ed. H. S Nalwa), (Ed. H. S Nalwa), John Wiley and sons, New York (1990).

2. S. S Hardaker, X. Wang, R. V. Gregory, Pol. Prints **39**, 123 (1998).

3. Loon-Seng Tan, S. R. Simko, Pol. Prints **3**, 2 (1998).

4. A.G MacDiarmid, W. Zheng, MRS Bulletin **22**, 29 (1997).

5. Yen Wei, Yan Sun, Xu Tang, Poly Print **3**, 1 (1989).

6. M. Lapowski, Mat. Sc. Forum, **122**, 51 (1993).

7. V.C. Ngu Yen, K. Potje-Kanloth, Thin Solid Films **338**, 142 (1999).

8. E.B Graper, Handbook of Thin Films Processing Technology, A1.11: 1-A1.1: 2, (1996).

9. S. M. Sze, Physics of Semiconductor Devices, (Ed. S.M. Sze), New York (1981).

10. W. Pukacki, Mat. Sc. Forum **122**, 261 (1993).

11. H. C. Montgomery, J. App. Phys. **42**, 2971 (1971).

12 Thermal Methods of Analysis-Applications and Problems, (Ed. P.J. Haines), London: Chapman and Hall (1992).

13. Introduction to Thermal Analysis – Techniques and Applications, (Ed. M. E. Brown), New York: Chapman and Hall (1990).

14. S. Bandyopadhyay, J. App. Phys. **85**, 3671 (1999).

15. Practical Sampling Techniques for Infrared Analysis, (Ed PB Coleman), Boca Raton: CRS Press, (1993).

Chapter 8

Results

Experimental results aimed at determining the charge transfer characteristics of CPs are presented in this chapter. The present work uses methods ranging from simple four-point probe conductivity measurements to conductivity measurements using the Montgomery method in the temperature range 30 – 450 K. Charge transfer at low temperatures is important in the determination of whether conductivity is metallic, semiconducting or insulating and also for the one, two or three dimensionality of conductivity in the material. In the light of this, several models shall be tested for fitness to the observed conductivity. Conductivity determining factors such as moisture content of the material, temperature, homogeneity of the material, geometrical forms of the sample, synthesis conditions and pressure used in the pressing of pellets are dealt with. These conductivity-determining factors are crucial and need to be mentioned when stating a sample's conductivity.

We used four types of Pan, commercial Pan (doped by camphor sulfonic acid (CSA)), electrochemically synthesized (doped by HCl), commercial Pan (doped by HCl) and chemically synthesized Pan (doped by HCl). Due to the low yield of electrosynthesized Pan, our work was based on the commercial forms of Pan and the chemically synthesized Pan.

8.1 Determining the mode of charge transfer

Measurements were made to ensure that no significant contribution to conductivity was occurring due to ionic conduction (drift of negatively and positively charged ions), by passing a constant current through a Pan pellet and monitoring the potential difference as a function of time using the four point probe method. As table 8.1 shows, there is no significant change in voltage with time for a constant applied current. We conclude from

these preliminary and important results underlying this work that conduction in Pan is predominantly electronic and that contribution to charge transfer from ionic mechanism are not of significance. In the event of ionic conduction, the potential difference would increase as the ions get depleted.

Table 8.1: Variation of voltage with a constant current of 2 x 10^{-5} A

Time (min)	*Voltage (mV) ± 0.01*
0	0.084
1	0.084
16	0.084
70	0.085
4320	0.085

8.2 Conductivity of Pan pellets at room temperatures

Pan powder (chemically synthesized and HCl doped) was compressed at 7.4 x 10^7 Pa to form pellets with an approximate diameter of 12 mm and a thickness of 0.22 cm. Figure 8.1 illustrates room temperature voltage/current characteristics of three pellets pressed from the same batch of powder. The procedures discussed in section 7.5 were used in acquiring these results. This figure indicates that the conductivity of Pan is ohmic at room temperature.

It must be noted that for pellet samples no congruent relationship exists between conductivity and thickness (table 8.2). However as table 8.3 shows for Pan film samples at room temperature, conductivity increase with film thickness[1].

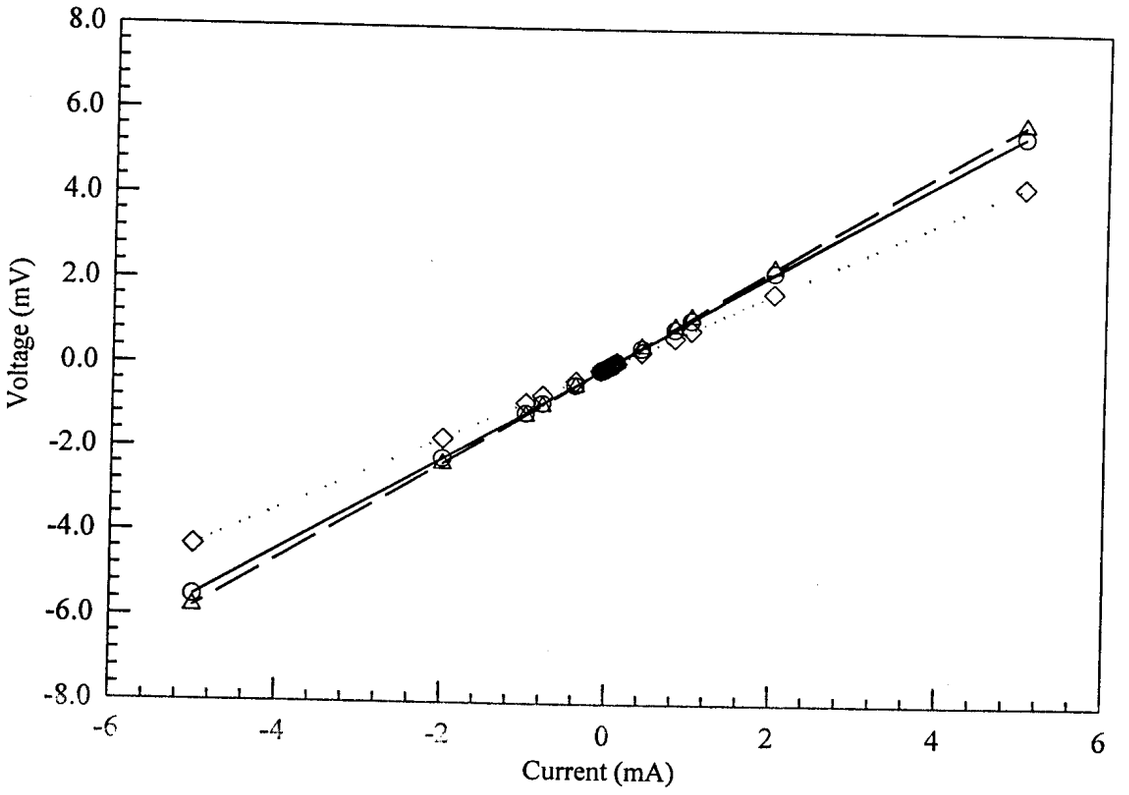

Fig (8.1): Room temperature current-voltage characteristics for three 0.022 cm thick Pan pellets pressed at 7.4 x 10^7 Pa.

Table 8.2: Conductivity of several pellets at room temperatures.

Sample	*Thickness (cm) ± 0.001*	*σ (S/cm) ± 0.2*
1	0.022	12.9
2	0.022	11.1
3	0.022	10.0
4	0.04	6.64
5	0.041	5.9
6	0.051	8.43
7	0.046	5.54
8	0.100	5.96
9	0.178	3.19
10	0.211	2.81

Table 8.3: Film thickness/conductivity relationship

Thickness ($\times 10^{-3}$) cm	*σ(S/cm)*
50	1×10^{-10}
100	1×10^{-7}
200	1×10^{-4}
300	1×10^{-4}
400	0.01
500	0.1

8.3 The effect of the temperature range, (30 < T (K) < 300), on the current-voltage properties of chemically synthesized Pan

It has been shown that temperature has an effect on the current/voltage characteristics of Pan[1,2]. The behavior of Pan has been determined as temperature varies from 30 K to 300 K using the Montgomery method. Currents up to 1 mA were applied over the temperature regime.

The spectra displayed in figures 8.2 ([A] and [B]) and figures 8.3 ([C] and [D]) illustrate the change in the current-voltage characteristics as the temperature increases from 30 K (figure 8.2 [A]) to 280 K (figure 8.3 [D]). As shown, the current-voltage characteristics of the material attain a direct relationship as temperature approaches 300 K (that is current/voltage spectra will be a straight line) for the particular fixed current range. The use of current values above 1 mA during the current-voltage measurements results in a heating effect due to the low conductivity of the polymer, thus measurements were restricted to reasonably low applied currents.

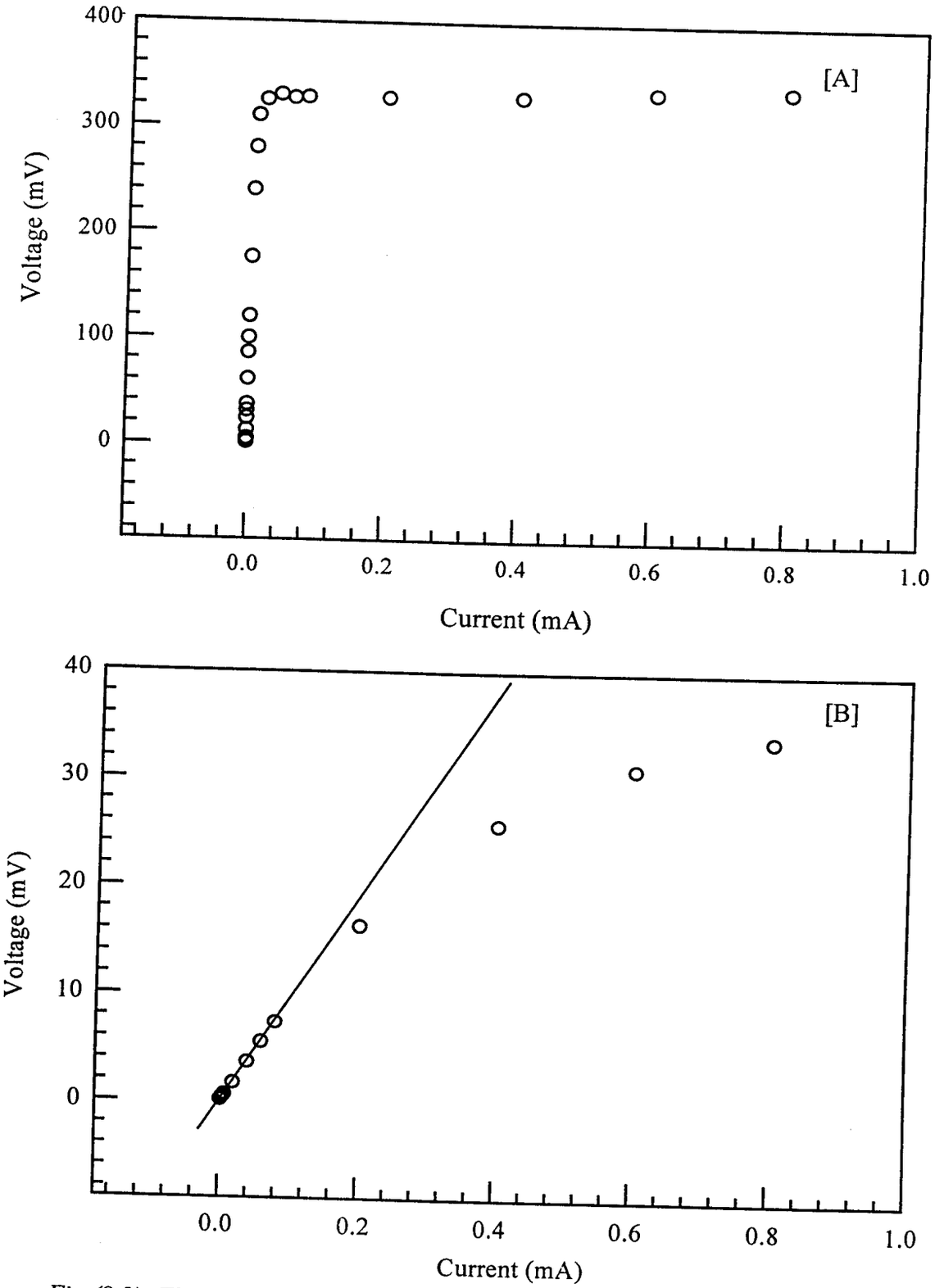

Fig (8.2): The current–voltage characteristics of chemically synthesized Pan at 30 K [A] and 80 K [B].

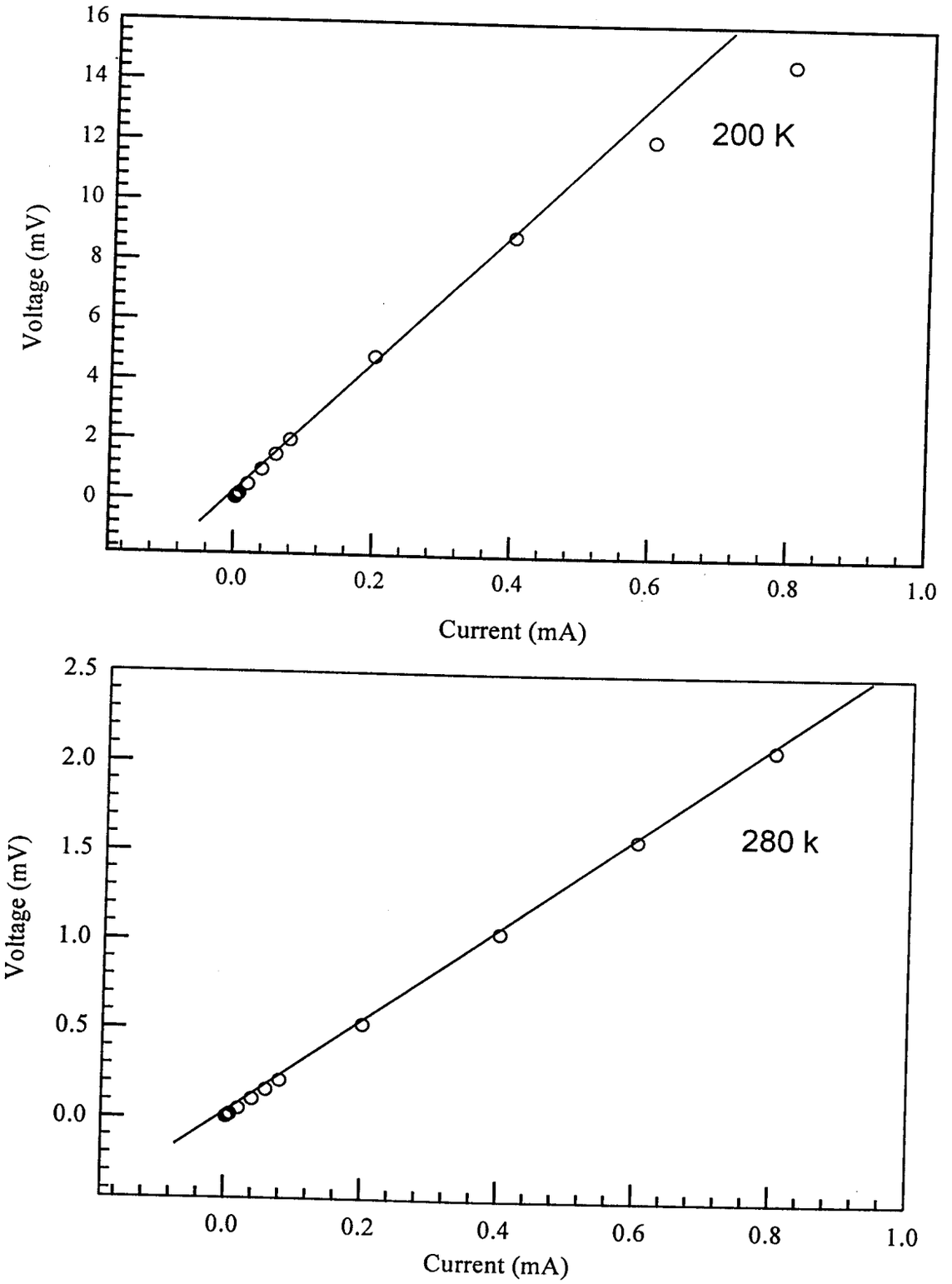

Fig (8.3): The current–voltage characteristics of chemically synthesized Pan at 200 K [C] and 280 K [D].

8.4 Scanning electron microscopy (SEM) images of Pan

SEM images of a Pan film and a pellet are shown in figure 8.4. Different magnifications were used because of the different surface profiles of the film and pellet. Magnifications above (× 1,000) did not provide further significant information for the film. The surface image of the pellets indicates the existence of cracks and inhomoginity in the bulk of the pellet, while the film has a uniform homogenous morphology.

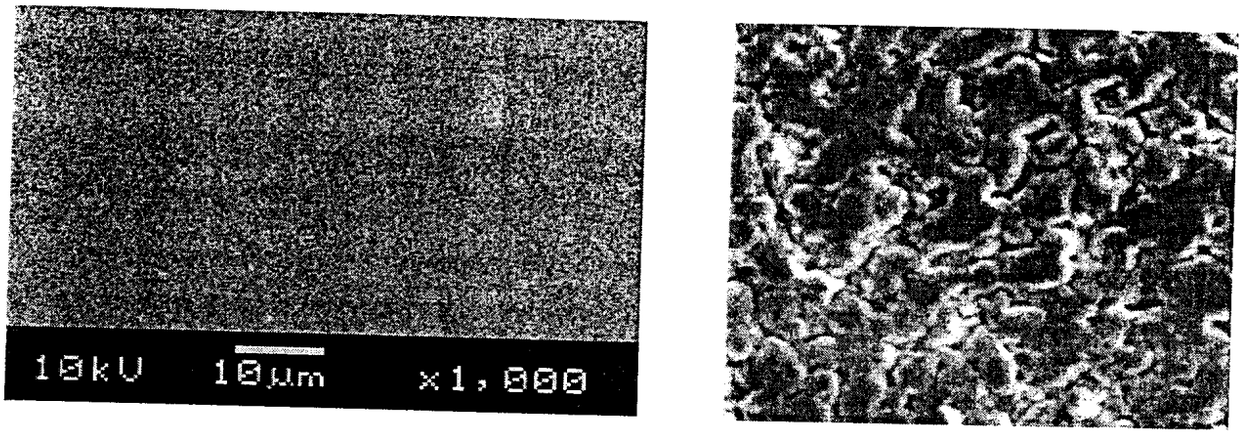

Fig (8.4): The surface images of Pan film (left) and pellet (right) pressed at 7.4 x 10^7 Pa

There is a limitation on conductivity caused by structural defects in the pellet. These results compelled us to measure conductivity at different positions on the pellet surface.

8.5 Positional conductivity for Pan pellets

The four-point probe method was used in obtaining conductivity results for different points on the same pellet, in so as to determine if the conductivity varied with location on the pellet. In this work chemically synthesized Pan was used. Due to the small size of the pellets, only three successive positions (1, 2 and 3) were used as indicated in figure 8.5. Further, table 8.4 outlines the results obtained in the case of two pellets (A and B).

It was observed that the conductivity at different positions on the pellet surface was not always the same. A possible explanation for this positional dependence of the conductivity for the pellet could partly be due to the surface inhomogenity as shown in figure 8.4.

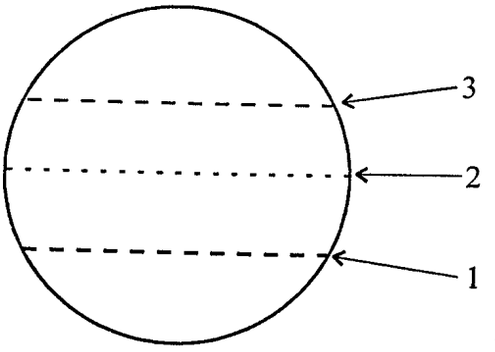

Fig (8.5): The positions on the pellet surface1, 2 and 3.

Table 8.3: Variation of conductivity (σ) on measurement position for Pan pellets (pressed at 47.4 x 10^7 Pa).

Pellet	*Thickness (cm) ± 0.005*	σ_1*(S/cm)*	σ_2*(S/cm)*	σ_3*(S/cm)*
A	0.040	5.58	4.83	6.64
B	0.051	8.43	7.59	8.34

8.6 The effect of pellet pressing pressure on conductivity

Measurements were performed to determine the effect of pressure used in the making of pellets on the conductivity.

The effect of pressure on conductivity can be visualized as denser packing of the material, enabling greater inter-chain contact in fibrilllar CPs. In theoretical terms, the electronic overlap between extended conjugation regions within the chain is partially

extended between chains and between fibers[1]. Pressures ranging from 7.4 x 10^7 to 17.6 x 10^7 Pa were used in pressing pellets. The relationship between conductivity and pressure for Pan in pellet form is shown in figure 8.6.

Within the pressure range used for this study (7.4 – 17.6) x 10^7 Pa there was no indication of a relationship between pressure and conductivity, (3 samples were produced for each pressure reading). However, a study of thin Pan films at pressures up to 22 GPa at room temperature appeared to show enhanced inter-chain charge transport due to sample compression[2].

Figure 8.6, also illustrates that the conductivity of pellets pressed under the same pressure are not necessarily of equal value and there is no clear relationship between pressure and conductivity.

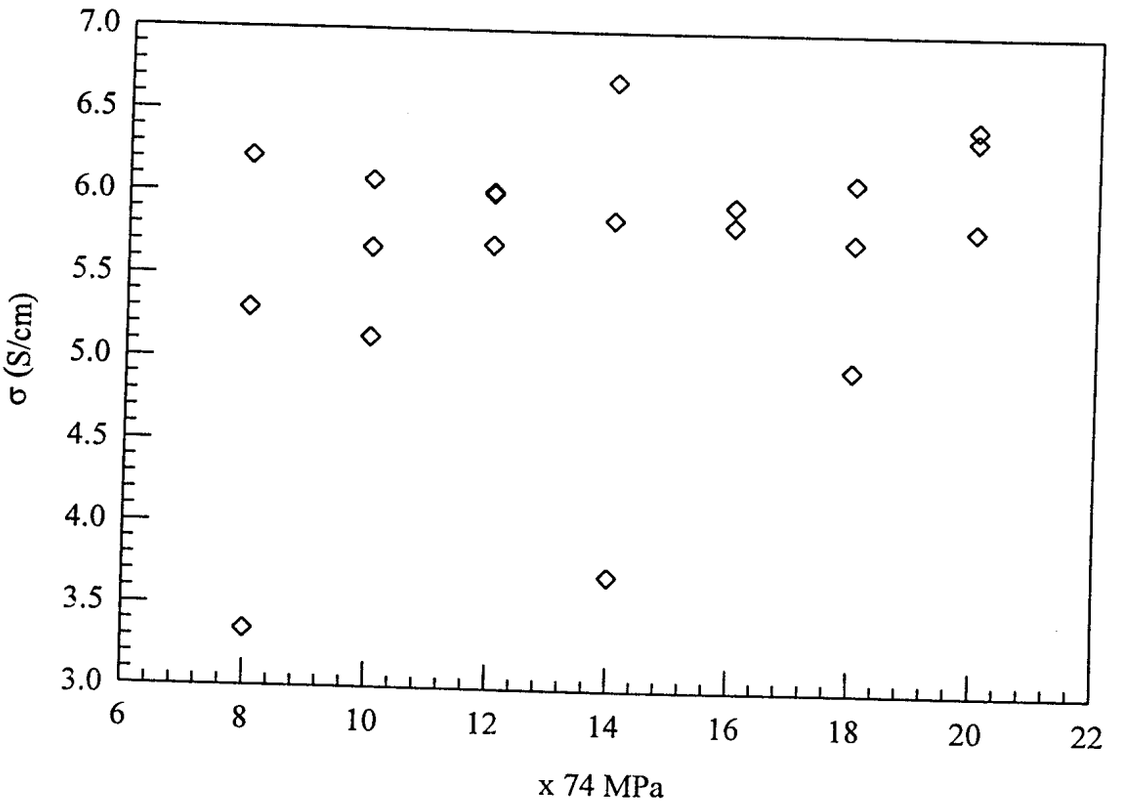

Fig (8.6): The relationship of pellet pressure and conductivity.

8.7 The generalized response of Pan (CSA and HCl doped) in both pellet and film form to annealing

Several factors including, temperature, dopant, moisture content, synthesis conditions and synthesis method differentiate the conductivities of Pan (CSA) and Pan (HCl). One of the aims of this study was to determine if these types of Pan display a generalized behavior under similar conductivity determining conditions. The Pan samples were analyzed at temperatures from 30 to 300 K.

Figure 8.7, illustrates the conductivity-temperature relationship of Pan (CSA) pellet, over the temperature range 30 – 300 K, measured using the Montgomery method. Results indicate; conductivity is responsive to temperature variations above 100K as the graph indicates.

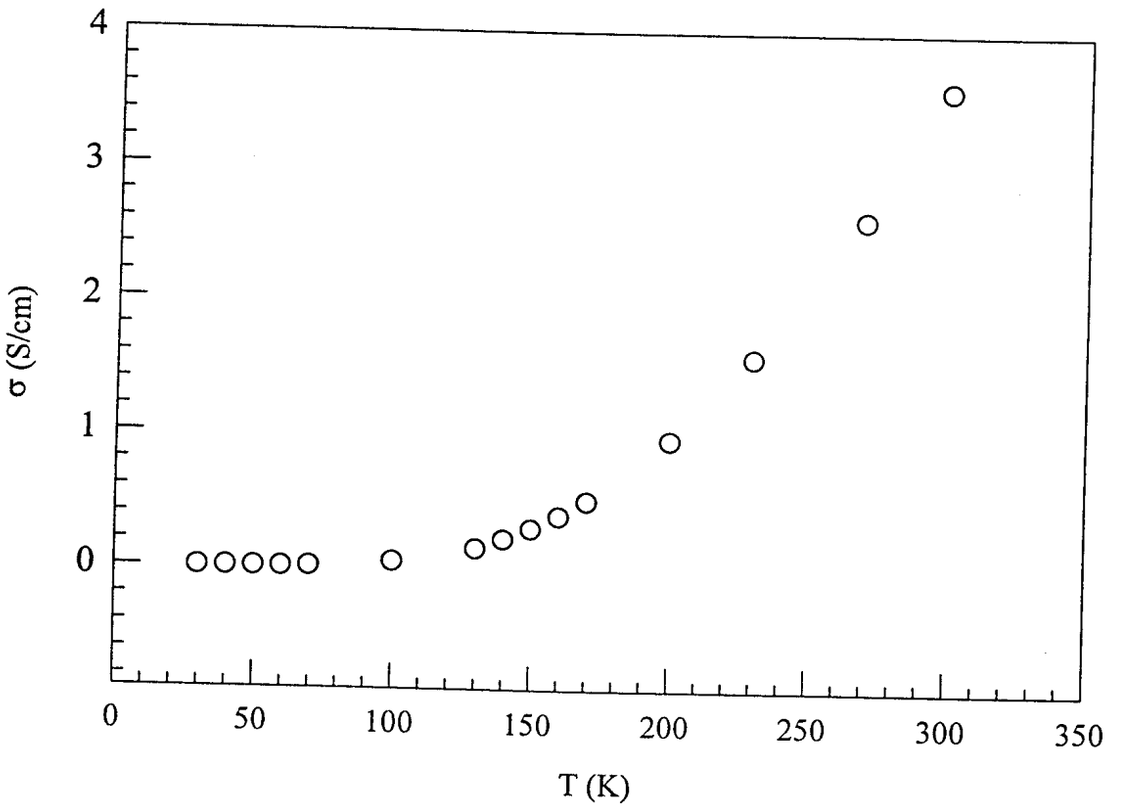

Figure (8.7): Response of Pan (CSA) pellet to temperature variations.

Preliminary experiments, involving annealing a pellet and comparing its current-voltage characteristics before and after annealing (figure 8.8), show an increase in resistance due to the annealing process. The sample was annealed at 373 K for 10 minutes.

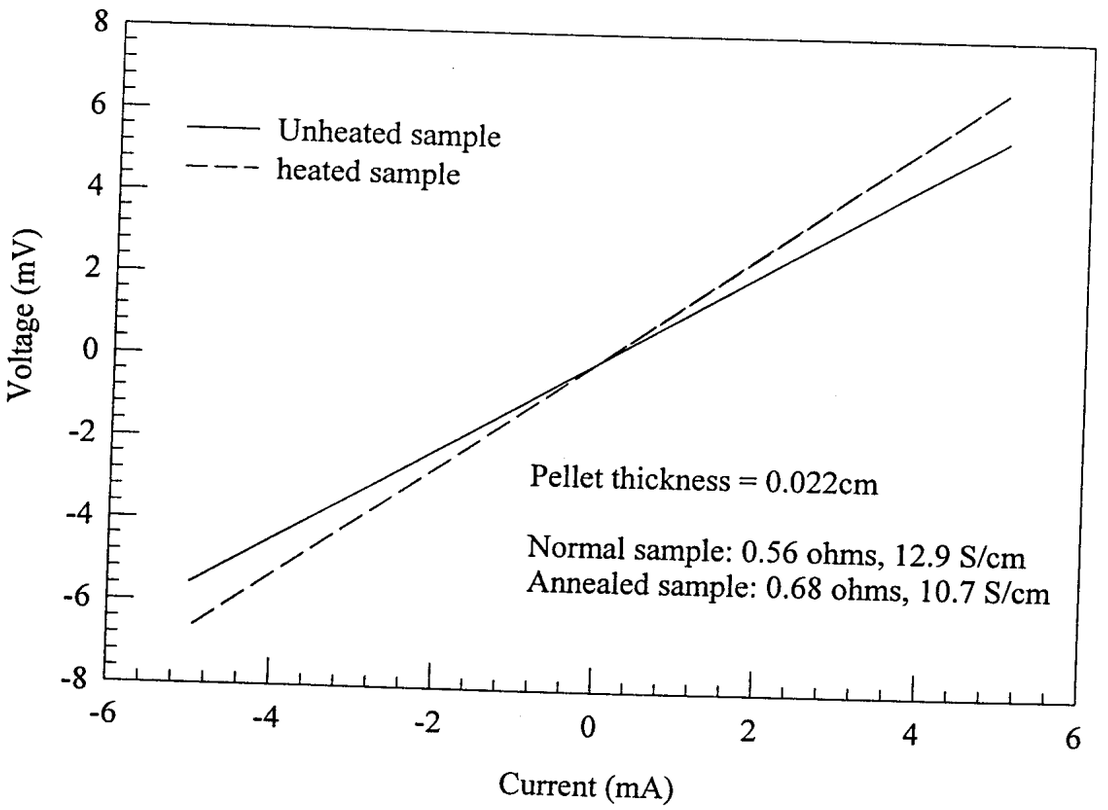

Fig (8.8): Influence of heating on the current-voltage characteristics of a Pan pellet

Further, investigations were done to determine the behavior of the Pan's conductivity as a function of varying temperature. Figure 8.9, illustrates the conductivity-temperature characteristics of Pan (CSA) from 300 to 380 K. The material's conductivity increases with increase in temperature, until approximately 328 K, where after it decreases.

The temperature dependence of conductivity from 300 to 325 K is linear. The decrease in conductivity from 335 to 380 K shows linear temperature dependence and is typical of metals. It would appear that the point $\delta\sigma/\delta T \cong 0$ is a semiconductor/metal transition

region. The point at which $\delta\sigma/\delta T \cong 0$ depends on a number of factors. The following section illustrates that sample annealing rate has a substantial contribution.

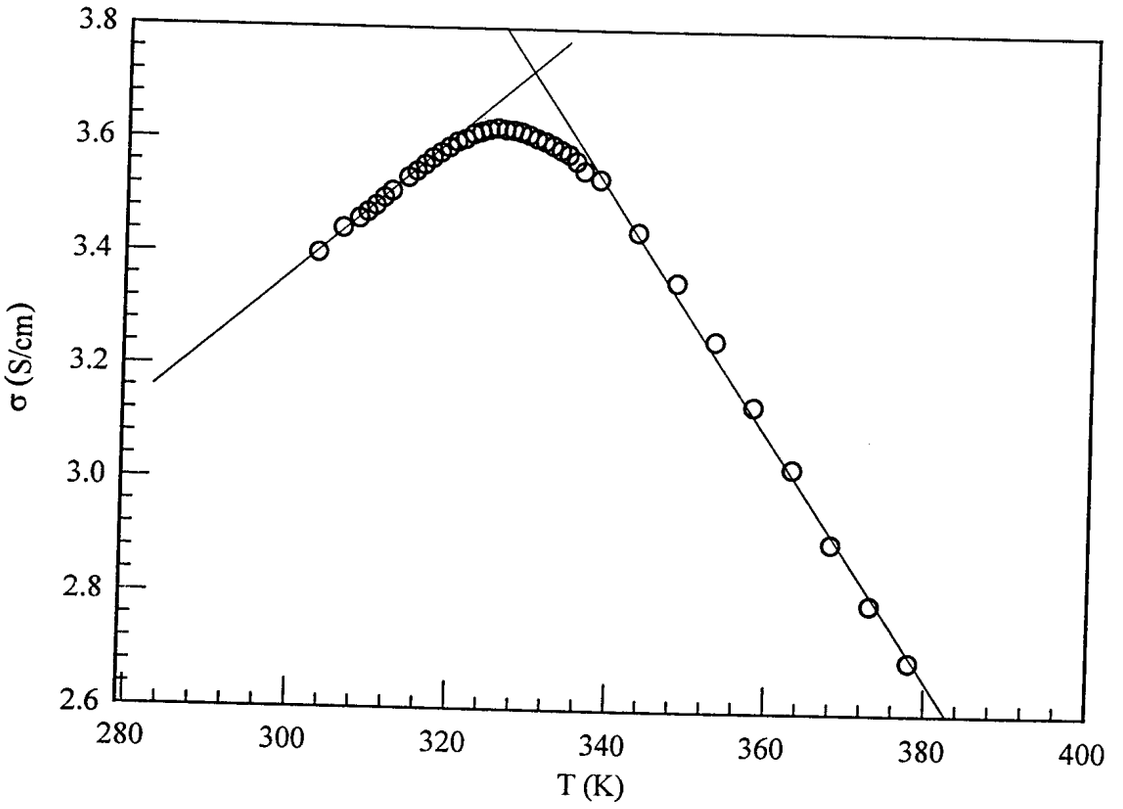

Fig (8.9): The temperature dependence of the conductivity of Pan material.

Thermal analysis shall be used in evaluating the conductivity-temperature relationship. This will be done in order to relate the change in conductivity to the mass loss of the polymer and other possibilities of polymer thermal degradation due to annealing processes.

8.7.1 Response of Pan (CSA) and Pan (HCl) doped to annealing temperature

The reproducibility of the electrical properties of Pan samples is illustrated in the case for Pan pellet and film samples. The conductivity-temperature characteristics of Pan in film

and pellet forms were analyzed and the results are shown in figure 8.10. It was concluded that the form of the Pan has no effect on the general conductivity-temperature response of the material, figure 8.11, both plots show conductivity reaches a point $\delta\sigma/\delta T \cong 0$.

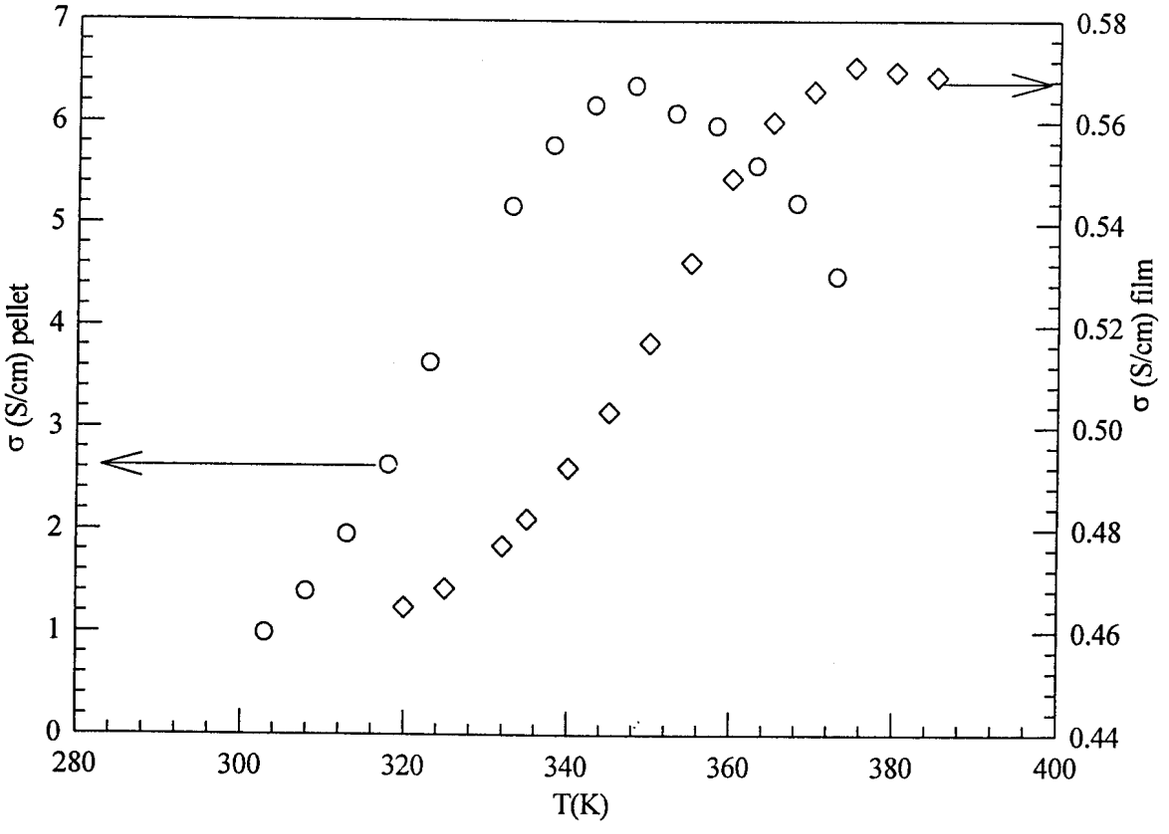

Fig (8.10): Pan (CSA) (o) pellet and Pan (HCl) film (◇) both measured using the Montgomery method.

No difference in behavior was observed for materials with different morphologies, forms and dopant types. **This suggests that transport predominantly involves monomer units and occurs independent of structure.**

8.7.2 The effect of annealing *rate* on Pan conductivity

The four-point probe method was applied for tracing the conductivity response of Pan pellets to annealing and annealing rate. It was found that the $\delta\sigma/\delta T \cong 0$ point depends on the annealing rate. The conduction mechanisms underlying the conductivity profile of figure 8.11 are analyzed in terms of conduction models.

Table 8.5 gives an **estimate** of the temperature readings at which $\delta\sigma/\delta T \cong 0$, for particular annealing rates, as derived from figure 8.11. The point $\delta\sigma/\delta T \cong 0$ shifts slightly to higher temperatures as annealing rate increases. Implying $\delta\sigma/\delta T \cong 0$, results from a heat energy activated process.

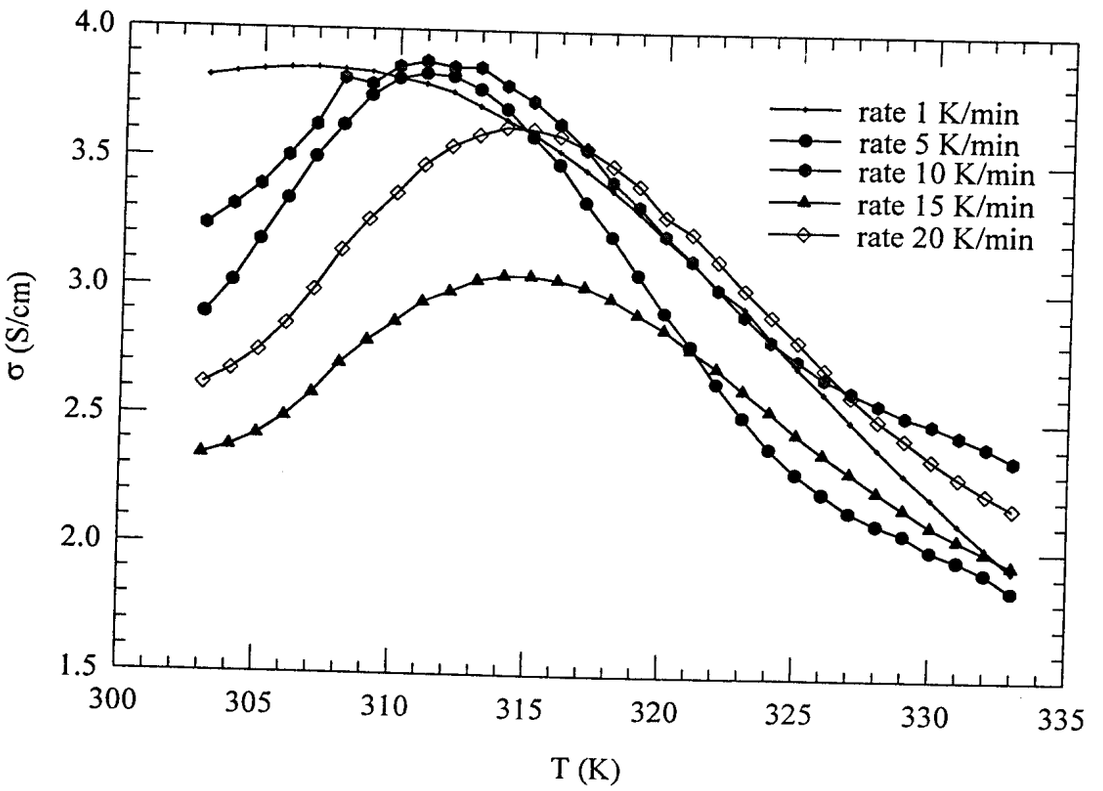

Fig (8.11): The change in conductivity with temperature for different annealing rates. Chemically synthesized Pan pellets were used to obtain these results.

Table 8.5: The relationship of annealing rate to the position $\delta\sigma/\delta T \cong 0$

Annealing rate (K/min)	Temperature at $\delta\sigma/\delta T \cong 0$
1	306
5	311
10	314
15	315
20	316

8.7.3 The conduction models for temperatures above 300 K

The work reported in the previous sections has shown that, the general conductivity response of Pan is similar regardless of the type of Pan and the form of the sample. Pan (CSA) and annealed at 1K/min was used to investigate the fitting of the variable range hopping and the activation energy models at temperatures above 300 K. These results together with thermal analysis and Fourier transform infrared (FTRI) results will help in explaining the conductivity-temperature profiles indicated in figure 8.12.

Figure 8.12 [A], represents Mott's VRH conduction of charge in three dimensions[2] between conducting islands (a plot of $\ln\sigma$ vs. $T^{-0.25}$). VRH model is obeyed for $T < 320$ K for the particular sample. The activated energy model ($\ln\sigma$ vs $T^{-0.5}$), figure 8.12 [B] is obeyed by this particular sample for $T < 319$ K. From the results we cannot state with absolute confidence whether conductivity is governed by VRH in three dimensions.

The thermally activated conductivity is attributed to electron hopping, but the origin and size of the electron localization centers and barriers have not yet been identified[3].

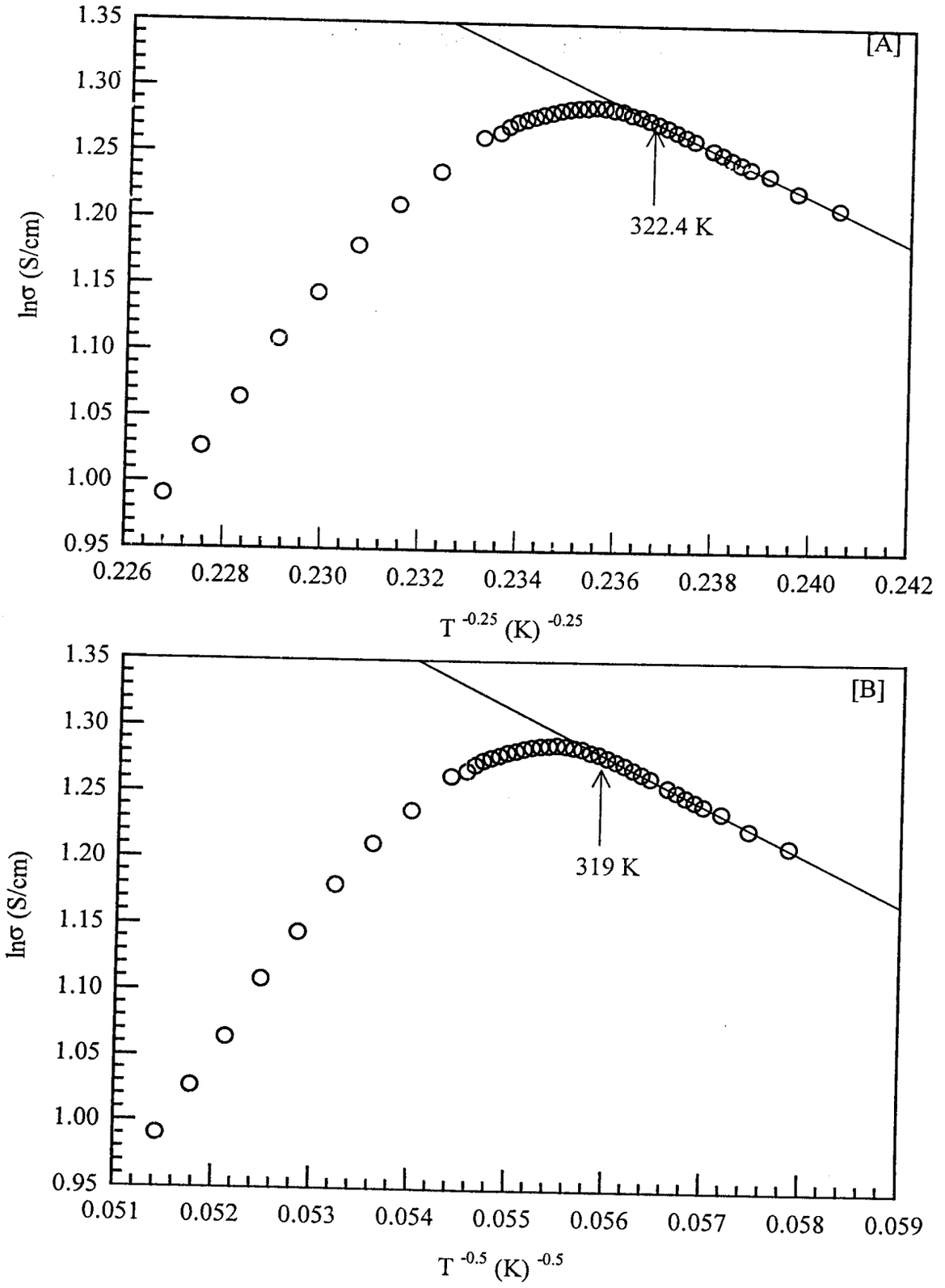

Fig (8.12): 3-D VRH model [A] and activation energy model [B] for Pan (CSA).

8.8 FTIR analysis

Fourier transform infrared spectroscopy was applied in analyzing the effect of annealing on the molecular structure of the polymer. The major objective was to deduce the relationship between conductivity-molecular structure changes as a result of annealing the polymer.

The observed change in conductivity with annealing could be a result of the loss in dopant ions from the polymer. In the event of a dedoping reaction, the spectra of the doped form is expected to change to that of the undoped form. Figure 8.13, shows a comparison of the spectra of the annealed forms of Pan (HC doped). From this figure and the experimentally obtained spectral values of undoped and doped Pan, table 8.6 was constructed. The measuring spectrometer used in this work had a resolution of 2 wavenumbers.

Assuming a dedoping reaction, the wavenumbers 1480 and 1563 cm^{-1} (representing the quinoid ring structure) are expected to move to higher wavenumbers by 17 and 33 values respectively. Tables 8.6 show an average movement of 10 and 18 cm^{-1} for the 1480 and 1563 cm^{-1} wavenumbers respectively, upon annealing. The changes in wavenumbers show a transition of the doped towards the undoped form. However, Pan (HCl doped) will not completely go to its undoped form with annealing as shown by annealing the Pan samples for 73 hrs at 373 K, table 8.6. Accompanying the wavenumber shift is a change in peak intensities, figure 8.13, indicating polymer degradation due to heat energy.

Upon heating the polymer with high intensity laser light, the Raman spectra of figure 8.14 shows that the spectra of doped Pan approaches that of carbon as expected of all polymers. Conclusively, the annealing process results in a slight transition of Pan from the doped to undoped form, loss of chloride ions and polymer degradation.

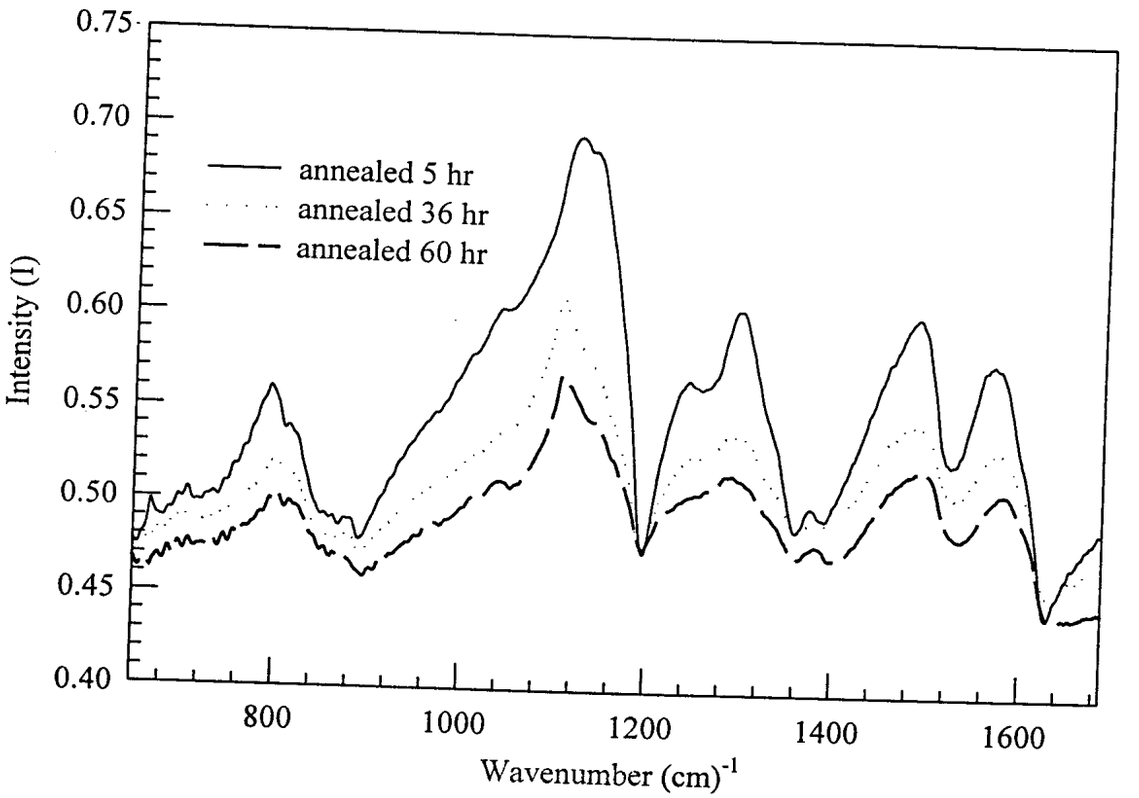

Figure (8.13): The spectral patterns of Pan (HCl doped) samples annealed at 100°C.

Table 8.6: Comparison of the peak positions for Pan samples

HCl doped	795	1106	1294	1480	1563
Annealed 5 hr	794	1119	1294	1490	1577
Annealed 36 hr	800	1103	1290	1490	1584
Annealed 48 hr	797	1103	1290	1490	1581
Annealed 60 hr	806	1103	1277	1494	1584
Annealed 73 hr	813	1110	1274	1490	1581
EB (undoped)	829	1165	1306	1497	1590

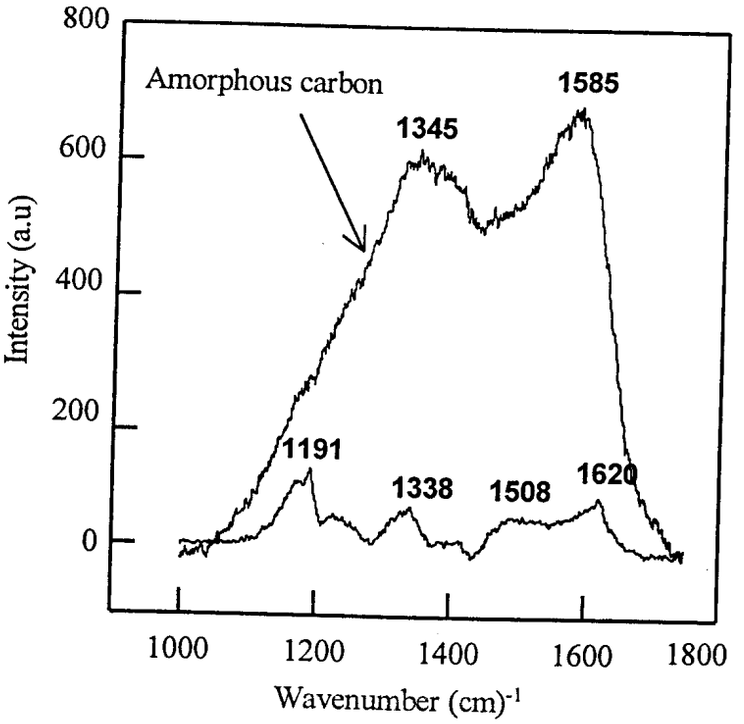

Fig (8.14): The Raman spectra of Pan (CSA) pellet compared to that of amorphous carbon.

8.9 Thermal analysis

Thermogravimetry was used to investigate the loss of moisture from the polymer as a result of annealing and to relate this result to the conductivity response discussed earlier in this chapter. The thermogravimetric (TG) curve, figure 8.15 shows a weight loss in the temperature region 25 – 100 °C, which is due to the loss of water. In this temperature range (figure 8.8-10) the conductivity of the Pan decreases. The second mass loss starting at about 250 °C is attributed to thermal degradation of the polymer.

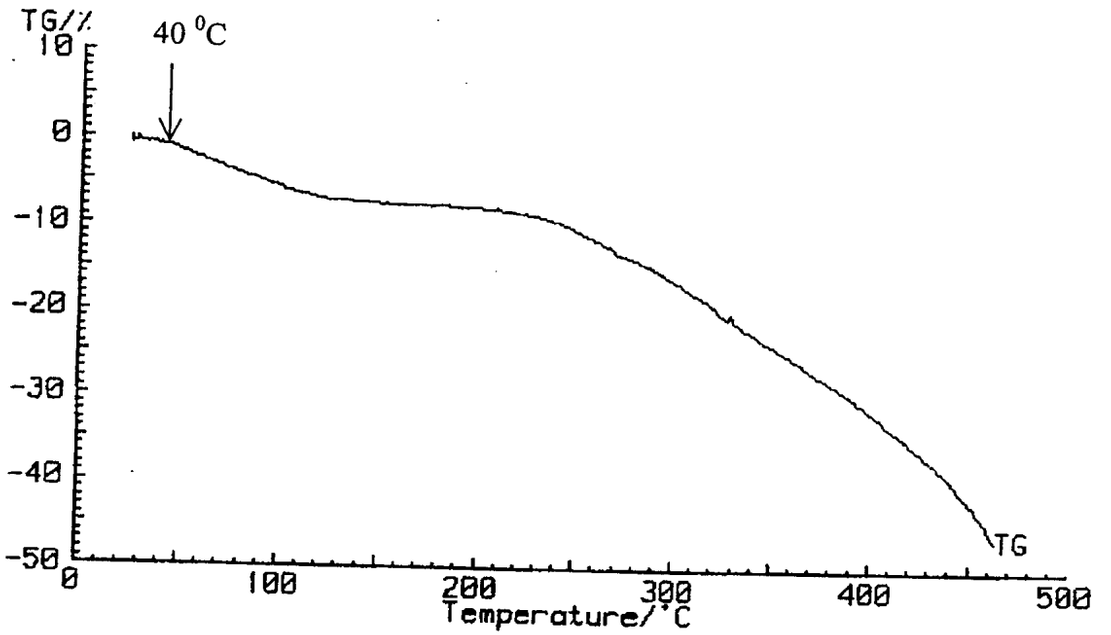

Fig (8.15): TG graph shows the loss of mainly water around 100 °C.

8.10 Conductivity in the temperature range 30 < T (K) < 300

Conductivity in the temperature range 30 < T (K) < 300, has been useful in determining the dimensionality of conduction in the polymer, conduction model of best fit and whether conduction in this temperature range is semiconducting, insulating or metallic.

Conductivity of the materials is analyzed in terms of the conduction models described in chapter 5. Figure 8.16 (for Pan (CSA) pellet sample) shows that resistivity (ρ) of the polymer is stable as temperature goes down from 300 to 100 K and increases from 100 to 30 K, the degree of temperature dependence of resistivity increases substantially at T < 100 K.

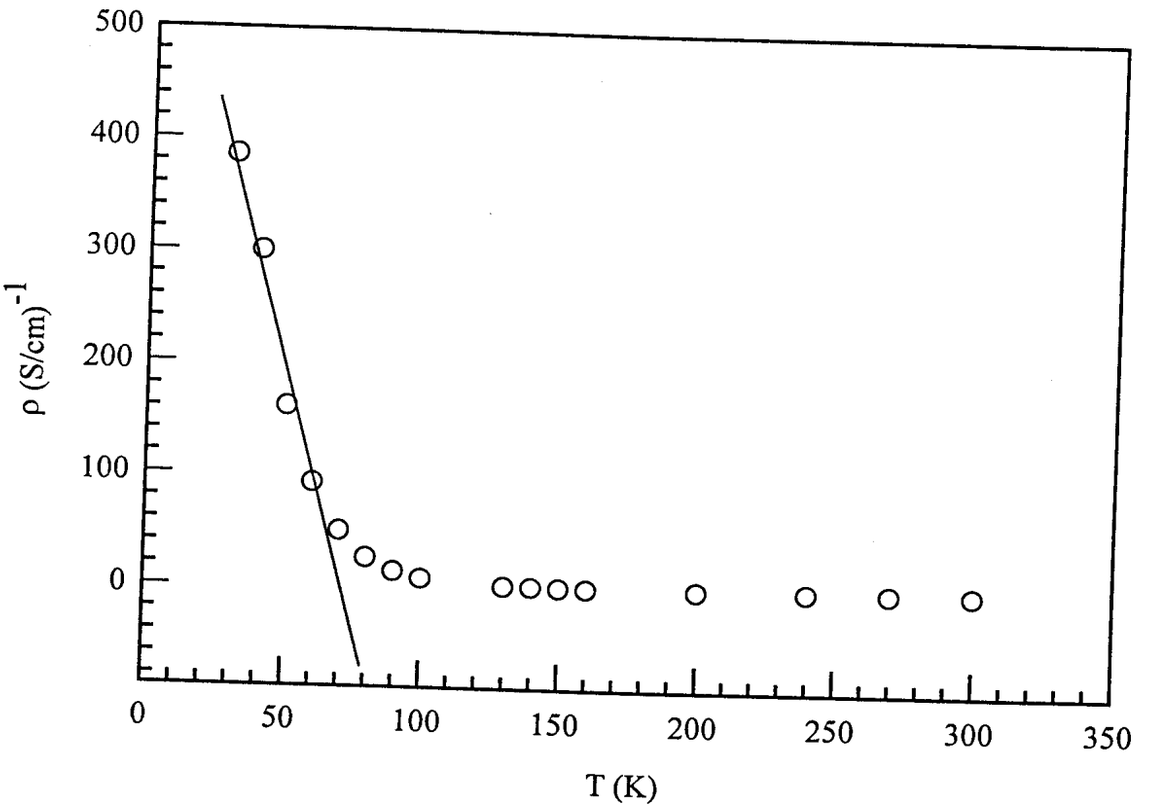

Fig (8.16): Variation of resistivity with temperature for chemically synthesized Pan.

The electrical properties of doped polymers are strongly dependent on the extent of disorder present in the material. The extent of disorder is generally characterized in terms of the temperature dependence of resistivity[2]. The resistivity coefficient of the material $\delta\rho/\delta T$, show little temperature dependence of conductivity for; $\rho_{(315\ K)}/\rho_{(310\ K)} = 1.02$, $\rho_{(320\ K)}/\rho_{(315\ K)} = 1.02$ and $\rho_{(325\ K)}/\rho_{(320\ K)} = 1.01$. But $\rho_{(300\ K)}/\rho_{(30\ K)} = 823.5$, indicating Pan is insulating at 30 K.

The Kivelson model and the VRH in 3-D were applied in analyzing the conductivity of Pan (CSA) and chemically synthesized Pan. From the previous sections there is not much significant difference between the activated model and VRH model in 2 and 3 D.

8.10.1 The conduction models

Several authors have examined the different conduction models and they have concluded that the VRH model in 3-D represents conduction in Pan satisfactorily. It is presumed however, that the overall conductivity observed, is a superposition of more than one conduction phenomenon.

The linear dependence of the measured variables (($\ln\sigma$ vs. $T^{-0.25}$) for the 3-D VRH model and ($\ln\sigma$ vs. $\ln T$) for the Kivelson model in figures (8.17, 8.18 and 8.19) would indicate an agreement between the conduction model and the conduction phenomenon. For the present section of this current chapter, the agreement between the conduction phenomenon and the conduction models is of prime importance. From these results, we shall deduce the model which best describes conduction in our samples of Pan.

8.10.1.1 Mott's VRH in 3-D

The micrographs of CP pellets and films demonstrate that the polymer solids consist of a heterogeneous structure of fibres and grains[1]. An idealisation of this structure was shown in figure 4.5 chapter 4 section 4.2.2. It is perhaps more accurate to characterize the conduction process in CPs as the hopping of electrons between these charged carriers, a basis for "hopping " models of conduction.

Figures (8.17, 8.18 and 8.19) are the Kivelson and 3-D VRH responses for the following materials; Pan (CSA) pellet, Pan (HCl) and Pan (CSA) film respectively. The Mott's VRH is a phonon assisted quantum-mechanical transport process in which a balance is obtained between the thermodynamic constraint on a charge carrier moving to a nearby localized state of different energy, against the quantum-mechanical restraint of a carrier moving in a localized state of a similar energy, but spatially remote[4]. This process leads to characteristic temperature dependence represented by the Mott's VRH conduction models, although there are other conduction mechanisms, which can, under certain conditions, also give such temperature dependence[4]. From the results we can conclude

that conduction phenomenon for our samples of Pan obeys the 3-D VRH model over the temperature range 30 – 300 K satisfactorily.

8.10.1.2 Kivelson model

This model has been largely used in representing the conductivity of lightly doped Pan samples. In this model, the conductivity follows the power law[3], $\sigma(T) \propto T^n$ where, n > *10.*

Figures ((8.17, 8.18 and 8.19)) are the responses of Pan (CSA) pellet, Pan (HCl) pellet and Pan (CSA) film respectively. Kivelson model is obeyed at T < 260, for all our samples. Estimates of the upper temperature limits for the Kivelson model are inserted in the figures.

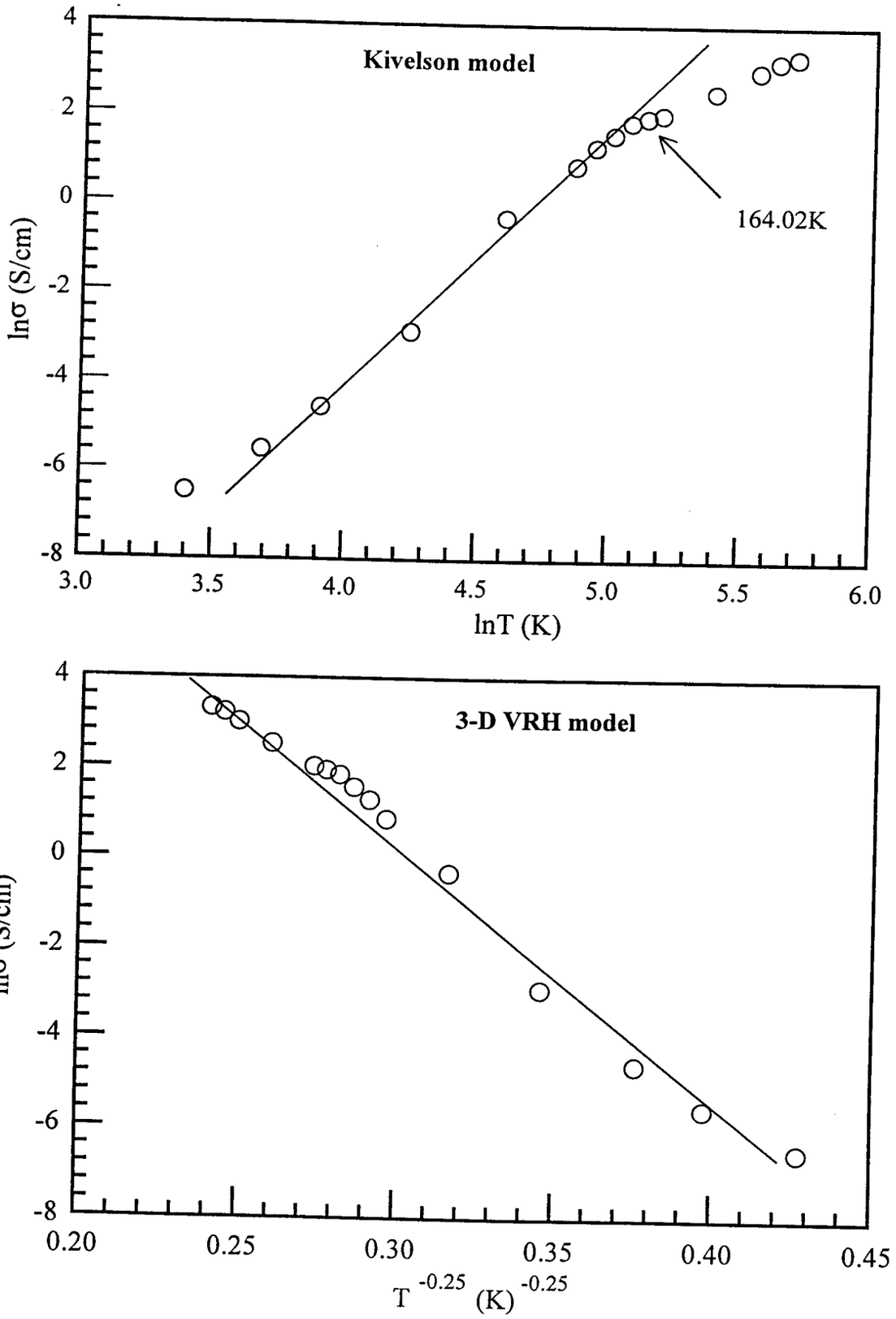

Fig (8.17) The Kivelson and 3–D VRH models for Pan (CSA) pellets.

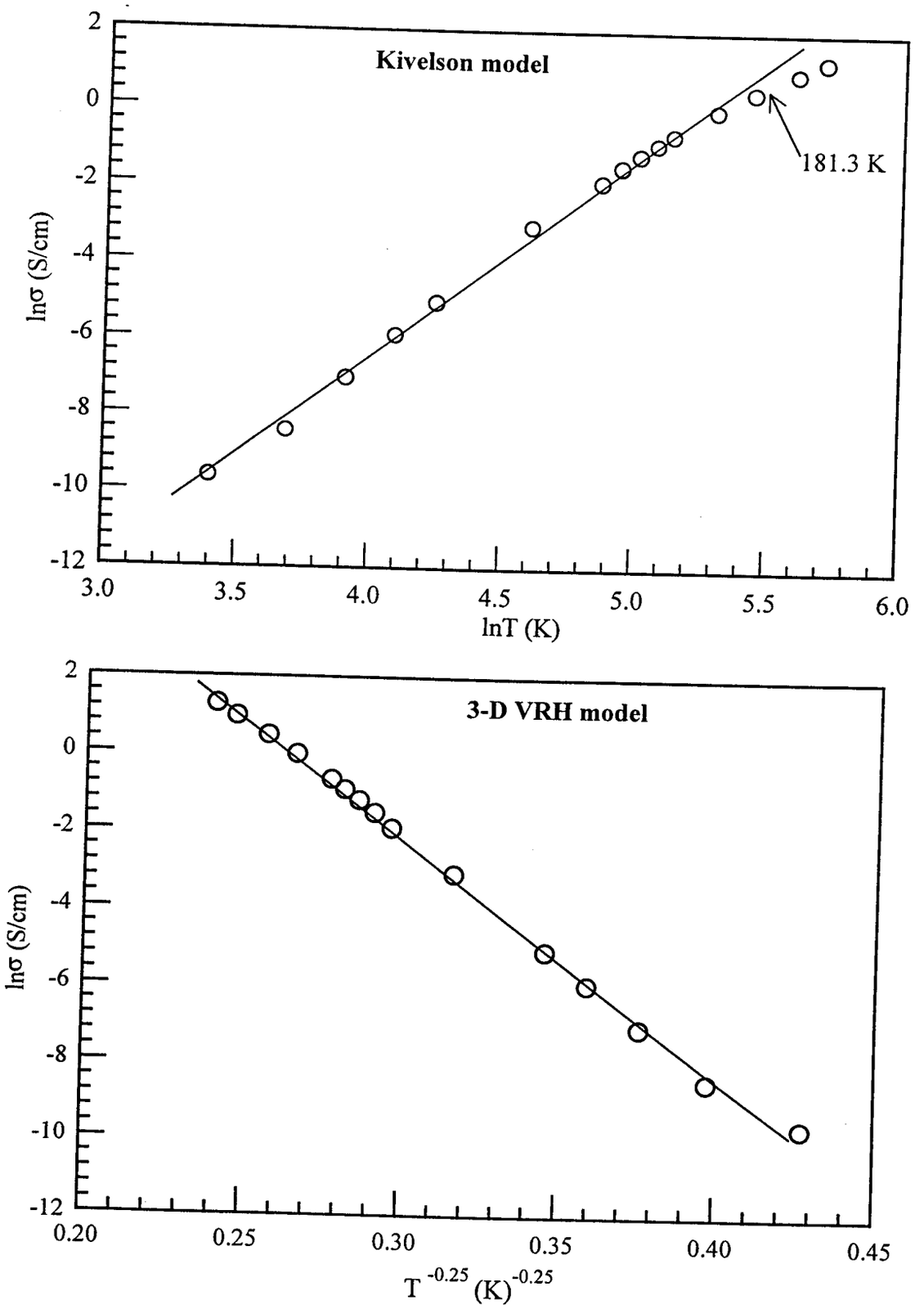

Fig (8.18): Kivelson and 3-D VRH models for Pan (HCl) pellets.

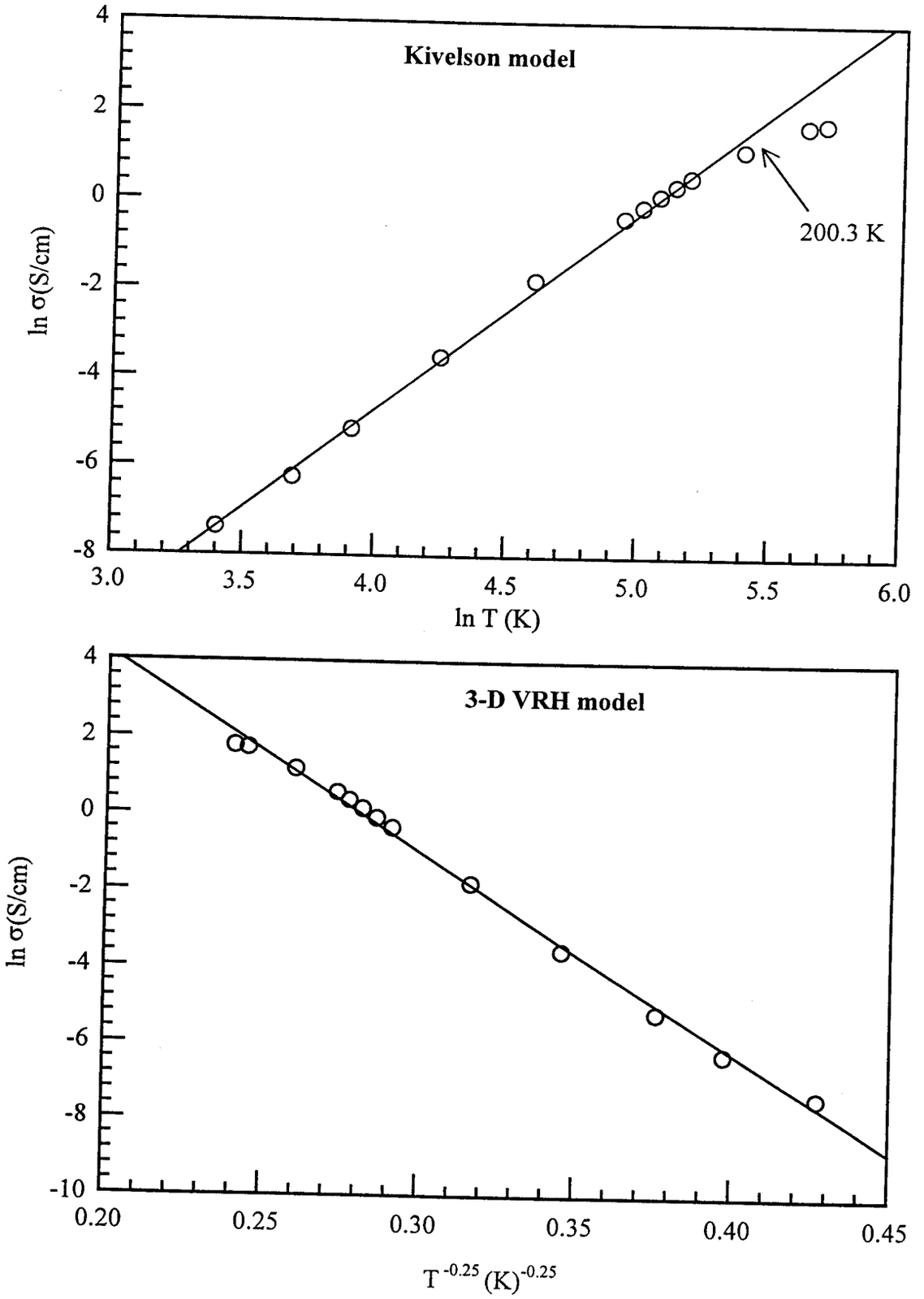

Fig (8.19): Kivelson and 3-D VRH models for Pan (HCl) films.

Reference

1. Conducting Polymers, Fundamentals and Applications, (Ed. P. Chandrasekhar), Kluwer academic publishers, Boston (1999).
2. R. Menon, C. O. Yoo, A. J. Heeger, Phys. Rev. **B 48**, 17685 (1993).
3. M. Gosh, A. Barman, S. Chatterjee, Phys. Lett. A **260**, 138 (1999).
4. D.S. Maddison, T. L. Tansley, J. App. Phys, **72**, 4677 (1992).

Chapter 9

Discussion

i. In stating the conductivity of a sample of Pan, other conductivity determining factors such as sample thickness, temperature, form of the sample and dopant used need to be mentioned.

ii. Specific conductivity values for CPs can not be reproduced even for samples derived from the same source.

iii. Low power dissipation of about 0.1 μWatt gives a more accurate measure of the material's electrical properties.

iv. The positive resistivity coefficient at temperatures below 300 K implies semiconducting behavior.

v. $\sigma(T)$ dependence is extremely weak for Pan materials used in the present work.

vi. Moisture is important for charge transfer.

vii. Conductivity is temperature activated.

viii. Annealed samples show Ohmic behavior.

ix. The fall in conductivity as a result of annealing the sample is attributed to the loss of moisture, degradation of the polymer and loss of the volatile hydrochloric acid.

x. There is a slight shift of the spectra of the doped form towards higher wavelength upon annealing.

xi. 3-D charge transfer sufficiently describes conductivity in Pan at $T < 320$ K.

xii. Application of conduction models to temperatures above 330 K is less accurate, since thermal analysis has shown the loss of water and other gaseous materials from the polymer.

xiii. The strong temperature dependence as temperature is lowered down to 30 K (compared to metals) arises from a combination of mesoscale inhomogeneity ("metallic islands") and microscopic disorder (localization of the electronic wave functions) both of which are indicative of the quality of the material. Thus Pan has

been characterized as a collection of metallic islands separated by insulating barriers[1].

Reference

1. M. Reghu, Y. Cao, A. J. Heeger, Phys. Rev. **B 47**, 1758 (1993).

Chapter 10

Conclusion

i. Thermal analysis has shown that the loss of moisture and other substances from Pan, affects polymer conductivity, a way of replenishing the moisture content of CP devices based on Pan will ensure their accuracy and longer device life span.
ii. The value of the applied current used for Pan materials has an effect on the current-voltage characteristics.
iii. The conductivity-temperature characteristics of all types of Pan are the same, (commercial Aldrich CSA and HCl doped, electrochemically synthesized and chemically synthesized.
iv. Conductivity values of Pan are not reproducible whether Pan is in pellet or film form.
v. Pan shows semiconducting behavior for $30 \leq T\ (K) \leq 300$.
vi. The VRH in 3 or 2 dimensions equally represented the conductivity in Pan.
vii. For hopping transport, conductivity increases with temperature in contrast to the decrease in conductivity with temperature for band conduction.
viii. The ratio σ (30 K)/ σ (300 K) for Pan at 30 K is indicative of insulating behavior.

Amongst other factors we could not study was the effect of vacuum on conductivity. It is assumed the process of pumping vacuum, in the cryostat, for low temperature measurements, results in dehumiditizing Pan and thus affects its conductivity.

Conductivity should be mainly due to hopping process that is hopping between localized electronic states, which are distributed at random in space and energy. The data do not really allow it to be possible to distinguish between two and three-dimensional conductivity.

Since there is a finite density of states at the Fermi energy (as inferred from the temperature-independent Pauli susceptibility) the increase in resistivity at low temperatures results from disorder-induced localization[1].

10.1 Motivation for future work

One of the major problems encountered with polyaniline was the varying of conductivity even for samples derived from the same powder source. This would imply one cannot state the conductivity value of polyaniline with absolute certainty. The study of the distribution of chain lengths in polyaniline should be undertaken together with a study to synthesis a polymer of uniform chain length.

The study of conducting polymers offers many opportunities. Even though charge transfer characteristics of conducting polymers are still not fully understood, the reproducibility of electronic, optical and photoelectrical properties to mention a few has allowed it possible to design and fabricate conducting polymer based devices. It is proposed that the next stage of this study should include a study towards coming up with devices that would have several advantages over the conventional material made devices. Devices of particular importance would be the study on polymer-based solar cells and polymer light emitting devices.

Several other conducting polymers including those mentioned in chapter 2, could be studied in place of polyaniline.

Reference

1. R. Menon, C. O. Yoo, A. J. Heeger, Phys. Rev. **B 48**, 17685 (1993).